POLITECNICO DI MILANO

FACOLTÀ DI INGEGNERIA CIVILE, AMBIENTALE E TERRITORIALE

Corso di Laurea Specialistica in Ingegneria Civile

MODELING CLIMATE CHANGE IMPACTS ON THE SEINE RIVER BASIN HYDROLOGY USING A CATCHMENT-BASED LAND SURFACE MODEL

Relatori:

Prof.ssa Maria Cristina Rulli

Dr. Agnès Ducharne

Laureando:

Olivier Crespi Reghizzi

Matr.: 708440

Anno Accademico 2007-2008

POLITECNICO DI MILANO

FACOLTÀ DI INGEGNERIA CIVILE, AMBIENTALE E TERRITORIALE

Corso di Laurea Specialistica in Ingegneria Civile

L'IMPATTO DEL CAMBIAMENTO CLIMATICO SUL CICLO IDROLOGICO NEL BACINO IDROGRAFICO DELLA SENNA: MODELLAZIONE TRAMITE IL MODELLO CATCHMENT BASED LAND SURFACE MODEL

Relatori:

Prof.ssa Maria Cristina Rulli

Dr. Agnès Ducharne

Laureando:

Olivier Crespi Reghizzi

Matr.: 708440

Anno Accademico 2007-2008

Summary

The present Master's thesis has been realised at UMR Sisyphe (CNRS - Université Pierre et Marie Curie) in Paris, France in the framework of the REXHYSS project focused on Climate change impacts on extreme hydrological events over the Seine and Somme river basins.

The aim of this thesis is to analyse climate change impacts on the hydrological variables over the Seine river basin using the Catchment Based Land Surface Model (CLSM) forced with various climate change scenarios. The present work benefited from a calibration of CLSM previously realised and from the recent implementation of a Muskingum routing model on the Seine river catchment.

In the framework of this thesis a validation of 6 runs of CLSM, with various calibrated parameter sets, has been realised, showing that the 6 runs had similar performances in correctly simulating observed discharges (1981-2002). It is a typical case of "equifinality". Then, the 6 "equifinal" runs forced with the SAFRAN dataset (based on observation) have been tested on historical time and with a climate change scenario on future time. This test shows that simulated impacts are robusts and not very much driven by the choice of the CLSM run.

Having chosen a run of CLSM within the 6 previously tested, a multi-scenario approach, classical in climate change impact studies, has been applied, realising an intercomparison of 11 climate change scenarios different each one from another for the Green-House Gases emission scenario (A1B and A2, IPCC SRES 2000), for the General Circulation model (8 GCMs) or for the downscaling technique (Weather Regime Approach, Variable Correction Method). In this way, uncertainties pending on simulated impacts are assessed and robustness of the impacts is ascertained.

The main simulated climate change impact is an important reduction of total runoff. E.g. mean total runoff at Poses would be nearly halved in 2081-2099 compared to the 1982-2000 value. The total runoff reduction is robust and confirmed in all the 11 climate scenarios. This reduction is particularly strong and allarming in spring and summer. Other impacts are a reduction of the soil moisture content and of the recharge of the deep acquifers represented in CLSM through a linear reservoir.

Sommario

La presente tesi di laurea è stata realizzata presso l'UMR Sisyphe (CNRS - Université Pierre et Marie Curie) di Parigi, Francia nell'ambito del progetto di ricerca francese REXHYSS riguardante la determinazione degli impatti dei cambiamenti climatici sugli eventi idrologici estremi nei bacini idrografici della Senna e della Somme.

Lo scopo della presente tesi è quello di analizzare gli impatti dei cambiamenti climatici sulle variabili idrologiche del bacino idrografico della Senna utilizzando il modello Catchment Based Land Surface Model (CLSM) alimentato con molteplici scenari di cambiamento climatico.

Si è usufruito di una precedente taratura del modello CLSM sul bacino idrografico della Senna e di un modello di propagazione di tipo Muskingum recentemente implementato. Si è quindi proceduto alla validazione di 6 "runs" di CLSM rispetto alle portate osservate in tempo storico (1981-2002). I 6 runs testati hanno rivelato capacità simili nel simulare correttamente le portate osservate. Si tratta quindi di un tipico caso di "equifinality". I 6 runs "equivalenti" in validazione sono stati quindi testati sia in tempo storico, con le osservazioni del dataset SAFRAN, sia in tempo futuro, con uno scenario di cambiamento climatico. Si mostra che gli impatti di cambiamento climatico simulati sono poco sensibili alla scelta del run di CLSM.

Scelto un run di CLSM all'interno di quelli testati precedentemente, si adotta un approccio multi-scenario, tipico degli studi sui cambiamenti climatici, realizzando un'analisi comparativa di 11 scenari di cambiamento climatico diversi tra loro per lo scenario di emissione di gas ad effetto serra (A1B e A2, IPCC SRES 2000), il modello di circolazione generale (8 GCMs) o per la tecnica di downscaling utilizzata (Weather Regime Approach e Variable Correction Method). In tale modo si accertano le incertezze gravanti sugli impatti simulati e si verifica la robustezza di tali impatti.

L'impatto principale del cambiamento climatico è la forte riduzione del deflusso totale. Ad esempio si prevede quasi un dimezzamento del deflusso totale medio a Poses negli anni 2081-2099 rispetto a 1982-2000. La riduzione del deflusso totale è robusta e confermata dagli 11 scenari di clima. Tale riduzione è particolarmente netta ed allarmante nei mesi primaverili ed estivi. Altri impatti riguardano la riduzione dell'umidità del suolo e della ricarica degli acquiferi profondi.

Acknowledgements

I would like to gratefully thank Dr. Agnès Ducharne for giving me this very interesting research opportunity and for her close support and advice. I also owe special thanks to Prof. Maria Cristina Rulli for her kind supervision.

I am grateful to Simon Gascoin, PhD Student at the Université Pierre et Marie Curie for his counseling and helpfulness and to all the researchers in UMR Sisyphe for their warm attitude towards me.

Last but not least, I would like to thank Didier Dagorne, Pierre Rigaudière and the French consulting company SAFEGE for kindly supporting this thesis.

Contents

Summary II

Sommario III

Acknowledgements IV

I Estratto sintetico in Italiano 1

0.1 Introduzione . . . 2
0.1.1 Contesto . . . 2
0.1.2 Il progetto REXHYSS . . . 3
0.1.3 Obiettivi del presente studio . . . 5
0.2 Gli scenari di cambiamento climatico . . . 6
0.3 Il modello idrologico CLSM . . . 7
0.4 Modellazione del bacino idrografico della Senna . . . 8
0.5 Impatti del cambiamento climatico . . . 10
0.6 Conclusione . . . 11

II Modeling climate change impacts on the Seine River basin hydrology 1

1 Introduction 2

1.1 Context . . . 3
1.2 The REXHYSS project . . . 4
1.3 Objectives of this thesis . . . 6
1.3.1 Climate change scenarios . . . 6
1.3.2 The CLSM model and the Seine river catchment . . . 7
1.3.3 Climate Change Impacts . . . 8

2 Climate change scenarios **9**
2.1 Emission scenarios . . . 11
2.2 General Circulation Model . . . 14
2.3 Downscaling techniques . . . 16

3 Catchment Based Land Surface Model **20**
3.1 A historical introduction . . . 21
3.1.1 Land surface models . . . 21
3.1.2 The role of vegetation . . . 22
3.1.3 Evapo-transpiration's formulation impact on runoff . . . 22
3.1.4 Subgrid variability . . . 23
3.2 CLSM model . . . 24
3.2.1 Overall framework . . . 25
3.2.2 A catchment based approach . . . 25
3.2.3 Subgrid variability . . . 26
3.2.4 Water and energy budgets . . . 34
3.3 CLSM model with linear storage reservoir . . . 37

4 Modeling the Seine river catchment **40**
4.1 The Seine river catchment . . . 41
4.2 Water management . . . 43
4.3 Modeling the Seine river basin . . . 44
4.3.1 Muskingum routing . . . 44
4.3.2 Reservoir management . . . 45
4.3.3 Data . . . 46
4.4 Validation of CLSM . . . 48
4.5 Equifinality . . . 51
4.5.1 SAFRAN annual mean cycle (1982-2000) . . . 52
4.5.2 Equifinality in climate change simulation (1950-2099) . . . 57

5 Modeling climate change impacts on hydrology **62**
5.1 Set of simulations . . . 63
5.1.1 Main set of simulations . . . 63
5.1.2 Additional simulations . . . 66
5.2 Testing initialization choices . . . 66
5.3 Assessment of simulations in present time observed climate . . . 69
5.3.1 Comparing climate . . . 71
5.3.2 ARPEGE climat v3+ and v4 versus SAFRAN and ERA-40: . 72
5.3.3 A1BCONT and seven IPCC AR4 simulations versus SAFRAN 82
5.3.4 Main results . . . 89
5.4 Climate change reference simulation . . . 90

5.4.1 Changes in mean annual cycle 90
5.4.2 Changes in probability distribution functions 95
5.4.3 Trends in annual mean values 97
5.5 General Circulation Model related uncertainties 102
5.5.1 Climate forcings 102
5.5.2 Impacts on hydrology 106
5.5.3 Main results 108
5.6 Downscaling techniques related uncertainties 109
5.6.1 Climate forcings 109
5.6.2 Impacts on hydrology 111
5.6.3 Main results 113
5.7 Emission scenarios related uncertainties 114
5.7.1 Climate forcings 115
5.7.2 Impacts on hydrology 117
5.7.3 Main results 119

6 Conclusion **120**
6.1 Overall approach 121
6.2 Synthesis of climate change impacts 121
6.2.1 Climate Forcings 121
6.2.2 CLSM outputs 122
6.3 Continuation of this work 128

List of Figures

2.1 Representation of the chain of models used for climate change impact studies . . . 10
2.2 Block diagram of the chain modeling process used for climate change impact studies . . . 11
2.3 Characteristics of the four SRES storylines . . . 12
2.4 Global GHG emission . . . 13
2.5 Example of a quantile-quantile plot for maximum precipitation in the Paris area . . . 18

3.1 Schematic representation of CLSM overall framework . . . 27
3.2 Water table and the catchment deficit . . . 29
3.3 Local moisture and catchment deficit . . . 29
3.4 Illustration of the catchment deficit and the surface and root zone excess . . . 29
3.5 Schematic representation of CLSM spatial partitioning process . . . 32
3.6 Subdivision of the catchment in 3 zones . . . 33
3.7 Probability density functions (pdfs) of equilibrium root zone soil moisture at various catchment deficits in the catchment . . . 33
3.8 Schematic representation of the energy budget performed by CLSM . 35
3.9 Schematic representation of the water balance calculations performed by CLSM . . . 36
3.10 Schematic representation of the water balance calculations performed by CLSM with a LR . . . 38
3.11 Soil moisture profile and water fluxes in CLSM-LR . . . 39

4.1 Topography and hydrographic network of the Seine basin . . . 42
4.2 Spatial distribution of annual mean precipitation over the Seine river basin . . . 42
4.3 Schema of river reach . . . 45
4.4 Unit catchment subdivision and vegetation . . . 46
4.5 Validation of CLSM - LRON version over 1981-2002 at Paris and Poses 50
4.6 Hydrographic network of the Seine river catchment . . . 51

4.7 Six runs of CLSM - SAFRAN dataset (1981-2002) - mean annual cycle of total runoff, evaporation, catchment deficit, linear reservoir water content, surface runoff and baseflow from linear reservoir 56
4.8 Annual mean trends - Arpege-v3+ - weather regime approach dataset(1950-2099). Six runs of CLSM - total runoff, evaporation, catchment deficit and linear reservoir water content 59
4.9 Six runs of CLSM - Arpege-v3+ - weather regime approach dataset (1981-2002) - mean annual cycle of total runoff, evaporation, catchment deficit, linear reservoir water content, surface runoff and baseflow from linear reservoir 60
4.10 Six runs of CLSM - Arpege-v3+ - weather regime approach dataset (2081-2099) - mimpacts on the mean annual cycle 61

5.1 Time partitioning 65
5.2 Spin up tests on A1BCONT 2079-2099 68
5.3 Trends on annual mean values over all the catchment upstream from Poses for precipitation, air temperature, evaporation, catchment deficit and linear reservoir's water content - SAFRAN, ERA-40, A1BCONT, ARP-v4-WR and ARP-v4-VCM - 1982-2000 74
5.4 Mean annual cycle over all the catchment upstream from Poses for air temperature, precipitation, air humidity and catchment deficit - SAFRAN, ERA-40, A1BCONT, ARP-v4-WR and ARP-v4-VCM - 1982-2000 75
5.5 Mean annual cycle over all the catchment upstream from Poses for total runoff, evaporation, recharge flux to the LR and LR's water content - SAFRAN, ERA-40, A1BCONT, ARP-v4-WR and ARP-v4-VCM - 1982-2000 76
5.6 Empirical relative frequency for air temperature and empirical probability of exceedance for precipitation and total runoff - SAFRAN, ERA-40, A1BCONT, ARP-v4-WR and ARP-v4-VCM - 1982-2000 . . 77
5.7 Trends on annual mean values over all the catchment upstream from Poses - SAFRAN, A1BCONT, and 7 others simulations from IPCC AR4 - 1982-2000 83
5.8 Mean annual cycle over all the catchment upstream from Poses - SAFRAN, A1BCONT, and 7 others simulations from IPCC AR4 - 1982-2000 84
5.9 Mean annual cycle over all the catchment upstream from Poses - SAFRAN, A1BCONT, and 7 others simulations from IPCC AR4 - 1982-2000 85

5.10 Empirical relative frequency for air temperature and empirical probability of exceedance for precipitation and total runoff - SAFRAN, A1BCONT, and 7 others simulations from IPCC AR4 - 1982-2000 . . 86
5.11 Monthly mean values over the entire watershed - A1BCONT simulation 92
5.12 Monthly mean values over the entire watershed - A1BCONT simulation 93
5.13 Changes in probability distribution functions for A1BCONT simulation 96
5.14 Trends on annual mean values over all the catchment for precipitation, air temperature, total runoff and evaporation 99
5.15 Trends on annual mean values over all the catchment for wilting areal fraction, catchment deficit, recharge to the linear reservoir and linear reservoir content 100
5.16 Mean annual runoff, overland flow and base flow at Poses for A1BCONT simulation 101
5.17 Assessment of GCMs related uncertainties on 21m impacts on the mean annual cycle. 104
5.18 Assessment of GCMs related uncertainties on 21f impacts on the mean annual cycle. 105
5.19 Empirical relative frequency for air temperature and empirical probability of exceedance for precipitation and total runoff - A1BCONT, and 7 others simulations from IPCC AR4 - 2081-2099 107
5.20 Assessment of downscaling techniques related uncertainties on 2081-2099 impacts on the mean annual cycle. 110
5.21 Empirical relative frequency for air temperature and empirical probability of exceedance for precipitation and total runoff - ARP-v4-VCM-A2 and ARP-v4-WR-A2 - 2081-2099 112
5.22 Assessment of GHGs emission scenarios related uncertainties on 2081-2099 impacts on the mean annual cycle. 116
5.23 Empirical relative frequency for air temperature and empirical probability of exceedance for precipitation and total runoff - ARP-v4-VCM-A2 and ARP-v4-VCM-A1B - 2081-2099 118

6.1 Main results on 2081-2099 impacts on the mean annual cycle 123
6.2 Trend on annual mean values for the 11 simulation ensemble: air temperature and precipitation 124
6.3 Trend on annual mean values for the 11 simulation ensemble: total runoff and evaporation 126
6.4 Trend on annual mean values for the 11 simulation ensemble: catchment deficit and linear reservoir water content 127

List of Tables

2.1 Comparative summary of the relative merits of statistical and dynamical downsclaing techniques. 17

4.1 Muskingum routing parameters 45
4.2 Validation of CLSM performances - SAFRAN 1981-2002 49
4.3 Mean, biases and impacts of six runs of CLSM - Total runoff and evaporation 53
4.4 Mean, biases and impacts of six runs of CLSM - Catchment deficit and Linear reservoir water content 54
4.5 Mean, biases and impacts of six runs of CLSM - Surface runoff, Topmodel's baseflow and LR's baseflow 55

5.1 Main set of simulations 64
5.2 General Circulation Models from IPCC AR4 66
5.3 Assessment of present time simulated air temperature over 1982-2000 years 78
5.4 Assessment of present time simulated precipitation over 1982-2000 years 78
5.5 Assessment of the present time simulated total runoff over 1982-2000 years 79
5.6 Assessment of the present time simulated catchment deficit and evaporation over 1982-2000 years 80
5.7 Assessment of the present time simulated recharge flux to the Linear Reservoir and LR's content over 1982-2000 years 82
5.8 A1BCONT annual mean values comparison for 21m, PT and 21f time periods. 98
5.9 Assessment of GCMs related uncertainties: precipitation, air temperature and total runoff. 103
5.10 Assessment of GCMs related uncertainties: evaporation, catchment deficit and LR's water content 108
5.11 Assessment of downscaling techniques related uncertainties: precipitation, air temperature and total runoff. 111

5.12 Assessment of downscaling techniques related uncertainties: evaporation, catchment deficit and LR's water content. 111
5.13 Assessment of GHGs emission scenarios related uncertainties: precipitation, air temperature and total runoff. 117
5.14 Assessment of GHGs emission scenarios related uncertainties: evaporation, catchment deficit and LR's water content 117

6.1 Climate change impacts on precipitation, air temperature and total runoff. 122
6.2 Climate change impacts on evaporation, catchment deficit and linear reservoir water content 128

Parte I

Estratto sintetico in Italiano

0.1 Introduzione

0.1.1 Contesto

Le recenti recenti pubblicazioni del Comitato Intergovernativo per i Cambiamenti Climatici[1] (IPCC-AR4 2007) affermano che "il riscaldamento del sistema climatico è inequivocabile" ed individuano nelle emissioni di Gas ad Effetto Serra ed aerosol una delle cause principali di tale riscaldamento globale.

Le ultime proiezioni dell'IPCC indicano che il riscaldamento medio globale alla superficie sarebbe compreso tra 1.5 e 6 °C alla fine del ventunesimo secolo. Tuttavia, sulle proiezioni di cambiamento climatico gravano incertezze legate ai modelli climatici utilizzati. Tali incertezze crescono passando da una scala globale ad una regionale, in particolare per tutte le variabili del ciclo idrologico.

Riguardo l'andamento delle precipitazioni in Europa, le proiezioni indicano un incremento delle stesse sull'Europa del Nord ed una riduzione sull'Europa Meridionale. La posizione della linea di separazione tra queste due aree oscilla a seconda del prescelto scenario di cambiamento climatico (Giorgi et al. 2004) ma, ad ogni modo, tale linea attraversa la Francia e il bacino idrografico della Senna si trova molto vicino ad essa.

Cambiamenti nel clima possono condurre a numerosi impatti sui sistemi fluviali e sulle risorse idriche. Ad esempio, un effetto previsto del cambiamento climatico in atto è che, in Europa, la frequenza degli eventi climatici estremi (siccità prolungate, esondazioni...) aumenti (Bates et al. 2008). Dal momento che l'acqua è un elemento essenziale per gli insediamenti umani sia in termini di risorse, che di rischio e vulnerabilità, gli impatti dei cambiamenti climatici sul ciclo idrologico sono l'oggetto di una ricerca attiva e crescente.

Il bacino idrografico della Senna copre una superficie di 78600 km^2 (a monte di Le Havre) che equivale al 14 % della Francia continentale. Tale area contiene 17 milioni di abitanti (circa 25 % della popolazione francese) con circa 10 milioni di persone nella sola agglomerazione parigina. Il 40 % delle attività industriali francesi è situato all'interno del bacino idrografico della Senna le cui acque sono ampiamente utilizzate per l'approvigionamento idrico, il raffreddamento di centrali termoelettriche e nucleari, l'industria e l'agricoltura. Una preoccupazione costante è stata la prevenzione delle piene fluviali, in particolare dal momento che le piene catastrofiche del 1910, 1955 e 2001 causarono ampi danni alla città di Parigi.

Sia la comunità scientifica che i decisori francesi concordano sulla primaria importanza del determinare gli impatti dei cambiamenti climatici su di un'area particolarmente strategica per la Francia come il bacino idrografico della Senna. Proprio

[1]IPCC : Intergovernmental Panel on Climate Change

a questo scopo venne avviato nel 2002 il progetto di ricerca GICC-Seine. Si trattava di un importante progetto di ricerca avente per tema "L'influenza dei cambiamenti climatici sul comportamento idrologico e bio-geochimico del bacino idrografico della Senna". Le istituzioni principali che partecipavano al progetto erano l'Università Pierre et Marie Curie (UPMC), il Centre National de la Recherche Scientifique (CNRS), l'Institut National de la Recherche Agronomique (INRA) e l'Ecole Nationale du Genie Rural des Eaux et des Forets (ENGREF). Il progetto GICC-Seine si è concluso nel 2004 (Ducharne et al. 2007 e Ducharne et al. 2004).

Il progetto GICC-Seine era parte del più ampio programma di ricerca francese GICC (Gestione e Impatti dei Cambiamenti Climatici). Il programma GICC è gestito dal Ministero francese dell'Ecologia e dello Sviluppo Sostenibile[2] in collaborazione stretta con la Missione inter-ministeriale sull'effetto serra[3]. Il programma GICC ha come missione di promuovere e sviluppare la ricerca scientifica riguardo agli impatti dei cambiamenti climatici e ai loro meccanismi fisici associati. L'obiettivo principale è quello di avere a disposizione argomentazioni scientifiche solide da utilizzare per ottimizzare le strategie di prevenzione e mitigazione degli impatti dei cambiamenti climatici.

Nell'ambito del programma GICC, venne avviato nel 2007 un nuovo progetto di ricerca sugli impatti dei cambiamenti climatici sul bacino idrografico della Senna. Si tratta del progetto REXHYSS ("Impact du changement climatique sur les Ressources en Eau et les Extrêmes Hydrologiques dans les bassins de la Seine et la Somme") descritto al paragrafo successivo. La presente tesi di laurea è stata realizzata nell'ambito di tale progetto di ricerca presso l'Unità Mista di Ricerca UMR Sysiphe[4] sotto la supervisione della D.ssa Agnès Ducharne[5].

0.1.2 Il progetto REXHYSS

Lo scopo del progetto REXHYSS è di valutare l'impatto dei cambiamenti climatici sugli eventi idrologici estremi nei bacini idrografici della Senna e della Somme. Il progetto beneficia dei progressi recenti nel campo delle tecniche di downscaling statistico degli scenari di clima prodotti dai modelli climatici. In particolare l'uso

[2]Ministère de l'Ecologie et du Développement Durable (MEDD), in francese)

[3]Mission Interministérielle de l'Effet de Serre (MIES), in francese

[4]L'Unité Mixte de Recherche Sisyphe è un centro di ricerca comune al Centre National de la Recherche Scientifique (CNRS), all'Université Pierre et Marie Curie (UPMC) e all'Ecole Nationale Supérieure des Mines de Paris (ENSMP).

[5]Dr. Agnès Ducharne, UMR Sysiphe, UPMC Case 105, 4 place Jussieu, 75252 Paris cedex 05, France ; agnes.ducharne@upmc.fr

della tecnica del Weather Regime Approach (Boé et al. 2006) e del Variable Correction Method (Déque 2007) permette di valutare le modificazioni della variabilità climatica a varie scale temporali, dalla scala giornaliera alla scala inter-annuale, oltre alla determinazione di un "impatto medio" dei cambiamenti climatici già realizzato in studi precedenti.

Il progetto REXHYSS si propone di caratterizzare quale sarà l'impatto dei cambiamenti climatici in termini di frequenza ed intensità degli eventi estremi (ad esempio eventi di piena, eventi di magra e siccità prolungate) utilizzando i classici metodi statistici. I dati richiesti per queste analisi sono le portate, l'umidità del suolo e le quote piezometriche prodotte da una serie di modelli idrologici che rappresentano la ricca diversità dello stato dell'arte nel campo. Il progetto si propone anche di caratterizzare le modifiche dell'estensione delle aree soggette ad esondazioni in alcune zone chiave dei bacini idrografici della Senna e della Somme per alcuni tempi di ritorno caratteristici. Inoltre verrano anche trattate le interazioni tra il sistema fluviale e l'agricoltura in materia di irrigazione, di produzione agricola e di inquinamento da nitrati utilizzando il modello accoppiato STICS-MODCOU.

Entrando maggiormente nei dettagli, il progetto REXHYSS si articola in 6 fasi di lavoro:

1. **Scenari di cambiamento climatico e downscaling:** in questa fase si producono e portano alla scala locale, attraverso techniche di downscaling, le variabili climatiche da fornire ai modelli idrologici utilizzati nella fase 2.

2. **Modellazione idrologica:** si realizza una analisi multi-modello utilizzando vari modelli idrologici basati su principi molto diversi tra loro. Tre tipi di modelli sono utilizzati: un modello concettuale e concentrato (GR4J: Perrin et al. 2003), due modelli idrogeologici distribuiti (MARTHE: Thiéry 1990; MODCOU: Ledoux et al. 1989) e 2 modelli distribuiti a base fisica di tipo Land Surface Model (CLSM: Koster et al. 2000 e Ducharne et al. 2000 ; SIM: Habets et al. 1999).

3. **Analisi statistica:** le variabili prodotte dai modelli idrologici saranno analizzate statisticamente con un approcio di tipo portata-durata-frequenza [6] (Javelle 2001 e Sauquet et al. 2003).

4. **Esondazioni:** dato un tempo di ritorno (per esempio 10 anni), gli idrogrammi prodotti nella fase 3 saranno inseriti in un modello idraulico numerico al fine di ottenere le altezze idriche e l'estensione delle aree di esondazione in alcuni zone strategiche del reticolo idrografico.

[6] Approche Qdf : débits - durée - fréquence.

5. **Agricoltura, irrigazione e inquinamento da nitrati:** date le modificazioni nel clima e nella disponibilità di risorse idriche, questa fase di lavoro quantificherà gli impatti sulle pratiche colturali, sui bisogni in irrigazione e fornirà indicazioni sulle ulteriori modificazioni nella disponibilità idrica causate dai cambiamenti nelle pratiche colturali. Questa fase sarà realizzata utilizzando il modello accoppiato idrologico ed agronomico STICS-MODCOU (Gomez et al. 2003).

6. **Interazioni con gli attori di bacino:** quest'ultima fase del progetto si interessa alle interazioni tra le modifiche nei sistemi fluviali e i sistemi sociali. I risultati ottenuti nelle fasi di lavoro precedenti saranno comunicati a tutti gli attori della gestione dell'acqua nei due bacini idrografici considerati. Lo scopo è quello di giungere ad una valutazione socio-economica dei cambiamenti nella frequenza e intensità degli eventi estremi. Tra le molte questioni sensibili vi sono, ad esempio, il drenaggio urbano delle acque a seguito di eventi di pioggia intensa o l'impatto delle esondazioni sulle infrastrutture, sui trasporti o sulla produzione elettrica. Quest'ultima fase del progetto beneficierà dell'interazione con enti "operativi" come Electricité de France (EDF), il Centre Scientifique et Technique du Batiment[7] (CSTB) e il comune di Parigi.

0.1.3 Obiettivi del presente studio

La presente tesi di laurea è stata realizzata presso l'UMR Sisyphe (CNRS - Université Pierre et Marie Curie, Parigi) sotto la supervisione della D.ssa Agnès Ducharne nell'ambito del progetto di ricerca REXHYSS. In particolare il presente studio si colloca nella fase 2 descritta precedentemente: *modellazione idrologica*.

L'argomento dello studio è la "Modellazione idrologica degli impatti dei cambiamenti climatici sul bacino idrografico della Senna tramite il modello Catchment based Land Surface Model (CLSM)" (Koster et al. 2000 e Ducharne et al. 2000). Avendo disponibili i dati climatici alla scala locale e utilizzando il modello CLSM già precedentemente tarato sul bacino idrografico della Senna, la presente tesi si propone di:

- Realizzare la validazione del modello CLSM, confrontando le portate simulate e osservate (sezione 4.4).

- Analizzare la sensibilità del modello CLSM rispetto a 6 versioni ("runs") dello stesso, aventi parametri tarati diversamente (sezione 4.5).

[7]EDF and CSTB partecipano entrambi al progetto GICC-IMFREX: "Impact des changements anthropiques sur la frequence des phénomènes Extremes de vent, de température et de précipitation".

- Realizzare la validazione degli scenari di cambiamento climatico confrontandoli, relativamente al periodo 1982-2000, alle simulazioni realizzate con dataset climatici basati sulle osservazioni[8] (sezione 5.3).

- Discutere gli impatti dei cambiamenti climatici sul bacino idrografico della Senna, analizzando le principali variabili idrologiche in termini di trend annuali, di ciclo medio annuale e di funzioni empiriche di ripartizione (sezione 5.4).

- Valutare le incertezze associate agli impatti e dovute ai vari elementi della catena di modelli usata per produrre gli scenari di cambiamento climatico: i modelli globali di circolazione (GCM: General Circulation Model), le techniche di downscaling e gli scenari di emissione di Gas ad Effetto Serra (GHGs: GreenHouse Gases). Queste analisi sono presentate rispettivamente alle sezioni 5.5, 5.6 e 5.7.

I risultati presentati in questa tesi saranno usati nell'analisi multi-modello della fase 2 di REXHYSS e nelle fasi successive del progetto. La realizzazione di questa tesi ha beneficiato di una grande quantità di dati prodotti da altri centri di ricerca e di un vasto lavoro di sviluppo e ottimizzazione del modello CLSM realizzato da altri ricercatori. Nelle prossime sottosezioni verrà descritto il lavoro svolto dall'autore, evidenziando pure le contribuzioni esterne di cui egli ha beneficiato.

0.2 Gli scenari di cambiamento climatico

I dataset climatici necessari come dato in ingresso per i modelli idrologici utilizzati per determinare gli impatti dei cambiamenti climatici sono prodotti attraverso una sequenza di modelli composta di tre fasi principali: la scelta di uno scenario di emissione di Gas ad Effetto Serra tra quelli prodotti dal IPCC nel rapporto speciale sugli scenari di emissione (SRES: Nakinovic and Swart 2000), un modello climatico di circolazione generale (GCM) e una tecnica di downscaling richiesta per trasferire i dataset climatici dalla grande scala dei GCMs alla risoluzione fine richiesta dai modelli idrologici.

Alle previsioni di clima futuro sono associate delle incertezze causate da ognuna delle tre fasi sopra elencate. La strategia consigliata, nell'ambito delle ricerche sui cambiamenti climatici, per considerare tali incertezze è quella di utilizzare un approccio multi-scenario. Nella presente tesi, sono stati quindi adottati 11 dataset climatici differenti come dati in ingresso per il modello idrologico CLSM. Tali dataset,

[8]In particolare ci siamo avvalsi per questo studio dei dataset SAFRAN (Durand et al. 1993) e ERA-40 (Uppala et al. 2005).

prodotti al CERFACS [9] e al CNRM[10] differivano gli uni dagli altri per lo scenario di emissione di Gas ad Effetto Serra (9 simulazioni basate sullo scenario A1B e 2 simulazioni basate sullo scenario A2), per il modello di circolazione generale (7 modelli GCM "classici" e 2 versioni diverse di un modello di circolazione a risoluzione variabile ARPEGE Climat, Gibelin and Déque 2003) e per la tecnica di downscaling (9 scenari basati sul Weather Regime Approach, Boé et al. 2006 e 2 scenari basati sul Variable Correction Method, Déque 2007).

Il capitolo 2 è dedicato alla descrizione delle tre fasi di cui sopra. La sezione 5.1 fornisce invece i dettagli sugli 11 scenari climatici utilizzati nel presente studio.

0.3 Il modello idrologico CLSM

Il modello CLSM è un modello idrologico distribuito a base fisica di tipo Land Surface Model. I Land Surface Models (LSMs) hanno come scopo di rappresentare i processi fisici che avvengono all'interfaccia tra il Suolo, la Vegetazione e l'Atmosfera. CLSM risolve le equazioni del bilancio idrico ed energetico, accoppiate tramite il flusso di calore latente. CLSM richiede come variabili in ingresso la precipitazione, la radiazione incidente ad onda lunga e ad onda corta, la temperatura dell'aria, l'umidità a 2m d'altezza e la velocità del vento a 10 m d'altezza. Tali variabili costituiscono il dataset climatico prodotto con la sequenza di modelli descritta precedentemente.

Il modello CLSM (Koster et al. 2000 e Ducharne et al. 2000) è particolarmente innovativo per due ragioni:

- Innanzitutto, la forma del Land Surface Element è il bacino idrografico unitario definito da frontiere topografiche, anzichè essere di forma rettangolare, funzione della risoluzione del dataset climatico che lo alimenta, come avviene in gran parte dei Land Surface Models.

- Inoltre, all'interno di ogni bacino idrografico unitario, CLSM si basa sui concetti di TOPMODEL (Beven and Kirkby 1979) per ottenere la distribuzione di umidità del suolo nella "root zone" e per permettere la separazione del bacino in aree sature, insature e sottoposte a stress idrico, descrivendo in tale modo l'eterogeneità spaziale della distribuzione dell'umidità del suolo.

Nell'ambito della presente tesi è stata utilizzata una versione recente di CLSM (Gascoin et al. 2008) che integra anche un serbatoio lineare profondo, con lo scopo di simulare meglio il comportamento di bacini idrografici in cui vi è una forte rilevanza

[9] Centre Européen de Recherche et de Formation en Calcul Scientifique - Toulouse, France

[10] Centre National de Recherche Meteorologique - Meteo France, Toulouse, France

del deflusso di base derivante dagli acquiferi profondi, come avviene in parte nel bacino idrografico della Senna.

Il capitolo 3 descrive il modello CLSM e CLSM-LR[11] (sezioni 3.2 e 3.3) dopo aver contestualizzato CLSM rispetto allo stato dell'arte dei Land Surface Model (sezione 3.1).

0.4 Modellazione del bacino idrografico della Senna

Il bacino idrografico della Senna copre 78600 km^2 (a Le Havre), il 14 % della Francia continentale. Si tratta di un bacino molto omogeneo da molti punti di vista (geologia, altimetria...). L'altitudine media è 160 m e meno dell'1% della superficie del bacino è situata a più di 500 m di altitudine. Il punto più alto si trova a 900 m. La Senna e i suoi tributari hanno pendenze ridotte (tra 0,01 e 0,02 m / 100 m) e scorrono quasi tutti da Est verso Ovest. La Senna sfocia nel canale della Manica presso Le Havre dopo un percorso lungo 776 km. Tuttavia nell'ambito di questa tesi, limiteremo il nostro studio al bacino idrografico situato a monte di Poses (160 km a monte di Le Havre) poichè a valle di tale sezione inizia l'area dell'estuario con acque salmastre e influenza idrodinamica da parte della marea (figura 4.1).

Le portate dei corsi d'acqua all'interno del bacino idrografico della Senna sono ben regolate per vari motivi:

- le precipitazioni sono ben distribuite nell'arco dell'anno con un regime idrologico di tipo oceanico,
- vi sono numerose formazioni geologiche di tipo sedimentario che hanno buone proprietà di ritenzione idrica,
- una parte importante delle portate provviene dal deflusso di base degli acquiferi profondi.

Un ulteriore capacità di regolazione è data dalla presenza di tre dighe di ritenuta sulla Marne, sull'Aube e sulla Senna, circa 200 km a monte di Parigi (vedi sezione 4.2). Una descrizione più ampia del bacino idrografico oggetto di studio è fornita alla sezione 4.1.

Il modello CLSM descrive il bacino idrografico della Senna a monte di Poses tramite 29 bacini unitari con un'area media di 2600 km^2. Il modello CLSM fornisce

[11]CLSM-LR: CLSM con serbatoio lineare.

le variabili in uscita (deflusso totale, evaporazione, umidità del suolo...) come medie spaziali dei valori giornalieri su di un bacino unitario.

CLSM si avvale di numerosi dati sperimentali per caratterizzare la zona di studio (vedi sezione 4.3.3). In particolare viene usato un modello digitale del terreno (risoluzione di 100 m) e la base dati ECOCLIMAP (Masson et al. 2003) specificamente pensata per i Land Surface Model. Da ECOCLIMAP vengono presi i dati riguardanti la vegetazione e alcuni parametri morfologici del suolo associati alla vegetazione alla scala temporale mensile. ECOCLIMAP contiene inoltre dati riguardanti il contenuto di sabbia ed argilla nel suolo, in base ai quali è possibile classificare il suolo in classi a cui associare poi caratteristiche idrauliche sulla base di quanto indicato da Cosby et al. (1984).

Cinque parametri sono oggetto di taratura poichè non è possibile assegnare loro un valore a priori: la conduttività idraulica a saturazione, la profondità del "bedrock depth" di TOPMODEL, il parametro ν di decadimento esponenziale della conduttività idraulica, il valore del catchment deficit massimo fino a cui avviene la ricarica del serbatoio lineare profondo ed infine la costante di tempo τ_G che regola la ricarica del serbatoio lineare. La taratura di CLSM è stata effettuata in passato nell'ambito del progetto GICC-Seine utilizzando il dataset SAFRAN sul periodo 1985-1991. Dato che all'epoca non era già stato implementato un modello di propagazione, la taratura era stata realizzata confrontando le medie su 10 giorni (Ducharne et al. 2004).

A seguito di recenti lavori all'UMR Sisyphe (Zhao 2006 e Bellier 2008), è stato associato al modello CLSM un modello di propagazione di tipo Muskingum (vedi sezione 4.3.1) di cui ci si è avvalsi nell'ambito del presente studio.

L'uso di un modello di propagazione ha reso possibile la validazione del modello sul periodo 1981-2002, confrontando portate giornaliere simulate ed osservate. Tale validazione è stata realizzata su 6 runs diversi di CLSM che si sono mostrati equivalenti in termini di corretta simulazione delle portate osservate (vedi sezione 4.4).

Si tratta di un tipica situazione di "equifinality" secondo la definizione di Beven (2006). Nell'ambito del presente studio si sono testati 6 "runs" di CLSM diversamente tarati sia su di una simulazione in tempo storico alimentata dal dataset climatico SAFRAN basato su osservazioni (sezione 4.5.1) sia su di una simulazione di cambiamento climatico in tempo futuro (sezione 4.5.2). Gli impatti del cambiamento climatico si sono rivelati poco sensibili alla scelta del run di CLSM, perciò un run tra i 6 testati è stato scelto e tutte le ulteriori simulazioni di cambiamento climatico (capitolo 5) sono state realizzate utilizzando quel run.

0.5 Impatti del cambiamento climatico

Gli impatti simulati con il run prescelto di CLSM sono ampiamente descritti ed analizzati al capitolo 5. Innanzitutto è stato realizzato un test circa le scelte di inizializzazione sulle simulazioni di cambiamento climatico disponibili in periodi di tempo discontinui (time-slices): sezione 5.2.

In seguito si è realizzata la validazione degli 11 scenari di cambiamento climatico rispetto alle osservazioni disponibili sul periodo 1982-2000 (dataset SAFRAN): sezione 5.3. In tale fase lo scenario Arpv4-VCM prodotto con la tecnica di downscaling del Variable Correction Method ha mostrato ampi errori rispetto alla simulazione basata sulle osservazioni SAFRAN mentre gli altri scenari si sono rivelati abbastanza simili a SAFRAN.

Avendo a disposizione uno scenario di cambiamento climatico continuo (1950-2100), si sono analizzati in dettaglio gli impatti simulati da esso, valutati su finestre temporali di 25 anni (sezione 5.4). Tali impatti sono stati analizzati sia in termini di ciclo annuale medio che di distribuzione empirica di probabilità.

In seguito sono state valutate le incertezze legate alla sequenza di modelli utilizzati per la produzione dei dataset climatici, analizzando e confrontando gli 11 scenari di cambiamento climatico a disposizione. La sezione 5.5 analizza 8 scenari prodotti da 8 modelli di circolazione generale diversi ma basati tutti sullo scenario di emissione A1B e sulla tecnica di downscaling del Weather Regime Approach. Le sezioni 5.6 e 5.7 sono dedicate invece alle incertezze legate alla scelta rispettivamente della tecnica di downscaling o dello scenario di emissione di gas ad effetto serra.

Tutte le analisi sono concordi nel mostrare una riduzione notevole e robusta del deflusso totale in seguito al cambiamento climatico. Tale riduzione dimezza quasi il valore del deflusso totale medio nel periodo 2081-2099 rispetto al valore relativo al 1982-2000 (si veda la figura 6.3). La riduzione del deflusso totale è particolarmente netta ed importante nei mesi primaverili ed estivi (figura 6.1).

Parimenti, anche gli impatti sull'umidità del suolo (catchment deficit) e sul contenuto d'acqua nel serbatoio lineare (figura 6.4) mostrano uno scenario futuro caratterizzato da una forte riduzione dell'umidità del suolo (netto aumento del catchment deficit di CLSM) e da una forte riduzione del contributo del serbatoio lineare profondo al deflusso totale. Infatti un'umidità del suolo fortemente ridotta implica una riduzione della ricarica al serbatoio lineare di CLSM, ossia agli acquiferi profondi rappresentati in CLSM come un serbatoio lineare.

0.6 Conclusione

I risultati della presente tesi di laurea saranno utilizzati nell'ambito del progetto REXHYSS. I dati in uscita verrano utilizzati per realizzare un'analisi comparativa tra i vari modelli idrologici (fase 2 di REXHYSS). Inoltre le portate verranno analizzate statisticamente presso il CEMAGREF[12] di Lyon utilizzando un approccio di tipo portata-durata-frequenza (Javelle 2001 e Sauquet et al. 2003) così da quantificare gli impatti dei cambiamenti climatici in termini di eventi estremi (siccità, esondazioni...).

Il riscaldamento globale di origine antropica e i cambiamenti climatici ad esso connessi sono fatti ampiamente accettati e confermati. Tuttavia sono ancora blande le iniziative di riduzione delle emissioni di gas ad effetto serra e di mitigazione dei cambiamenti climatici messe in atto dai decisori e dai cittadini. Questo è dovuto in parte anche al fatto che essi difficilmente comprendono il legame esistente tra cambiamenti climatici alla scala globale e gli impatti sulla vita quotidiana di ognuno alla scala locale. Perciò, la Ricerca sugli impatti dei cambiamenti climatici deve svolgere il ruolo essenziale di rendere comprensibili, ai cittadini e ai decisori, gli impatti alla scala locale del riscaldamento globale.

Gli impatti dei cambiamenti climatici, quantificati nella presente tesi ed ulteriormente approfonditi nelle fasi successive del progetto REXHYSS, saranno molto utili a tutti gli attori e decisori che hanno un ruolo nella gestione del bacino idrografico della Senna. Vi è la speranza, inoltre, che la previsione di impatti importanti (per non dire catastrofici) e robusti sulle grandezze idrologiche del bacino idrografico della Senna induca i decisori politici francesi non solo ad adottare politiche di adattamento ai nuovi scenari ma anche (e soprattutto) politiche globali di mitigazione e riduzione delle emissioni di gas ad effetto serra.

[12]Il Cemagref è un ente pubblico di ricerca francese che si propone di ottenere risultati direttamente utilizzabili operativamente nella gestione del territorio e delle risorse idriche.

Part II

Modeling climate change impacts on the Seine River basin hydrology

Chapter 1

Introduction

1.1 Context

Major climate change as a result of anthropogenic emission of green-house gases (GHGs) is now widely accepted. Recent projections by the Intergovernmental Panel on Climate Change (IPCC) indicate that global mean surface temperature will increase by 1.5°C to 6°C by the end of the 21st century with increased uncertainties at the regional scale, especially regarding the water cycle (IPCC, Fourth Assessment Report IPCC-AR4 2007).

Concerning precipitations, projections are of an increase over Northern Europe and of a reduction at the South of Europe. The climate divide between these two areas crosses over France and oscillates depending on the climate change scenario (Giorgi, Bi, and Pal 2004). Anyway, the Seine river catchment, which is the field of study of this thesis, is very close to this edge.

Changes in climate imply impacts on river systems and hydrology such as changes in river flow or groundwater storage. For example, extreme hydrological events such as floods and droughts would increase their frequency over Europe (Bates et al. 2008). Because of the importance of water for human settlement in terms of resource and risk factors, climate change impacts on the water cycle are the object of growing active research.

The Seine River catchment covers 78600 km^2 (at Le Havre), that is 14 % of the surface of continental France. This area contains 17 millions of inhabitants (25 % of the national population) with 10 millions in the single agglomeration of Paris. 40% of the national industrial activities are located within the Seine river catchment. The Seine is largely used for water supply, power plants cooling, industry and agriculture. Moreover, there is a major concern on flood occurence since the events of 1910, 1955 and 2001 damaged rather largely Paris.

Both French policymakers and scientists agree of the primary importance of ascertaining what will be the impacts of climate change over such a strategic area of the country. That is how the GICC-Seine research project took place in 2002-2004. GICC-Seine was an important research project focused on the "Influence of climate change on hydrological and bio-geochemical behavior of the Seine river catchment". Main partners of the GICC-Seine project were the "Université Pierre et Marie Curie" (UPMC), the "Centre National de la Recherche Scientifique" (CNRS), the "Institut National de la Recherche Agronomique (INRA) and the Ecole Nationale du Genie Rural, des Eaux et des Forets (ENGREF). GICC-Seine project was concluded in 2004 (Ducharne et al. 2007 and Ducharne et al. 2004).

GICC-Seine was part of GICC, a larger French research program which is focused on the: "Management and Impacts of Climate Change" or "Gestion et Impacts du Changement Climatique (GICC)" in French. GICC is essentially managed by the

Ministry of Ecology and Sustainable Development[1] in close collaboration with the Inter-Ministerial Mission on Greenhouse Effect (Mission Interministérielle de l'Effet de Serre, MIES, in French). The mission of GICC is to promote and develop scientific research on identifying national 'Impacts of Climate Change' and associated physical mechanisms. The main objective, downstream, is to provide sound scientific arguments in order to participate in the tuning of adaptive tools and techniques. This will allow policy and decision makers from the public sector to optimize strategies for prevention and mitigation of those impacts.

In the framework of the GICC program too, the REXHYSS ("Impact du changement climatique sur les Ressources en Eau et les Extrêmes Hydrologiques dans les bassins de la Seine et la Somme") project started in 2007. This master's thesis was realised at the "UMR[2] Sysiphe"), under the supervision of Dr. Agnès Ducharne[3], as a part of the REXHYSS project.

1.2 The REXHYSS project

The aim of this project is to assess the impact of climate change on extreme hydrological events in the river basins of the Seine and Somme (France). The project will benefit from recent advances in the statistical downscaling of climate simulations. A weather regime approach and a variable correction approach allow to account for changes in climate variability at daily to inter-annual time scales, in addition to mean climate change considered in previous studies.

REXHYSS will characterize how climate change is susceptible to impact the distribution of extreme events, regarding high and low flows and droughts, using classical frequency analyses. The input are the discharge, soil moisture and piezometric heads simulated by a set of state-of-the-art hydrological models. The project will also focus on some manifestations of these extremes to which societies are particularly sensitive. Regarding floods, it will assess the changes in their extension in some key areas of the two basins (Somme valley upstream from Abbeville, Seine valley including Paris and the alluvial plain of the Bassée) and for selected return periods. It will also consider the relationships between agriculture and the river system, with respect to irrigation demand and its impact on water resources, crop production and nitrate pollution, which can be simulated by the coupled model

[1]Ministère de l'Ecologie et du Développement Durable, (MEDD, in French)

[2]The "Unité Mixte de Recherche Sisyphe" is a joint research unit between the Centre National de la Recherche Scientifique (CNRS), the Université Pierre et Marie Curie (UPMC) and the Ecole Nationale Supérieure des Mines de Paris (ENSMP).

[3]Dr. Agnès Ducharne, UMR Sysiphe, UPMC Case 105, 4 place Jussieu, 75252 Paris cedex 05, France ; agnes.ducharne@upmc.fr

STICS-MODCOU. When assessing how these processes and their feed-backs may be modified under climate change, it will distinguish the impact of mean climate vs. climate variability.

Specifically, the REXHYSS project is composed of 6 main work packages:

1. **Climate scenarios and downscaling:** this work package will produce, and downscale to a finer resolution, the climate forcings essential for "feeding" the hydrologic impact models of package 2.

2. **Hydrological models :** a multi-model analysis will be realised using various hydrological models very different for their conceptual assumptions. Three families of model will be used: a lumped conceptual model (GR4J, Perrin, Michel, and Andréassian 2003), two hydrogeological distributed models (MARTHE, Thiéry 1990; MODCOU, Ledoux, Girard, and de Marsily 1989) and two distributed Land Surface Models (CLSM, Koster et al. 2000 and Ducharne et al. 2000 ; SIM Habets et al. 1999).

3. **Frequential analysis :** outputs from the hydrological models will be statiscally analysed with a discharge-duration-frequency[4] approach which has been recently developed (Javelle 2001 and Sauquet, Javelle, and Le Clerc 2003).

4. **Floods :** given a return period (e.g. 10 years), hydrographs from step n°3 will be inserted in a hydraulical model in order to obtain the water heights and the extension of flood areas in some strategic points of the hydrographic network.

5. **Agriculture, irrigation and nitrate pollution:** given the changes in climate, water resources availability and in soil root zone moisture content, this work package will quantify impacts in terms of agricultural practices, irrigation needs and changes in water resources availability driven by modified irrigation practices. This will be done through the STICS-MODCOU coupled hydrogeological and agronomical model (Gomez et al. 2003).

6. **Interactions with all the stake holders:** this last part of the project addresses the feed-backs between the changes in rivers systems and social systems. Results will be communicated to all the actors of water management in the two studied watersheds. The aim is to obtain a a socio-economic assessment of the simulated changes in extreme hydrological events. Among the sensitive questions, one can find urban storm water effluents or the impacts of floods on infrastructures, transportation or energy production. This kind of

[4]Approche Qdf : débits - durée - fréquence.

analysis, although qualitative, is important to support adaptation strategies to climate change. This last step of the project will benefit from existing close relationships with operational institutions such as, among the others, Electricité de France (EDF), the Centre Scientifique et Technique du Bâtiment[5] (CSTB) and the Mairie de Paris[6].

1.3 Objectives of this thesis

This master's thesis was realised at UMR Sisyphe (CNRS - Université Pierre et Marie Curie, Paris) under the supervision of Dr. Agnès Ducharne in the framework of the Rexhyss project. More specifically, it is a part of the previously described "work package 2" of REXHYSS: hydrological modeling.

The subject of this master's thesis is the modeling of climate change impacts on the Seine river catchment using a Catchment Based Land Surface Model (CLSM) (Koster et al. 2000 and Ducharne et al. 2000). The results of this master's thesis will be used in the multi-model comparison of climate change impacts and in the other work packages within the REXHYSS project. Realising this thesis has benefited from a large amount of data produced by other research team and from a large amount of work realised previously by other researchers in developing and optimizing the CLSM model. In the next subsections it will be specified what has been done specifically by the autor and the original contributions brought within this master's thesis.

1.3.1 Climate change scenarios, general circulation models and downscaling

Climate forcings required as an input for hydrological models used in climate change impacts studies are produced through a complex modeling sequence composed of three main steps: the Green-House Gases (GHGs) emission scenario, the General Circulation Models (GCMs) and the Downscaling Technique required to transfer the climate forcings from the coarse resolution of GCMs to the finer one of hydrological impact models.

Uncertainties are pending on these predicted future climate scenarios due to each part of the modeling sequence. The recommended strategy for taking into account these uncertainties is to use a multi-scenario approach. In the present thesis, it

[5]EDF and CSTB both participate to the GICC-IMFREX project: "Impact des changements anthropique sur la frequence des phénomènes Extremes de vent, de température et de précipitation" that is Impact of anthropogenic change on frequency of extremes (wind, temperature and precipitation).

[6]Mairie de Paris: Municipality of Paris

meant using 11 climate forcings datasets, to feed the CLSM model. Each of the 11 scenarios is different from one another for the GHGs emission scenario, for the General Circulation Model (GCM) or for the downscaling technique.

Climate scenarios were selected and downscaled at the "Centre National de Recherche Meteorologique - Meteo France" (CNRM - Toulouse, France) and at the "Centre Européen de Recherche et de Formation en Calcul Scientifique" (CERFACS - Toulouse, France) in the framework of the Rexhyss project.

Chapter 2 makes the state of the art in the field of climate change scenarios predictions and analyses critically the modeling sequence employed for producing the various scenarios we used.

1.3.2 The CLSM model and the Seine river catchment

The Catchment Based Land Surface Model (CLSM) (Koster et al. 2000 and Ducharne et al. 2000) has been already calibrated and used for modeling climate change impacts on the Seine watershed within the GICC-Seine project (Ducharne et al. 2004 and Ducharne et al. 2007).

Within this thesis, a modified version of CLSM with an additional deep linear reservoir (CLSM-LR) has been used too (Gascoin et al. 2008).

Chapter 3 gives an overview of Land Surface Models and describes CLSM and CLSM-LR (with deep linear reservoir) models.

Until now and in particular when calibration of CLSM was realised, CLSM did not include any runoff routing procedure on the Seine river basin. Thus, runoff used to be compared to observed discharge over 10 days averages. In the last two years a Muskingum routing model for the Seine river basin was developed in the framework of two master's thesis at the Université Pierre et Marie Curie, Paris (Zhao 2006 and Bellier 2008).

Within this thesis, CLSM with Muskingum routing was used for producing daily discharges and for realising validation of CLSM on a longer period of time. The routing procedures was not used for producing mean annual trends and annual mean cycle. It was instead very useful for realising validation of the model and for analysing results in terms of empirical probability distributions.

In the calibration previously realised, 6 parameter datasets gave very similar performances over the calibration period (1985-1991). Within this thesis, we realised a validation of these 6 runs of CLSM (with routing) obtaining similar and equally acceptable performances over the validation period (1982-2002). This is a typical case of "equifinality" (Beven 2006) which opens an essential question in climate change impact studies: how do the six runs "equifinal" in calibration behave in future time? What is the range of variation of the simulated impacts using these six runs? To discuss this issue, we realised a 150 years long climate change driven

simulation with these 6 runs of CLSM to discuss the issue of equifinality of CLSM calibration datasets in predicting climate change impacts.

Chapter 4 after shortly describing the Seine river catchment and the non-meteorological data used within this thesis, is focused on the discussion of the validation and of the "equifinality" issues.

1.3.3 Climate Change Impacts

The key part of this thesis's work is presented in chapter 5. The chapter is focused on the analysis of climate change impacts through a multi-scenario approach (11 climate change scenarios) and on the assessment of uncertainties associated to these predicted impacts.

First (§ 5.2), a test is made, concerning the impact of initialisation choices on climate change simulations available on time-slices mode (due to high computational costs, climate scenarios are usually produced only for selected periods of time which are called "time-slices").

Secondly, an assessment of the 11 climate change scenarios ability to represent historical climate is realised (§ 5.3).

We have available a continuous climate change simulation over the 1950-2100 time period, we chose this simulation as the "reference climate change simulation" and realised a detailed analysis of its results and impacts (§ 5.4).

Then uncertainties related to the various part of the modeling sequence (GHGs emission scenario, GCMs and downscaling technique) which produces the climate forcings are analysed and quantified (§ 5.5, 5.6 and 5.7).

A synthesis of the projected impacts and uncertainties is given in § 6.2.

Chapter 2

Climate change scenarios

Future climate on a local scale is the main input for modeling climate change impacts on hydrology. In this chapter we will describe shortly how these future climate forcings necessary for hydrological models are produced. Specifically we will focus our attention on how the climate forcings used within this thesis have been built.

A three main step modeling sequence is required to produce climate forcings required at a local scale by local impact models. The modeling sequence is described in figure 2.1 and in figure 2.2.

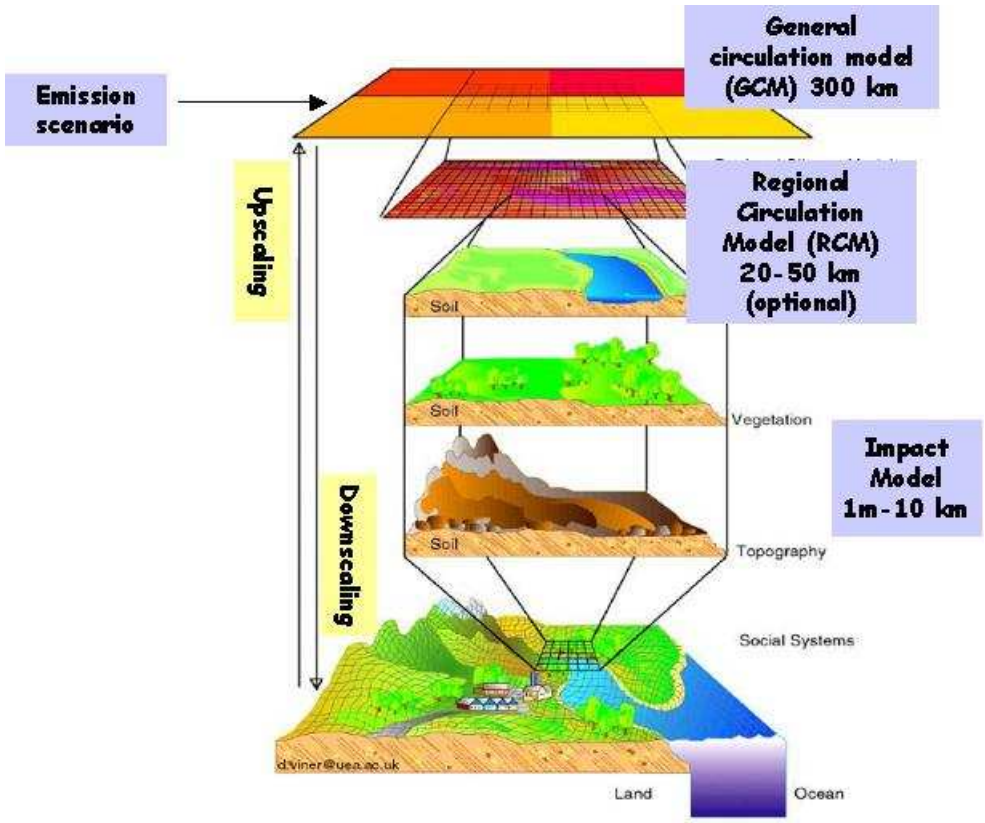

Figure 2.1: Representation of the chain of models used for climate change impact studies, source : CRU, University of East Anglia

The first step is the choice of one or more emission scenarios from the Intergovernmental Panel on Climate Change(IPCC). Some directions concerning this choice are given in §2.1. Once an emission scenario has been chosen, a general circulation model (GCM) is used to predict future climate on a global scale (§2.2). Last but not least an appropriate downscaling technique (§2.3) is used to transform data from the coarse resolution of GCM to the fine scale required by hydrological models.

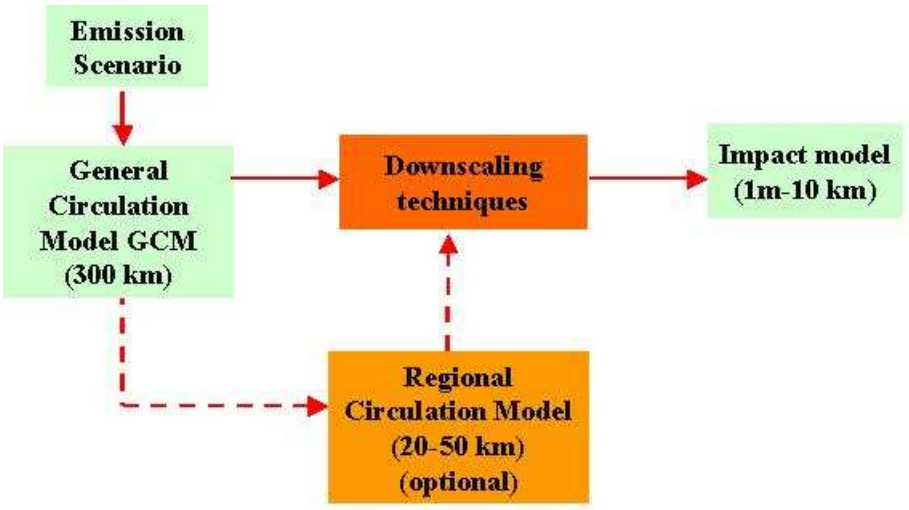

Figure 2.2: **Block diagram of the chain modeling process used for climate change impact studies**

2.1 Emission scenarios

IPCC stated in the Fourth Assessment Report (IPCC-AR4 2007) that:

> There is high agreement and much evidence that with current climate change mitigation policies and related sutainable development practices, global GHG emission will continue to grow over the next few decades.

Emitting this statement has been possible thanks to green house gases (GHGs) emission scenarios produced by the Intergovernmental Panel on Climate Change(IPCC) and published in the Special Report on Emission Scenarios (Nakinovic and Swart 2000) which is part of the IPCC Third Assessment Report (2001).

All the SRES emission scenarios are based on the following assumptions:

- The scenarios do not include additional climate initiatives and do not explictly assume implementation of the United Nations Framework Convention on Climate Change (UNFCCC) or the emission targets of the Kyoto Protocol. Thus all scenarios are "in absence of additional climate policies". However GHG emissions are directly affected by non-climate change policies concerning (demographic change, social and economic development, technological change, ressource use and pollution management).

- The main forces of future GHG trajectories are and will continue to be : demographic change social and economic development and the rate and direction of technological change.

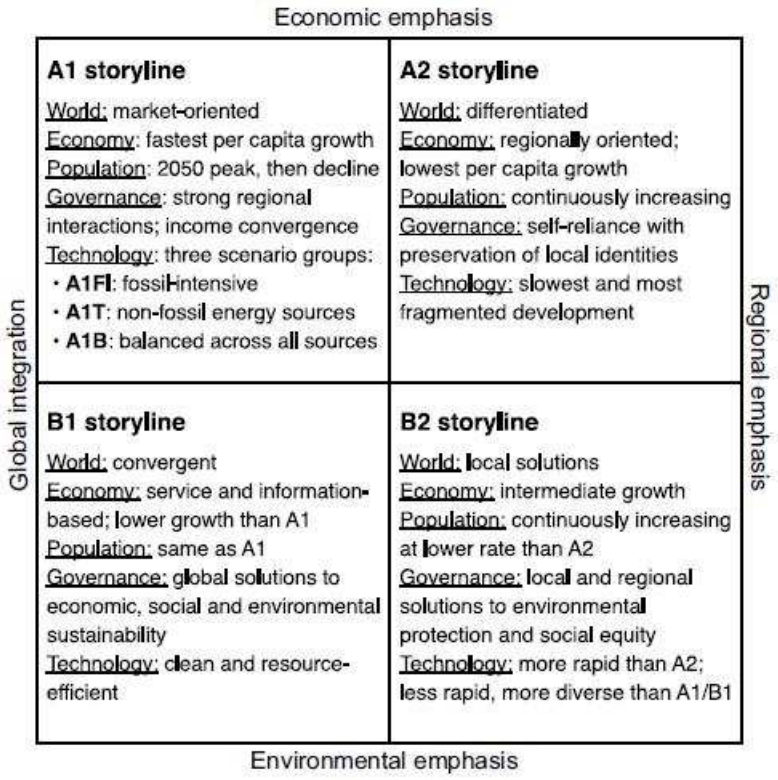

Figure 2.3: Characteristics of the four SRES storylines, source: (Bates et al. 2008)

The four IPCC SRES storylines (see in figure 2.3), which form the basis for many studies on projected climate change and related impacts on hydrology, consider a range of plausible changes in population and economic activity over the 21^{st} century:

A1: It describes a world of very rapid economic growth, global population that peaks in mid-century and declines thereafter, rapid introduction of new and more efficient technologies, convergence among regions and reduction in regional differences in per capita income. A1B scenario is distinguished by a "balanced" energy related technological change which means *not relying too heavily on one particular energy source, with similar improvement rates applied to all energy supply and end use technologies* (Nakinovic and Swart 2000). Scenarios A1Fl (fossil fuel intensive) and A1T (predominantly non fossil fuel) are much less used by scientific community for impact studies.

A2: This scenario describes a very heterogeneous world where self-reliance and preservation of local identities are predominant. There is a continously increasing global population. Economic development is mainly regional. Economic growth and technological change is slower and more fragmented than in other

storylines.

B1: There is the same population trend as in A1 storyline but with a very rapid changes toward a service and intormation economy with lower material-intensity and clean and ressource efficient technologies. There is en emphasis on global solutions to sustainability and equity.

B2: Emphasis is on local solutions to economic, social and environmental sustainability. Population increases continously but at a slower rate than in A2 storyline.

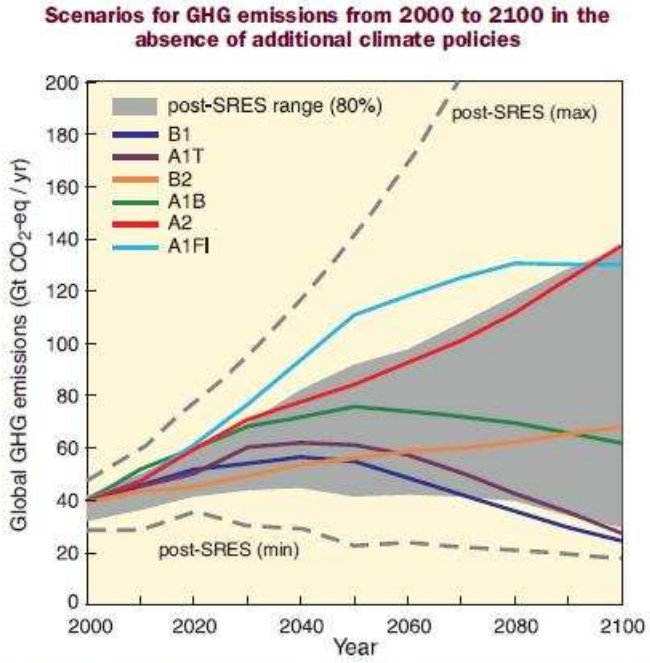

Figure 3.1. Global GHG emissions (in GtCO$_2$-eq per year) in the absence of additional climate policies: six illustrative SRES marker scenarios (coloured lines) and 80th percentile range of recent scenarios published since SRES (post-SRES) (gray shaded area). Dashed lines show the full range of post-SRES scenarios. The emissions include CO$_2$, CH$_4$, N$_2$O and F-gases. {WGIII 1.3, 3.2, Figure SPM.4}

Figure 2.4: Global GHG emission, source: (IPCC-AR4 2007)

The 4 storylines described above and summarized in figure 2.3 produce a CO_2 emission scenarios represented in figure 2.4. Depending on the chosen scenario there are large differences in the predicted CO_2 emission values. In the framework of the REXHYSS project climate change scenarios used for the present thesis have been produced under A1B and A2 emission scenarios. This GHGs emission scenario choice is common practice in climate change research since B1 and B2 scenarios seem

unrealistically optimistic due to the weakness of current climate change mitigation policies.

Differences between simulated impacts under A1B and A2 GHGs emission scenarios are discussed in § 5.7.

2.2 General Circulation Model

After choosing a GHG emission scenario, a general circulation model (GCM) gives predictions on future climate. It transforms the information about GHG and aerosol concentration into the information about the changes in the atmospheres and ocean conditions and circulations (Déque 2007). Confidence in general circulation models estimates comes from the foundation of the models in accepted physical principles and from their ability to reproduce observed features of current climate and past climate changes. Confidence in model estimates is higher for temperature than for precipitation. Confidence in the changes projected by global models decreases at smaller scales and other techniques such as regional models or downscaling techniques are required for producing climate estimates at a finer scale (Randall et al. 2007).

IPCC simulations in Fourth Assessment Report of the Intergovernmental Panel on Climate Change, 2007 have been undertaken using more than 20 general circulation model coupling representation of the ocean-atmosphere and of the ice-regions). These multi-model simulation had the objective of representing more robustly climate's recent and future evolution under many GHGs and aerosols emission scenarios. To better understand what is the idea behind this multi-model simulation and intercomparison we will give here some useful definitions inspired from Bony, S. and Dufresne, J. in Terray and Braconnot 2006:

The climate sensitivity is a global indicator used for characterising earth surface temperature variation caused by a perturbation (for example the doubling of CO_2 concentration).

The radiative forcing is a variable used to quantify the perturbation according to which the climate sensitivity is monitored. The perturbation is quantified in terms of its effect on the upper level atmosphere's energy budget, assuming all the others variables being unchanged.

Feedback loop : given a radiative forcing[1], the earth surface temperature will change causing a change in all the other climate variables (wind, humidity,

[1]which is an inbalance in the atmosphere energy budget

clouds, rain, snow...) as well. Some of these variations will cause another imbalance (radiative forcing) in the upper level atmosphere's energy budget which will induce another change in the earth surface temperature and in other climate variables. This process is called a **feedback loop**.

There are three main feedback loops in GCMs:

The water vapour feedback: temperature's increase induces higher presence of water vapour in the atmosphere and strengthens the green house effect (**positive feedback**).

The cryospheric feedback: temperature's increase induces faster snow and ice melt causing earth's surface to reflect a smaller part of solar radiation (change in albedo) (**positive feedback**).

The cloud feedback: changes in water vapour and atmospheric circulation change clouds covering and their radiative effect. Those changes modify the green house effect, the part of solar radiation reflected from the atmosphere and the energy balance. It can be either a **positive or negative feedback**.

Until IPCC AR3 (Third Assessment Report of Intergovernmental Panel on Climate Change, 2007) there was a lack of analytical studies concerning the above feedbacks. Since IPCC AR3, some GCMs models intercomparison projects have been undertaken and feedback effects magnitude has been estimated. This intercomparison reaffirms that spread of climate sensitivity estimates among models arises primarily from inter-model differences in cloud feedbacks (Randall et al. 2007).

Since IPCC AR3 (Third Assessment Report of Intergovernmental Panel of Climate Change, 2007), all the components of those climate models have been improved, for example : the atmosphere (convection, clouds, aerosols, orography), the oceans (free surface formulation), the sea-ice regions(rheology) and the continents (land use). The resolution and the coupling between model's components have been improved too (Terray and Braconnot 2006). However, the multi-model intercomparison realised for the IPCC AR4 shows also that climate models still have large bias and uncertitudes. This fact confirms that it is essential in climate change research to apply a multi-model approach for obtaining robust results concerning future climate and impacts.

Due to high computational requirements of GCMs and to the present limitation of scientific computer offer, the horizontal resolution of GCMs is most of the time restricted to 200-300 km. Thus, forcings on a regional and local scale are produced using a downscaling technique and/or a finer scale regional circulation model with boundary conditions given by a general circulation model or by observed data.

Another approach, applied in French climate models is to adopt a variable horizontal resolution, fine on the area of interest and coarse on the rest of the world.

Specifically, four climate scenarios[2] used within this thesis have been produced with the ARPEGE Climat from the CNRM - Toulouse[3] (Gibelin and Déque 2003) which has a variable resolution of 50 km over France and up to 450 km over the Southern Pacific.

The principal advantage of the variable resolution approach is that the model such as ARPEGE Climat does not require the boundary conditions essential to a regional model which are often source of great errors and uncertainties. An inconvenient of ARPEGE Climat is that the circulation model is not coupled to an ocean atmosphere module since a coupled variable resolution model would imply an inacceptable computational costs. Then, ARPEGE Climat requires a sea surface temperature (SST), taken from a "classical" coarse resolution GCM.

In the framework of this thesis we have used 11 climate scenarios which are described in § 5.1. Seven of them are issued from as many "classical" coarse resolution GCMs (within the IPCC AR4 intercomparison project, see table 5.2). Four other scenarios are issued instead from two different versions of variable resolution ARPEGE Climat model. Climate forcings produced with both "classical" and variable resolution GCMs have been directly downscaled (see §2.3): no intermediate regional circulation model has been used. Next section is focused on downscaling techniques.

2.3 Downscaling techniques

Brindging the gap between the resolution of climate models and regional and local scale processes represents a considerable problem for the impact assessment of climate change, including the application of climate change scenarios to hydrological models as in the present thesis.

Two fundamental approaches exists for the downscaling of large scale GCM output to a finer spatial resolution. The first of these is a *dynamical* approach where a higher resolution regional climate model (RCM) is forced by large scale and lateral boundary conditions from a GCM. The second approach is to use *statistical* methods to establish empirical relationships between GCM-resolution climate variables and local climate. Sometimes, a dynamical downscaling (RCM) is applied first and a statistical one afterwards to obtain local scale variables. A review from Fowler, Blenkisop, and Tebaldi (2007) contains a very interesting analysis of the main advantages and limitations of each one of these approaches (figure 2.1).

[2]In particular our "reference" continous climate change scenario has been produced with this variable resolution GCM.

[3]Centre National de Recherche Meteorologique - Toulouse - Meteo France

	Statistical downscaling	Dynamical downscaling
Advantages	• Comparatively cheap and computationally efficient • Can provide point-scale climatic variables from GCM-scale output • Can be used to derive variables not available from RCMs • Easily transferable to other regions • Based on standard and accepted statistical procedures • Able to directly incorporate observations into method	• Produces responses based on physically consistent processes • Produces finer resolution information from GCM-scale output that can resolve atmospheric processes on a smaller scale
Disadvantages	• Require long and reliable observed historical data series for calibration • Dependent upon choice of predictors • Non-stationarity in the predictor-predictand relationship • Climate system feedbacks not included • Dependent on GCM boundary forcing; affected by biases in underlying GCM • Domain size, climatic region and season affects downscaling skill	• Computationally intensive • Limited number of scenario ensembles available • Strongly dependent on GCM boundary forcing

Table 2.1: Comparative summary of the relative merits of statistical and dynamical downsclaing techniques., source: (Fowler, Blenkisop, and Tebaldi 2007)

Within this thesis no dynamical downscaling has been used to produce climate forcings. The 11 scenarios issued from coarse scale GCM or from finer scale variable resolution model have been statistically downscaled without any use of a Regional Climate Model[4]. We will shortly make a state of the art of the existing downscaling techniques in the next subsection focusing our attention on the two downscaling techniques which have been used to produce climate forcings within the Rexhyss project.

In **statistical downscaling** an empirical relationship linking large scale information and local or regional variables is first established for current climate, then applying this relationship, local variable for future climate are derived from large scale values simulated by a General Circulation Model. Thus, Statistical Downscaling techniques are all based on the **strong hypothesis** that the empirical relationship established for present climate is still valid under altered climate conditions. This stationarity assumption is the major theoretical weakness of statistical downscaling as it is not verifiable.

The perturbation method (or delta change approach) is the first and simplest statistical downscaling approach. It consists in assuming the constancy through time of model bias. With this approach, simulated future climate is assumed to have the same bias that exists on observed historical time data. This approach is obviously not sufficient for representing extremes since it does not care about changes in the

[4]However, three scenarios are issued from the variable resolution model ARPEGE Climat, which has a fine resolution, similar to a Regional Circulation Model, over France.

variability or spatial pattern of climate. For example, the temporal sequence of wet days is unchanged, when change in wet and dry spells may be an important component of climate change (Fowler, Blenkisop, and Tebaldi 2007).

More sophisticated statistical downscaling methods have been developed for feeding local hydrologic impact models with robusts extreme events. We will shortly describe here the concepts beyond the **variable correction method** and the **weather regime approach** through which climate forcings used within this thesis have been produced.

The variable correction method (VCM) is a statistical downscaling approach designed for obtaining an acceptable representation of extreme events (precipitation and temperature). This method compares model and observation using a "quantile-quantile" (q-q) plot which consists in plotting a model value against an observed one, both corresponding to the same probability. When one deals with the same number of data in both observation and model dataset, the method is very easy to implement: the two dataset are ranked by increasing order, the first pair (model, observation) corresponds to the first point in the diagram, the second pair to the second point, and so on. An example of such a plot for precipitation is given in figure 2.5: if the model was perfect, the plots should align along the diagonal, the model is instead too wet in the low precipitation and too dry in heavy summer precipitation. Heavy winter precipitation are correctly reproduced.

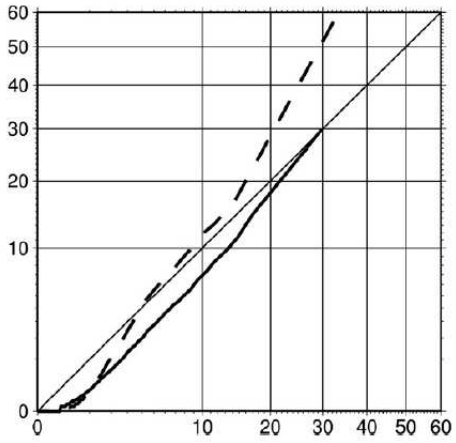

Figure 2.5: Example of a quantile-quantile plot for maximum precipitation in the Paris area [mm/d]. Model (ARPEGE Climat v3) on the x-axis and observation on the y-axis. Solid line is winter and dash line is summer. Source: Déque 2007

The variable correction method (Déque 2007) is based on the assumption that the model is able to predict a ranked category of temperature or precipitation but not a correct value for this variable. It uses the q-q plot as a correction function, for

example transforming a "very high precipitation" from the model of 30 mm/d in the associated "very high precipitation" of 60 mm/d from the observation (figure 2.5).

The weather regime approach This statistical downscaling technique (Boé et al. 2006) is based on the assumption that regional climate is conditioned both by the large scale circulation (mostly correctly represented by GCMs) and by small scale features. This method is based on the assumption that similar weather conditions "weather types" should lead to similar local surface variables in present and future climate. First, discriminating weather types (large scale circulation patterns) for local surface variables are determined on present climate through a complex algorithm. Then these weather types are used as "predictors" in future climate to determine local scale surface variables through a conditional resampling process (Boé et al. 2006). In other terms, with such a technique climate change is estimated by evaluating the change in the frequency of the weather types simulated by the GCM.

Uncertainties deriving from the choice of the downscaling technique are analysed in sections 5.3.2 and 5.6.

Chapter 3

Catchment Based Land Surface Model

In this chapter we will firstly give a state of the art of Land Surface hydrological Models. We will then analyse in detail the Catchment Based Land Surface Model (CLSM) and CLSM model with Linear Reservoir.

3.1 A historical introduction

In this section, we will make a state of the art, giving a historical overview based on the article of Koster et al. (2000).

3.1.1 Land surface models

Land surface models (LSMs) were first introduced in atmospheric general circulation models (GCMs) to generate water and energy fluxes to the atmosphere. Indeed, as we have seen in the previous chapter, general circulation models are useful tools for examining the mechanisms behind climate variability, for characterizing the sensitivity of climate to anthropogenic forcing and for predicting future climate. *To be of some value, a GCM has to correctly represent a realistic climate through a reliable modelisation of physical processes. Over continents in particular, a proper representation of the land surface energy and water balance is critical* (Koster et al. 2000).

Land surface models were originally coupled with a GCM for simulating the diurnal cycle of land surface water and energy fluxes as a function of near-surface meteorology (precipitation, short-wave and long-wave incident radiation, surface pressure, air temperature and humidity at 2 m, wind speed at 10 m of altitude). Concerning the energy flux, a LSM is designed for partitioning correctly the net incoming radiative energy into latent heat flux, sensible heat flux, ground heating and snowmelt (cf. §3.2.4.1). As for the water balance, we expect a LSM to properly partition the precipitation at the surface into evaporation, runoff and moisture storage. *The two budgets are then coupled by the latent heat flux* (Gascoin et al. 2008).

The first scheme that took hydrological processes interactively into account in GCMs was the *bucket model* (Manabe 1969). That model was based on two main assumptions:

- the evaporation rate is computed by multiplying the potential rate by an aridity coefficient, which is a simple function of total soil moisture content.

- All water reaching the soil until saturation is infiltrated; afterward, runoff takes place to remove the excess water at the surface.

3.1.2 The role of vegetation

Since 1969, Manabe's model has been adapted in many different ways. Some years later a new approach started with the so called *soil-vegetation-atmosphere-transfer* (SVAT). In SVAT models vegetation has a direct role in determining the surface energy and water balance, particularly by allowing stomatal conductance to decrease in response to increased environmental stress.

With the SVAT approach a reliable evapotranspiration (sum of transpiration by vegetation, interception loss from wet leafs and soil evaporation) rate was computed taking into account vegetation. The evaporation formula is generally described with the aid of a resistance diagram, similar to that of the Penman-Monteith evaporation formula (Monteith 1965). An intercomparison project, the Project for the Intercomparison of Land Surface Parameterizations Schemes(PILPS) (Henderson-Sellers, Yang, and Dickinson 1993), showed that the SVAT approach is the most popular within LSMs.

The issue of correctly representing vegetation in LSMs is far from being simple since vegetation is not uniform over a GCM grid-box. How can heterogeneity be represented? In the *Simple Biosphere model* (SiB) (Sellers et al. 1986) it was done through the definition of a mean value of the vegetative cover.

Another way is to define a mosaic of vegetation types inside a grid-box, to compute for each of them the water exchanges of land surface with atmosphere, and to average the fluxes (Koster and Suarez 1996):

> Using vegetation maps, every surface grid cell in the GCM is subdivided into relatively homogeneous subregions or "mosaic tiles", each tile containing a single vegetation or bare soil type. Energy and water balance calculations are performed over each tile at every time step, and each tile maintains its own prognostic variables (moisture reservoirs and temperatures). The tiles in a grid square respond to the mean conditions in the overlying GCM grid box; this grid box, in turn responds to the areally weighted fluxes of heat and moisture from the tiles. The tiles in a grid square do not interact with each other directly, though they can affect each other through the overlying atmosphere.

This kind of approach is applied in CLSM model where the vegetation tiles are subregions of a unit catchment. Fluxes are areally weighted and averaged over using the vegetation tiles.

3.1.3 Evapo-transpiration's formulation impact on runoff

Koster et al. (2000) notice that with SVAT models, great importance has been given to a correct representation of evapo-transpiration: canopy interception and

environmental influences on stomatal conductance are generally well represented using some complex functions. In addition some research has been undertaken on photosynthetic control over transpiration and carbon uptake (Dickinson et al. 1998).

However Koster and Milly (1997) showed in a pioneering work that the runoff formulation controls evaporation rates as much as the evaporation formula. They concluded that *one requirement for an accurate simulation of a region's water budget (and thus energy budget) is compatibility between the LSM' evaporation and runoff formulation.* Furthermore *even a 'perfect' description of canopy structure and stomatal behavior does not ensure realistic evaporation rates if the runoff remains relatively crude or incompatible with the evaporation formulation.* In fact the water budget within the continental water cycle implies that the improvement of the evaporation computation is limited if the runoff generation mechanisms are not properly represented.

3.1.4 Subgrid variability

Koster et al. (2000) point out that most standard SVAT models are mainly one-dimensional[1] in their structure. However, the modeler should not forget that runoff in nature is largely dependent on spatial heterogeneity in precipitation, surface and vegetation characteristics.

Overland flow[2] in hydrological models is generally represented through one of the following mechanisms:

- The **Dunne** mechanism requires rainfall to impinge on a saturated ground surface, typically a small fraction of the land area receiving the rain.
- The **Horton** mechanism generates overland flow when rainfall rate exceeds the infiltration capacity of the soil. This infiltration capacity of the soil varies considerably in space with both soil texture and water content.

Baseflow or **subsurface flow** represents the slow component of river discharge and is essential for sustaining low flows. This term reflects (physically or synthetically) the correct representation of the water table and of its three-dimensional structure (Koster et al. 2000).

Koster et al. (2000) underline that both subsurface and overland flow produced by a land surface model cannot be realistic if the chosen LSM does not consider somehow the three dimensional structure of the water table and of the catchment's surface and vegetation.

[1] This fact encourages even more the detailed description of vegetation and canopy structure

[2] Total runoff is the sum of baseflow and overland flow, (Dingman 2002)

Different approaches have been used in the past to consider three dimensional nature of runoff's generation:

- The *mosaic* approach (Koster and Suarez 1992,Koster and Suarez 1996) is named for its use of the mosaic[3] strategy to account for subgrid heterogeneity in surface characteristics.
- Famiglietti and Wood (1994) were the first to include a TOPMODEL[4] based formulation in a land surface model for taking into account the relationships between topography and subgrid variability of hydrological processes.
- Some proposals for a more accurate computation of *subsurface flow* are among the others Wood, Lettenmaier, and Zartarian 1992 and Ducharne, Laval, and Polcher 1998.

The two first items listed above inspired the Catchment Land Surface Model (CLSM) (Koster et al. 2000 and Ducharne et al. 2000) which has been used in the present work. CLSM is described further in section 3.2. The third item somehow inspired instead the insertion of a linear subsurface reservoir in the original CLSM (Gascoin et al. 2008), a solution that has been used too in the present thesis and on which we will give some detail in section 3.3.

3.2 CLSM model

In this section we will describe the main features of the Catchment Based Land Surface Model, which has been used in this thesis work.

The catchment-based land surface model (Koster et al. 2000 and Ducharne et al. 2000) provides a physically based description of the influence of climate on hydrology. As a land surface model (LSM), it is designed to simulate the diurnal cycle of land surface water and energy fluxes as a function of near-surface meteorology (precipitation, short-wave and longwave incident radiation, surface pressure, air temperature and humidity at 2 m, wind speed at 10 m) and can either be coupled to a GCM or used off-line as in the present study. It is an innovative land surface model for the following two reasons:

- The shape of the land surface element is the unit **hydrological catchment** with boundaries defined by **topography** instead of a quasi-rectangular element with boundaries defined by the overlying GCM atmospheric grid (see § 3.2.2).

[3]Refer also to §3.1.2, where the mosaic approach is shortly described.

[4]We will give more details on TOPMODEL formulation in §3.2.3.1

- Within each catchment, soil moisture is assumed to vary significantly and this heterogeneity is represented using the well known TOPMODEL (Beven and Kirkby 1979). TOPMODEL is used for determining the distribution of soil moisture in the root zone and for allowing the separation of the catchment into specific hydrological regimes (saturated, stressed and intermediate fractions of the catchment) see § 3.2.3.1.

At each time step water and energy budgets are solved independently in each areal fraction according to classical SVAT parameterizations, mostly taken from the Mosaic LSM (Koster and Suarez 1996, Koster and Suarez 1992). These issues are shortly described in § 3.2.4.

CLSM model has been validated in the Arkansas-Red river catchment (Ducharne et al. 2000) and in the Seine river basin where it has already been used as a tool to assess the impact of climate change on hydrology in the framework of the french research project GICC-Seine (Ducharne et al. 2004 ; Ducharne et al. 2007).

3.2.1 Overall framework

The CLSM model is applied to a **single unit catchment**. It is possible however to link one unit catchment to the others using one of the standard hydrological routing techniques. In our study a Muskingum routing technique has been applied (section 4.3.1).

Within each unit catchment a process made of two main parts is applied:

1. The catchment is partitioned into three subdivisions according to their soil moisture regime (saturated, stressed or intermediate). This process is described in §3.2.3 and in figure 3.1.

2. The coupled energy and water budget are computed separately for each subdivision according to the appropriate hydrological regime. See §3.2.4.

3.2.2 A catchment based approach

In CLSM the hydrological river catchment is the land surface element. The catchment approach is an important aspect of this model for many reasons:

- It allows us to compare simulated discharges and observed ones. This is an important mean of validation, owing to the wealth of flow river data, whereas other hydrological variables as soil moisture or evaporation are still poorly known.

- It makes possible to use classical hydrological models (e.g. TOPMODEL) and tools (e.g. Muskingum routing methods).

On the other hand using catchment as land surface element makes necessary an algorithm that downscale or upscales the atmospheric forcing. In our case, an upscaling is required from the $8km \times 8km$ grid box available for this work to the unit catchment size.

3.2.3 Subgrid variability

A rather interesting process is used in CLSM for taking into account subgrid heterogeneity in moisture profile. This process is described in the figure 3.1 and requires a few steps:

1. The topographic index distribution over all the catchment is obtained through a gridded *digital elevation model* (DEM) of the watershed. See 3.2.3.1.
2. Using TOPMODEL equations the spatial distribution of the water table depth d is obtained. See §3.2.3.1.
3. Under TOPMODEL and equilibrium assumptions a *Catchment Deficit* M_d is calculated from the spatial distribution of d. See §3.2.3.2.
4. Two other soil moisture variables (the *root zone excess* M_z and the *surface excess* M_s) are used to better characterize soil moisture conditions that are obviously not under equilibrium conditions (see §3.2.3.2). Transfers between these three moisture reservoirs are described in § 3.2.3.3.
5. Starting from the three moisture variables values and through manipulation of a probability density function (pdf) of root zone moisture, the catchment is subdivided into three distinct regions (saturated, wilting[5] and transpiration[6] one), each one with its own areal fraction A_{sat}, A_{tr} and A_{wilt}. See §3.2.3.4.

The process described above is undertaken at each 20 minutes time step. The output of the process are the three areal fraction A_{sat}, A_{tr} and A_{wilt}. The coupled energy and water budgets are then applied separately for each areal fraction at the next time step. See §3.2.4.

3.2.3.1 TOPMODEL framework

TOPMODEL (Beven and Kirkby 1979) is an hydrological model where runoff generation is based on Dunne mechanism[7]. According to that mechanism, runoff is

[5] stressed

[6] intermediate

[7] See §3.2.3.

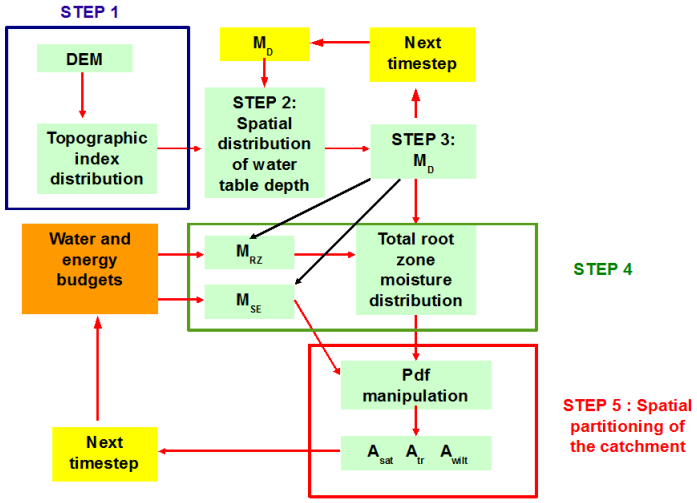

Figure 3.1: Schematic representation of CLSM overall framework

due to the saturation of subsurface soil layers caused by a raise in the water table which is due both to precipitation and subsurface flow[8].

TOPMODEL simulates the dynamical behavior of the runoff contributing area A_c of a catchment. In TOPMODEL, the contributing area is defined as the saturated part of the catchment, where the water table intercepts the soil surface.

In each point i of the catchment the following variables are defined :

- the bedrock depth D_i measured from the ground,
- the water table depth d_i measured from the ground,
- the slope $\tan\beta_i$,
- the upstream area a_i that contributes to flow (per unit contour),

Water table in CLSM is based on the same **assumptions** of TOPMODEL:

Hyp1: The saturated hydraulic conductivity decreases exponentially with depth z($z = 0$ at the surface and positive underground):

$$K_s = K_0 \cdot e^{(-\nu \cdot z)} \tag{3.1}$$

K_s is the saturated conductivity at the soil surface, constant over all the catchment,
K_0 is K_s at $z = 0$,
ν is the decay parameter with depth of the hydraulic conductivity.

[8]Some detail on TOPMODEL principles have been inspired from (Mancini and Montaldo).

Hyp2: At all time steps the water table distribution results from a steady state under the uniform recharge rate at the time step. The water table recharge process is slow enough to consider a water table distribution at equilibrium.

Hyp3: The water table is nearly parallel to the soil surface, i.e. the hydraulic gradients are approximated by the topographic gradients.

Under these assumptions, applying the continuity equation between the bedrock depth and the ground surface, considering a constant value of precipitation over all the catchment, it is possible to obtain the following relationship between the water table depth at a point and the mean water table depth (Koster et al. 2000):

$$d_i = \overline{d} - \frac{1}{\nu} \cdot \left(\ln \frac{a_i}{\tan(\beta)} - \overline{x} \right) \tag{3.2}$$

$\ln \frac{a_i}{\tan(\beta)}$ is the *topographic index* at the point,
$\overline{x}$ is the mean catchment value of the topographic index

After computing the topographic index for all the catchment from a gridded Digital Elevation Model (DEM), CLSM uses equation 3.2 to derive, at each 20 minutes time step, a spatial distribution of the water table depth, only from the mean water table depth $\overline{d}$. This is an essential task for obtaining the catchment deficit M_d variable described in the next subsection.

3.2.3.2 Soil moisture variables

The *catchment deficit* M_d is the key variable used by CLSM to describe the soil moisture : it is the average amount of water, per unit area, that would need to be added to saturate all of the catchment, assuming that the vertical moisture profile results from hydrostatic equilibrium.

M_d is the main prognostic variable of CLSM and is related to $\overline{d}$ by a one to one relationship. Figure 3.2 shows the equilibrium profile of soil moisture with depth at an arbitrary point in the catchment. The expression of the equilibrium profile comes from the relations of Clapp and Hornberger (1978):

$$w(z) = \left(\frac{\Psi_s - z}{\Psi_s} \right)^{-\frac{1}{b}} \tag{3.3}$$

w is the degree of saturation, i.e. the *wetness*[9].
Ψ_s is the matrix potential in the soil at saturation
b is a soil parameter.

It is possible then to vertically integrate $1 - w(z)$ between the water table and the ground surface, obtaining a *local moisture deficit* D (figure 3.2). The figure 3.3

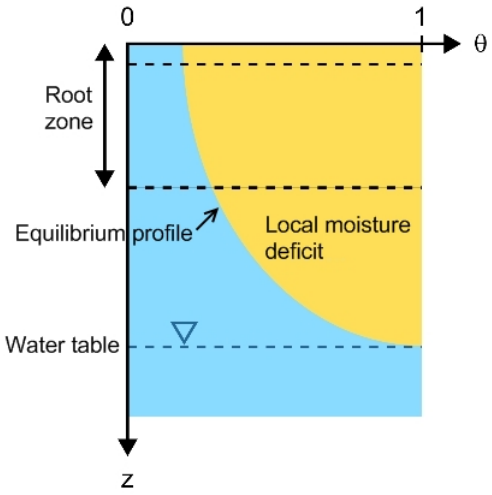

Figure 3.2: Water table and the catchment deficit, adapted from Gascoin.

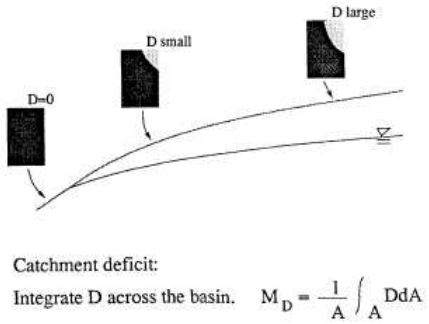

Figure 3.3: Local moisture and catchment deficit, source: (Koster et al. 2000)

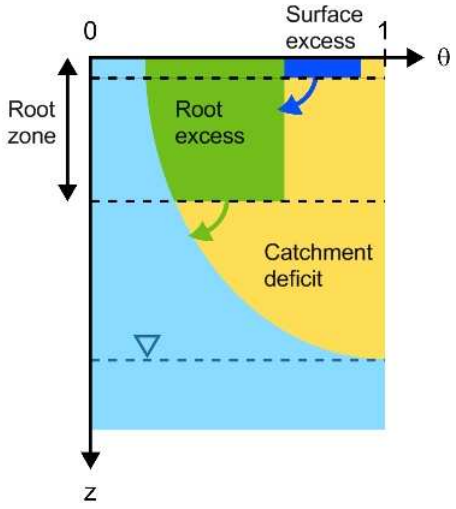

Figure 3.4: Illustration of the catchment deficit and the surface and root zone excess, adapted from Gascoin

shows that the local deficit varies within the catchment : there are large values of D where the water table is deep and D=0 where the ground is fully saturated. The catchment deficit M_d is the integral of the local deficit D across the catchment's area.

A bedrockdepth is assumed and CLSM model imposes a maximum catchment deficit based on estimated soil profile depths. The importance of this maximum value is expressed in §3.2.3.4 and in §3.2.4.2.

Two additional variables, the *root zone excess* M_{RZ} and the *surface excess* M_{SE} allow to account for non equilibrium conditions which are obviously the rule in nature but are ignored by catchment deficit value.

According to Koster et al. (2000) :

Definition 1. *The* ***root zone excess*** *at a given point is the amount by which the moisture in the root zone exceeds (or is less than) the moisture content implied by the local equilibrium moisture profile. The root zone excess for all the catchment* M_{RZ} *is the average amount of water, per unit area, by which condition sin the root zone across the catchment are out of equilibrium.*

Total root zone moisture distribution, which is the sum of equilibrium root zone moisture and root zone excess, is used in CLSM for partitioning the catchment into three subregions. See §3.2.3.4 .

Definition 2. *The* ***surface excess*** *of the catchment is the average amount per unit area by which the moisture in the top 2 cm is different from the value implied by the equilibrium profile.*

The concepts of surface and root zone excess are illustrated in the figure 3.4. M_{RZ} and M_{SE} are positive after a storm and negative when evaporation exceeds precipitation over an extended period of time. In the next subsection, we will shortly describe how transfers between these 3 soil moisture reservoirs are computed.

3.2.3.3 Transfers between moisture variables

The transfers between the root zone excess and the water table and between the surface excess and the root zone excess are computed in order to bring the total system closer to equilibrium conditions. The first transfer, ΔM_{RZ}, goes from the root zone excess M_{RZ} to the water table M_D when $M_{RZ} > M_D$. It goes in the opposite direction otherwise.

The vertical water flux ΔM_{RZ} is based on Richards equation (Richards 1931). It is computed as (Ducharne et al. 2000):

$$\Delta M_{RZ} = M_{RZ} \cdot \frac{\Delta t}{r_1} \tag{3.4}$$

Δt is the time step length.
r_1 is an empirical parameter

The timescale r_1 is estimated off-line as an empirical function of M_{RZ} and M_D as described in Ducharne et al. 2000. In essence, r_1 decreases with decreasing M_D and with increasing M_{RZ}.

The transfer between the surface excess and the root zone excess follows the same path:

$$\Delta M_{SE} = M_{SE} \cdot \frac{\Delta t}{r_2} \tag{3.5}$$

Δ t is the time step length.
r_2 is an empirical parameter depending on M_{SE} and M_{RZ}
The value of r_2 decreases with an increase in M_{SE} or in M_{RZ}.

3.2.3.4 Spatial partitioning within the catchment

The three moisture variables described above, combined with the topographic information, allows to partition the catchment into three fractions, each with a different moisture status (saturated, stressed, intermediate) and thereby a different parametrization of runoff and evapotranspiration.

The subdivision of a catchment into three subregions is illustrated in figure 3.6. According to Koster et al. (2000) definitions, the **saturated region** consists of all points for which the root zone is fully saturated and it has a fractional area of A_{sat}. The **transpiration region** of areal fraction A_{tr} includes all points having subsaturated root zone moistures that lie above the vegetation-specific wilting point θ_{wilt}. The **wilting region**, consisting of all points for which transpiration is shut off completely, has a fractional area of A_{wilt}. The water budget is then computed differently in each region (see § 3.2.4.2) leading to *a more credible estimates of evaporation and runoff across the catchment* (Koster et al. 2000).

Referring to the steps and to the block diagram of §3.2.3, the current paragraph goes more into detail the step number 5. How does the CLSM model subdivide the total catchment area into the three areal fraction values A_{sat}, A_{tr} and A_{wilt}? The answer to the question is given in papers Koster et al. 2000 and Ducharne et al. 2000 where the complex process is described in detail. We will only give here a short glimpse on that process.

The areal fractions are determined through manipulation of probability density functions (pdf) of the root zone soil moisture. Considering first the case of water table depth being above the assumed bedrock depth of the catchment (i.e. the catchment deficit M_D being below the assumed maximum catchment deficit), it is possible to follow the conceptual path of the block diagram in figure 3.5:

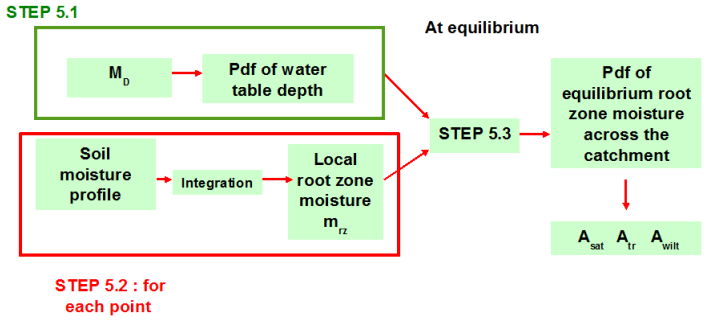

Figure 3.5: Schematic representation of CLSM spatial partitioning process

1. There is a one to one relationship between the catchment deficit M_D and the probability density function of the water table depth d within the catchment.

2. A specific equilibrium moisture profile is given through equation 3.3. It is possible to integrate this equation vertically for obtaining a local equilibrium root zone moisture at a given point m_{rz} (Koster et al. 2000):

$$m_{rz} = \frac{1}{d_{rz}} \cdot \int_{\overline{d}-d_{rz}}^{\overline{d}} w(z)dz \tag{3.6}$$

   where d_{rz} is the depth of the root zone.

3. Combining equations 3.3 and 3.6 allows to transform the pdf of water table depth into a pdf of equilibrium root zone moisture across the catchment. A typical shape for this pdf is labeled (A) in figure 3.7.

Referring to the figure 3.7:

Pdf B corresponds to the assumption of the mean water table depth being equal to the bedrock depth, having a catchment deficit M_D^B and a zone moisture θ_B.

Pdf C refers to the onset of wilting ($\theta_0 = \theta_{wilt}$), having a catchment deficit M_D^C and a zone moisture θ_C.

Pdf D corresponds to complete wilting and is a simple delta function centered at θ_{wilt}.

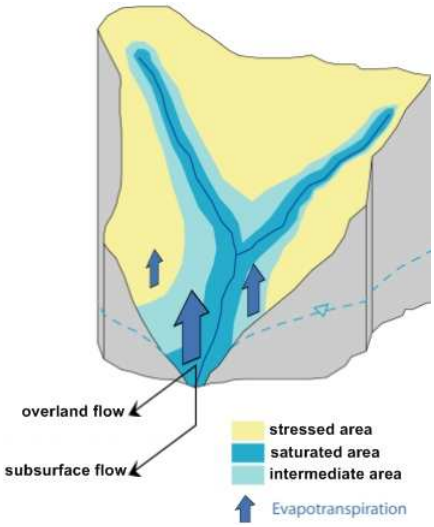

Figure 3.6: Subdivision of the catchment in 3 zones, source: Gascoin

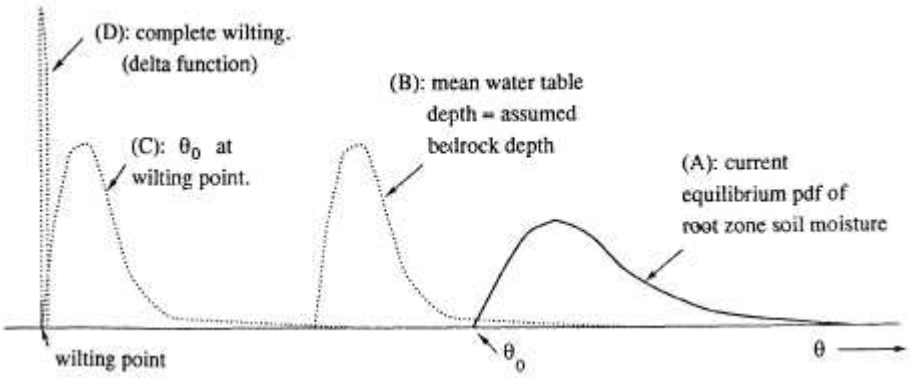

Figure 3.7: Probability density functions (pdfs) of equilibrium root zone soil moisture at various catchment deficits in the catchment, source: Koster et al. 2000.

It is important to point out that : *the shapes of B and C are the same because prior to wilting evapotranspiration is assumed for convenience to act uniformly on the root zone moisture: unstressed transpiration does take place, after all, in both the saturated and transpirations fractions. Thus the soil in the non wilting catchment is assumed to dry uniformly, leading to a simple translation of the pdf.* (Koster et al. 2000).

Then the fractional areas A_{sat}, A_{tr} and A_{wilt} are obtained in CLSM according to the block diagram in figure 3.5. Different formulations for A_{sat}, A_{tr} and A_{wilt} are given in the appendix A of (Koster et al. 2000) depending on position of the pdf A of root zone soil moisture at equilibrium and on the value of the root zone excess θ_{exc} (which is obtained from M_{RZ}) compared to the value of M_D^B and to the position

of the pdf C.

A first question concerns whether $M_D < M_D^B$ or not (meaning that the mean water table depth is above the assumed bedrock depth or not). A second issue is whether the θ_{exc} value brings the pdf A below wilting point or not.

Depending on the answers to those two questions different formulations are given in (Koster et al. 2000) for A_{sat}, A_{tr} and A_{wilt} values. For example the simpler one for the case $M_D < M^B$ and no part of the pdf A below wilting point is :

$$\begin{aligned} A_{sat} &= \int_{\infty}^{1} f(\theta - \theta_{exc}) d\theta \\ A_{tr} &= 1 - A_{sat} \\ A_{wilt} &= 0 \end{aligned}$$

where $f(\theta)$ is the equilibrium pdf A.

3.2.4 Water and energy budgets

At each time step the water and energy budget are solved independently in each areal fraction according to the classical SVAT parametrization (see §3.1.2), mostly taken from the Mosaic LSM (Koster and Suarez 1996).

3.2.4.1 The energy budget

According to (Koster and Suarez 1996), the energy balance calculations within each areal fraction are performed in the following way (figure 3.8):

> A fraction of the incoming solar radiation is immediately reflected. The sum of absorbed solar radiation and downward longwave radiation is balanced by upwelling longwave radiation, outgoing latent heat, outgoing sensible heat, ground heat storage, and snowmelt. Canopy resistance, which controls transpiration rates, is allowed to vary with environmental stress. Heat transfer into the deep soil updates a deep soil temperature. A strict energy balance is maintained for the surface/canopy system and for the deep soil at every time step; energy is never created or destroyed, except possibly through numerical round-off.

The surface energy balance equation (in the absence of snowmelt) is :

$$R_{SW-net} + R_{lw}^{\downarrow} = \frac{C_H \delta T_c}{\Delta t} + R_{lw}^{\uparrow} + H + \lambda E + G_D \tag{3.7}$$

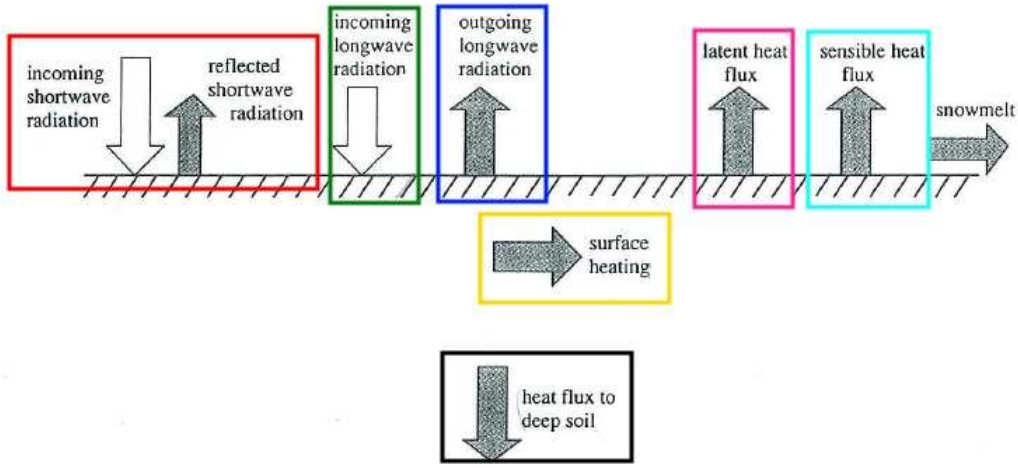

Figure 3.8: Schematic representation of the energy budget performed by CLSM, adapted from Koster and Suarez 1996

where

R_{SW-net}	is net shortwave radiation absorbed at the surface,
$R_{lw}^{\downarrow}$	is the longwave radiation absorbed at the surface,
C_H	is the heat capacity associated with surface-canopy temperature,
δT_c	is the change in surface-canopy temperature T_c over time step,
Δt	is the time step duration,
$R_{lw}^{\uparrow}$	is the upward longwave radiation at surface,
H	is the sensible heat flux,
λ	is the latent heat of vaporization,
E	is the evaporation rate, and
G_D	is the heat flux to deep soil.

More details on computation of the above energy balance for Mosaic LSM and for CLSM are given in (Koster and Suarez 1996). Being a catchment based model, CLSM computes a separate water balance for each subregion (Koster et al. 2000) :

> in accordance with the modeled distribution of soil moisture, the resistance applied to the evapotranspiration calculation vary significantly between the subregions. Resistance to bare soil evaporation, a function of surface soil moisture is very small in the saturated region, is moderate in the transpiration region, and is high in the wilting region.

CLSM assumes the same small non zero resistance for both the saturated and transpiration regions and a high value for the wilting region where transpiration is completely shut down. There is no explicit smoothing of the evapotranspiration

regimes between the subregions. However an implicit smoothing is accomplished by the dynamically varying areas of the subregions (Koster et al. 2000).

Each subregion maintains its own surface/canopy temperature but temperatures at deeper levels are assumed to be spatially homogeneous.A three layer snow model from Lynch-Stieglitz 1994 has been coupled to CLSM. It is fully described in (Stieglitz et al. 2001).

3.2.4.2 The water budget

Figure 3.9 illustrates water balance calculations for CLSM in its original version (without linear reservoir, see also §3.3).

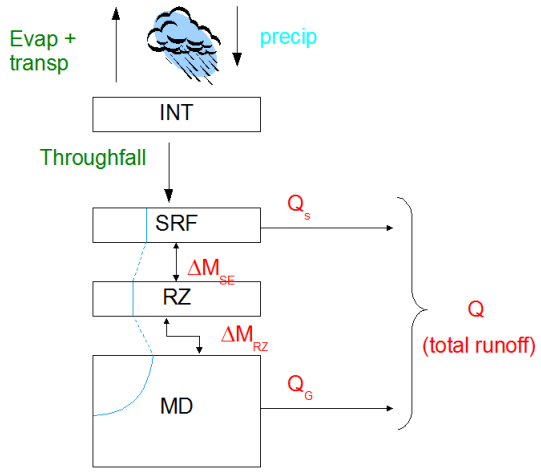

Figure 3.9: Schematic representation of the water balance calculations performed by CLSM, adapted from Koster and Suarez 1996 and Ducharne

Of the precitation water falling on the land surface, some is added to a canopy interception reservoir (INT), which accounts for the ability of leaves and ground litter to hold small amounts of "free-standing" water from which evapo-transpiration occurs unhindered (EVAP + TRANSP). The rest of the precipitation goes into the surface layer (SRF), and this *throughfall* is in turn partitioned into surface runoff (overland flow) and infiltration into the root zone layer. More details on these 3 reservoirs (surface, root zone and subsurface) have been given in §3.2.3.3. Transfers between this root zone layer and the main subsurface layer MD are computed as described in §3.2.3.2.

The total runoff is the sum of two components as in TOPMODEL : the subsurface downslope flow (TOPMODEL's base flow) Q_B and the surface runoff Q_S. The latter includes two terms, excess saturation overland flow and excess infiltration overland flow.

Throughfall P_T falls uniformly on all three catchment subregions. Then:

- Throughfall impinging on the saturated region is immediately converted into surface runoff (excess saturation overland

$$Q_S = P_T \cdot A_{sat} \quad M_{SE} < 0. \tag{3.8}$$

- On other areas, throughfall infiltrates the soil, unless the surface excess M_{SE} is positive[10]

$$Q_S = P_T A_{sat} \quad M_{SE} < 0 \tag{3.9}$$

$$Q_S = P_T \left(A_{sat} + A_{tr} \frac{M_{SE}}{M_{SE-max}} \right) \quad M_{SE} > 0 \tag{3.10}$$

where
M_{SE-max} is the maximum possible value of the surface excess given the current values of catchment deficit and root zone excess.

Subsurface flow is equivalent to TOPMODEL's "base flow" (Beven and Kirkby 1979):

$$Q_B = \frac{K_0}{\nu} e^{-\overline{x}-\nu\overline{z}} \quad M_D < M_D^B \tag{3.11}$$

$$Q_B = 0 \quad M_D \geq M_D^B \tag{3.12}$$

where:
$\overline{x}$ is the mean catchment value of topographic index. maximum possible value of the surface excess given the current values of catchment deficit and root zone excess.
M_D^B is the catchment deficit corresponding to the mean water table being at the soil depth. See §3.2.3.4.

As already written in §3.2.3.2, CLSM defines an active soil depth D[11] and takes care that the mean water table depth is not lower than D (Gascoin et al. 2008 and Koster et al. 2000).

3.3 CLSM model with linear storage reservoir

The TOPMODEL framework of CLSM has the limitation of representing only a shallow water table. It is not adapted to catchments characterised mainly by

[10] indicating a rain-induced excess of moisture near the surface:

[11] or bedrock depth

slow subsurface flow. The shallow aquifer represented by TOPMODEL[12] is not comparable to thick aquifers which have lower hydraulic gradient resulting in slower Darcy's velocity and longer response time to recharge events.

This is exactly the case of the Somme[13] river basin and CLSM model in its original version did not manage to correctly represent observed discharges in the Somme river (and particularly the 2001 major flood event). Thus Gascoin et al. worked on an adaptation of CLSM model to the Somme catchment and in general to thick and deep aquifers. They better represented observed discharges adding a Linear Reservoir (LR) to CLSM. Since the Seine river catchment is very close to the Somme watershed and since a large part of the Seine river basin has a geological structure similar to the Somme river (sedimentary soil formations), CLSM with linear reservoir has been used on the Seine river basin too within the present thesis. Details on the implementation of the model are given in chapter 4.

In CLSM with LR (CLSM-LR) there is an additional runoff term Q_G to account for ground water storage in a deep aquifer. Thus, total runoff in CLSM-LR is composed of three terms:

$$Q = Q_S + Q_B + Q_G. \tag{3.13}$$

The deep component Q_G is generated from the additional LR. This reservoir has no spatial variability and is connected to the original version of CLSM as shown in the figure 3.10.

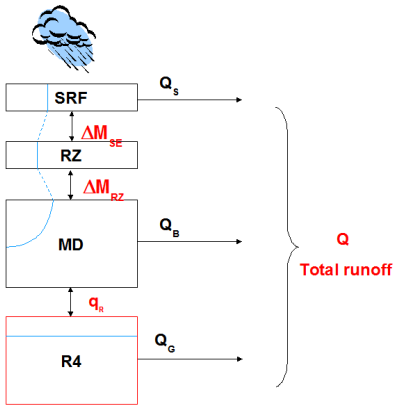

Figure 3.10: Schematic representation of the water balance calculations performed by CLSM with a LR, adapted from Ducharne and Gascoin

[12]with the assumption of the hydraulic gradient being equal to the surface slopes.

[13]The Somme river is located in the North of France, not far from the Seine river basin. The Somme river is fed by the thick and deep Chalk aquifer.

Some details on CLSM-LR are given below and in figure 3.11:

- The LR does not exert any control on the surface, as the flux q_r which recharges it from the soil layer is always greater or equal to zero:

$$q_r = (M_G - M_D)\frac{dt}{\tau_R} \quad M_D < M_G \tag{3.14}$$

$$q_r = 0 \quad M_D \geq M_G \tag{3.15}$$

- $M_G = \alpha M_D^B$, is the maximum deficit up to which the recharge is allowed, LR's recharge takes place only when the catchment is sufficiently wet. M_D^B has been defined in §3.2.3.4. The timescale τ_R controls the rate of recharge.

- Water flow toward LR is uniformly removed from the soil layer and thus added to the catchment deficit.The flow Q_G coming out from the LR is computed using a linear storage relation controlled by a single timescale parameter τ_G which is specific to the catchment. In the above equations S_G is the amount of water (in mm) in the LR:

$$M_D = M_D + q_r \tag{3.16}$$

$$S_G = S_G + q_r \tag{3.17}$$

$$Q_G = S_G\frac{dt}{\tau_G} \tag{3.18}$$

- CLSM-LR is constrained by three more parameters than the original CLSM : M_G, τ_R and τ_G.

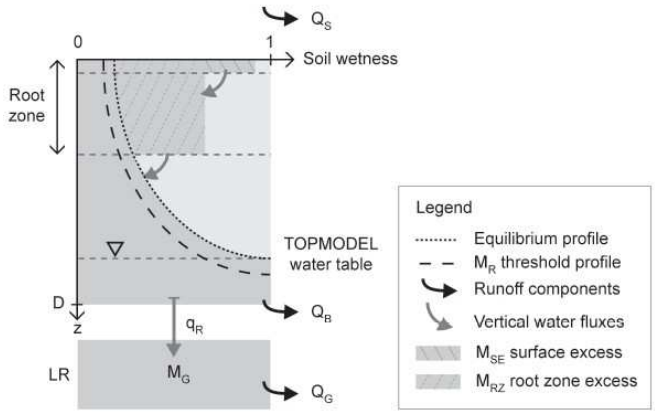

Figure 3.11: Soil moisture profile and water fluxes in CLSM-LR, source: Gascoin et al. 2008

Chapter 4

Modeling the Seine river catchment

This chapter is focused on the Seine river basin and on its representation through the CLSM model. First, a short geographical description is given. Then, data used and choices made to represent the Seine river basin with CLSM are described. Last but not least, the validation of CLSM with respect to observed discharge at Poses is discussed and since 6 runs showed similar performances on historical time, the "equifinality" of these various run in simulating climate change impacts is analysed.

4.1 The Seine river catchment

The Seine River catchment covers 78600 km^2 (at Le Havre), that is 14 % of the surface of continental France. Most of the Seine basin is part of the "Bassin Parisien" a geological area that include important aquifers separated by semi-permeable formations. Deeper and more ancient aquifers are wider than the basin itself. There are several concentric sedimentary formations consisting of tertiary rocks (alternating clay, sandstone and limestone). These formations lie on a basement of ancient massifs outcropping at the extreme South East and North East of the basin. The basin has altitudes generally lower than 300m, culminating to 900 m in Morvan (figure 4.1). Average altitude is 160 m and less than 1% of the territory of the basin has an altitude higher than 500 m (Meybeck, de Marsily, and Fustec 1998).

Due to this moderate altitude, the Seine and its tributaries have weak slopes (0,01 to 0,03 m / 100 m). Most of them flow towards the west. The Seine flows into the English channel at Le Havre after a 776 km long course. However the estuarine domain (brackish water, hydrodinamically influenced by the tides) starts 166 km upstream of Le Havre in Poses. River Seine is generally considered 7th order from the confluence with river Yonne, and becomes 8th order after the confluence of the river Oise downstream from Paris. River Marne is 6th order. The three main tributaries (Seine upstream from Paris, Marne and Oise rivers) all cross about the same portion sof concentric geological formations and have therefore quite similar morphological and hydrological charcteristics.

River discharges are generally well regulated due to multiple factors such as :

- a pluviometry distributed over the whole year with an "oceanic" hydrologic regime.
- the presence of sedimentary formations that have good water retention properties,
- an important part of discharges coming from baseflow from deep aquifers.

The dominating oceanic westernly winds supply rather constantly the basin in humidity as in an oceanic regime. This lead to large precipitations firstly on coastal

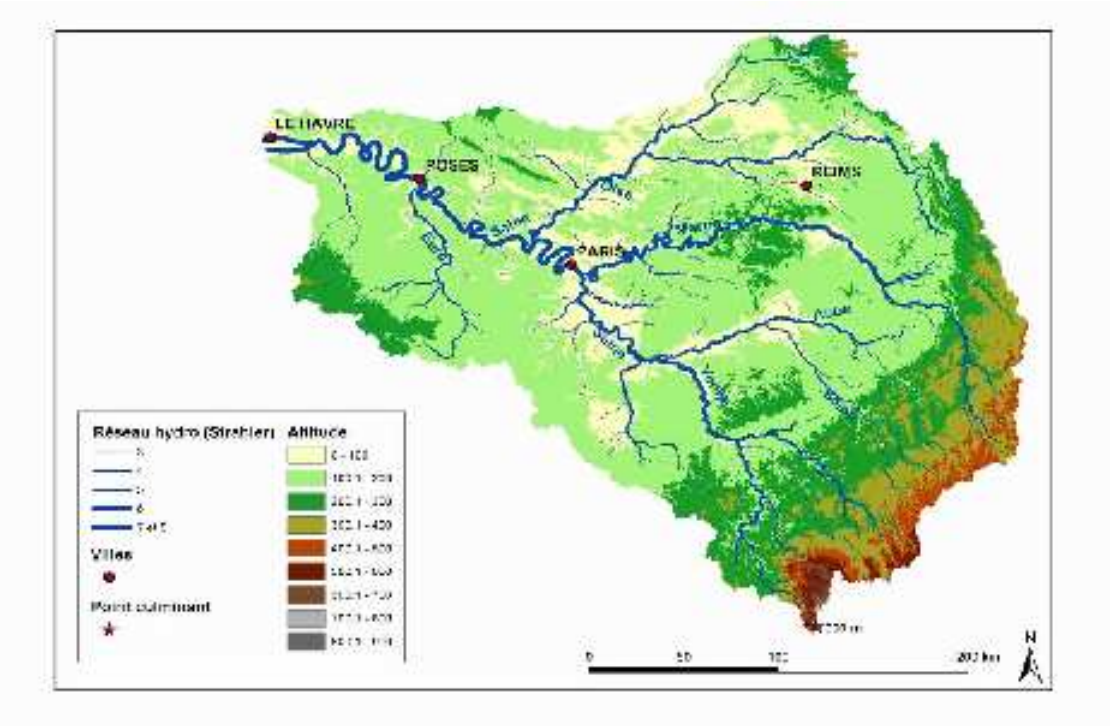

Figure 4.1: Topography and hydrographic network of the Seine basin. Altitudes, main tributaries and main cities are labeled. Strahler stream orders from 3 to 8 are represented only. The highest point in Morvan is marked with a star. Source: Ducharne et al. 2004

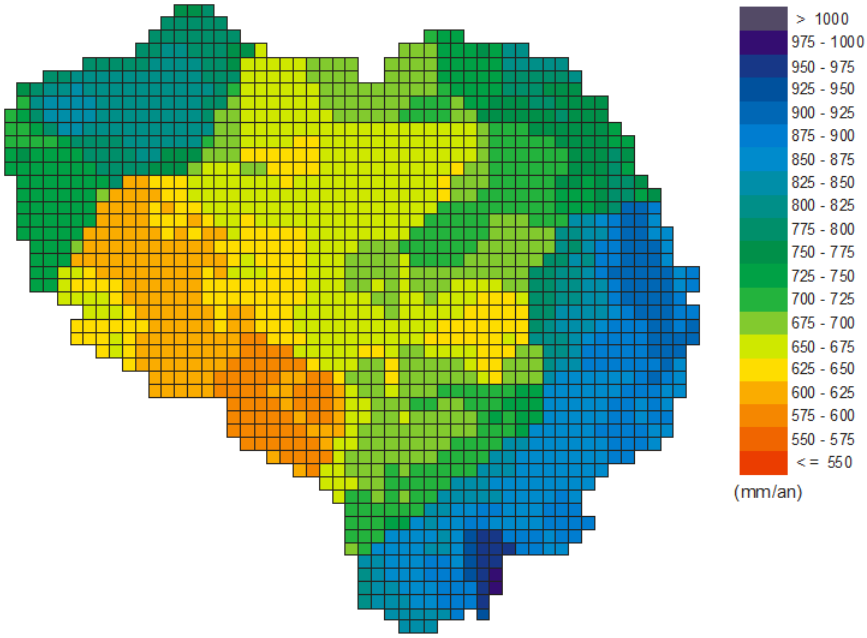

Figure 4.2: Spatial distribution of annual mean precipitation over the Seine river basin. Mean values in mm/y have been computed from SAFRAN 1970-1990. Source: Ducharne et al. 2004.

parts of the basin and then on the eastern orographic obstacles (figure 4.2). Annual mean precipitation over the basin is 750 mm/y (mean value over 1931-1960, Ducharne et al. 2004). It splits into 550 mm/y of evaporation and 200 mm/y of runoff. This last value is smaller than other French rives that flows from higher montainous areas with higher precipitation. The Seine river is also the French river less influenced by snow regime: snow days are rare (except on Morvan where there can be up to 40 days/year of snow). Snow influence on the Seine river hydrologic regime is negligible.

The Seine river has a "pluvial-oceanic" hydrologic regime more driven by evapotranspiration than by precipitation which is well distributed over the year. Discharge maxima are in winter when evapotranspiration is little and minima in summer when evapotranspiration is enhanced. At Poses, annual mean discharge is 480 m^3/s with a minimum of 240 m^3/s in august and a maximum of 805 m^3/s in february (average over 1974-2000). Major flood events in 1910, 1955 and 2001 had peak discharges at Poses of 2500, 2300 and 2200 m^3/s respectively.

The Seine river basin has a very homogeneous topography, geology and pluviometry. Thank to this fact, all the main tributaries have similar and homogeneous hydrologic regimes.

In the framework of this thesis we have made the choice of analysing the results mostly in Poses which is the last gauging station not to be in the estuarine domain of the Seine. We will discuss all our results as averages over all the Seine river basin upstream from Poses unless otherwise stated. This choice makes sense and is justified because of the great homogeneity that characterises the Seine river catchment.

4.2 Water management

The Seine River catchment (78600 km^2 (at Le Havre), that is 14 % of the surface of continental France) contains 17 millions of inhabitants (25 % of the national population) with 10 millions in the single agglomeration of Paris. 40% of the national industrial activities are located within the Seine river catchment.

In such an important area of the country, water related issues are given a very large attention. Water resources availability is not presently a major concern on the Seine river basin due to the large pluviometry and to the important aquifers. Flood protection is instead a very important issue because of the strategic importance of the areas within the Seine watershed. The construction of reservoirs in the upstream from Paris watersheds was planned after the 1910 flood event, which had caused large damages to Paris.

Three main storage-reservoirs were built between 1966 and 1989 on the Seine, Marne and Aube rivers on a clay ring-shaped formation 200 km upstream from Paris. On a regional scale, they have a spilling flood effect while, in Paris, they have mainly

the function of sustaining low flows in late summer and fall. In fact, output from these three reservoirs can be up to 60 m^3/s which means nearly doubling low flows discharge of the Seine at Paris (Meybeck, de Marsily, and Fustec 1998). Output from the three reservoirs improves water quality in low flows. Water supply for the Paris area comes mainly from the Seine through various intakes, thus, the three water reservoirs have the essential functions of allowing a reliable water supply in low flows.

4.3 Modeling the Seine river basin

The Seine river basin has been subdivided in 29 unit catchments with an average area of 2600 km^2. The CLSM model returns output variables such as runoff, evaporation and catchment deficit as averages over a unit catchment on a daily basis. Total are given over a unit catchment.

Until now, CLSM did not include any runoff routing procedure on the Seine river basin. Thus, runoff was compared to observed discharge over 10 days averages in order to take into account delay effects. In the last two years, a Muskingum routing procedure has been developed in the framework of two master's thesis at the Université Pierre et Marie Curie, Paris (Zhao 2006 and Bellier 2008).

Within the present thesis, Muskingum routing has been applied to produce daily discharges used for realising the validation (§ 4.4) and the empirical probability distribution analysis (chapter 5). Monthly and annual mean values have instead been computed without any routing procedure.

4.3.1 Muskingum routing

Muskingum routing is a lumped conceptual routing method based on the continuity equation and on an empirical storage relation:

$$\frac{dS}{dt} = I(t) - Q(t) + q(t) \tag{4.1}$$

$$S(t) = k[x \cdot I(t) + (1 - x) \cdot Q(t)] \tag{4.2}$$

S is the storage [m^3],
I is the inflow [m^3/s],
Q is the outflow [m^3/s],
q is the contributing lateral runoff [m^3/s],
x is a weighting factor $0 \leq x \leq 0.5$ [-],
k is the wave travel time in the reach [sec.].

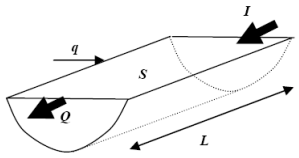

Figure 4.3: Schema of river reach. Source: Zhao 2006.

If the water storage in the channel is only controlled by the downstream condition we have x=0. On the contrary, x=0,5 gives same weight at both the inflow and the outflow (Musy and Higy 1998). The wave travel time k is expressed as :

$$k = \frac{L}{v} \tag{4.3}$$

L is the reach length [m],
v is the mean velocity in the reach [m/s].

Equations 4.2 are integrated with a finite difference method. Best compromise between acceptable computational costs and computing errors was found to be a Euler 1st order implicit integration method (Bellier 2008) with a timestep of 10800 seconds.

The wave travel time k and the x coefficient have been calibrated, and initial storage conditions have been defined through:

$$S_0 = A_0 \cdot L \tag{4.4}$$

A_0 is initial wet section [m^2],
S_0 is initial storage each [m^3].

At the end, Muskingum routing has been applied with the following parameters values:

Parameter	Unit	Value
x	[-]	0,02
v	[m/s]	1,45
A_0	[m^2]	10
dt	[s]	10800

Table 4.1: Muskingum routing parameters: x is a weighting parameter, v is the mean velocity over the reach, A_0 is the initial wet section, and dt is the chosen time step

4.3.2 Reservoir management

The three reservoirs on the Seine, Aube and Marne rivers are managed by the "Institution Interdepartementale des Barrages-reservoirs du bassin de la Seine".

Reservoir records (outflows) are available on the 1981-2002 time period. These records have been used on validation (§ 4.4) for comparing simulated and observed discharge values at various gauging stations .

When dealing with climate scenarios instead, it is not possible to guess what decisions would be taken in terms of reservoir management. Thus, a mean reservoir management year has been built averaging reservoirs management record over the 1981-2002 time period. Simulated and routed discharges from climate scenarios have been corrected taking into account this mean reservoir management year.

4.3.3 Data

A high-resolution **digital elevation model** (100-m resolution DEM) was used to characterise the distribution of the topographic index in each unit catchment.

The **vegetation** properties have been derived from the ECOCLIMAP dataset (Masson et al. 2003) which has a resolution of 1km and reflects land use in the 1993. ECOCLIMAP has 215 vegetation classes which have been translated in the 8 vegetation types of CLSM. It gives information on vegetation phenology and associated soil morphology parameters (such as root zone depth) at the monthly timestep. Figure 4.4 shows the percentage of woods within each unit catchment.

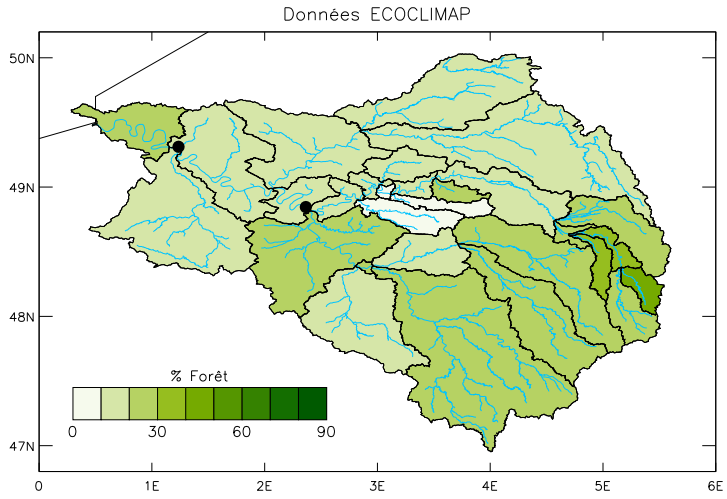

Figure 4.4: Unit catchment subdivision and vegetation. The Seine river basin has been subdivided into 29 unit catchments. Green color indicates the percentage of woods in each unit catchment. Points indicate the gauging station at Paris and Poses. Source: Ducharne

ECOCLIMAP also contains information on sand and clay content based on FAO global data and soil map of France (Jamagne et al. 1995). Using the USDA classification it is possible to link sand and clay content to a soil texture class. Then, for each texture class, **soil hydraulic parameters** are derived according to the values

indicated in Cosby et al. 1984: hydraulic conductivity, matrix potential in the soil at saturation, wilting point, b parameter of equation (3.3).

ECOCLIMAP dataset is not sufficient for characterising three important parameters of CLSM for which a calibration has been required (Ducharne 2008) : hydraulic saturated conductivity, the decay parameter ν and the total soil depth [1].

It has been already discussed (§ 4.3.1) that CLSM did not include until now any routing model. **Calibration** of the CLSM model for the GICC Seine project was done in 2003-2004 running the SAFRAN[2] observed climate dataset between 1985-1991 and comparing its runoff values to the observed discharges (taking into account the historical records concerning reservoir management, refer to § 4.3.2). **Observed daily streamflow data** have been collected from the *Banque Hydro* database[3].

Since there was no routing procedure, performances were evaluated in terms of 10 days averages with the **Nash-Sutcliffe coefficient** N :

$$N = 1 - \frac{\sum_i^n (Q_{sim} - Q_{obs})^2}{\sum_i^n (\bar{Q}_{obs} - Q_{obs})^2} \tag{4.5}$$

where

Q_{sim}	is the simulated discharge
Q_{obs}	is the observed discharge
$\bar{Q}_{obs}$	is the mean observed discharge over the whole period
n	is the number of days in the period

Nash efficiency coefficient can assume values between -∞ and 1. Optimal value is 1, meaning that the model predict perfectly observed discharges. A zero value of the Nash coefficient means instead that the model does not predict observed discharges better than substituting simulated values with the mean observed discharge (Nash and Sutcliffe 1970). It is classical to consider that a model is acceptable if it has a Nash criterium above 0,7.

Five parameters of CLSM were calibrated (3 concerning the TOPMODEL's framework and 2 concerning the linear reservoir):

- The hydraulic conductivity[4] at saturation.
- The TOPMODEL soil depth D.

[1]Soil depth is calibrated since it is a poorly known parameter, contrary to the root zone depth which is constrained by the vegetation cover.

[2]Details on the SAFRAN dataset are given in §5.3.

[3]www.hydro.eaufrance.fr

[4]See §3.2.3.1.

- The third calibration parameter is ν which is the decay parameter with depth of the hydraulic conductivity (equation (3.1)).
- The maximum catchment deficit M_G up to which there is a recharge to the deep LR's reservoir is calibrated too
- The fifth calibration parameter is the LR's discharge flux timescale τ_G. The recharge to the LR timescale parameter τ_r has not been calibrated since it showed very little influence.

The 29 unit cactchment were all calibrated over 1985-1991 time in order to obtain a Nash coefficient as great as possible on all existing gauging stations and especially at Poses. 6 calibration datasets gave very similar and acceptable Nash coefficients (see next section).

4.4 Validation of CLSM

CLSM model has been used on the Seine river catchment for many years. It has been already used for modeling climate change impacts on the Seine watershed in the framework of the GICC-Seine project[5] (Ducharne et al. 2004 and Ducharne et al. 2007).

Since the Muskingum routing is now working and since SAFRAN, reservoir management records and observed discharges are now available on a longer time period, in the framework of this thesis a validation of the CLSM model has been conducted on 1981-2002 time period.

The following six calibrated versions have been tested:

LRON: it is the version which had the best performances on the previous calibration. It was calibrated through maximising Nash's coefficient in the upstream unit catchments first (in red in figure 4.6) and in the downstream reaches afterwards. CLSM with linear reservoir is applied, even if the linear reservoir is not activated in all catchments. All simulations analysed in chapter 5 have been realised with this run.

NOLR: it is the best version of the CLSM without linear reservoir. It was calibrated with same technique as above.

Stockmin: it was calibrated with two criteria: obtaining acceptable Nash coefficients and a minimum linear reservoir content.

[5]GICC-Seine is the "Gestion et Impact du Changement Climatique" research programme supported by the French "Ministère de l'Ecologie et du Developpement Durable".

Stockmax: it was calibrated with two criteria: obtaining acceptable Nash coefficients and a maximum linear reservoir content.

Downstream LRON: Upstream unit catchment (figure 4.6) were calibrated as in "LRON" run while downstream unit catchments parameters were uniformly chosen for a CLSM version with linear reservoir.

Downstream NOLR: Upstream unit catchment (figure 4.6) were calibrated as in "LRON" run while downstream unit catchments parameters were uniformly chosen for a CLSM version without linear reservoir.

NOLR is the only run which does not include a deep linear reservoir. The other 5 runs described above all include a linear reservoir at least in some unit catchments. We will refer to these 5 runs as the "CLSM with LR" runs.

Table 4.2 summarises mean observed and simulated discharges and Nash-Sutcliffe efficiencies for the six calibrated versions at Paris and Poses for calibration (1985-1991) and validation (1981-2002). The six simulations have very similar Nash-Suttcliffe coefficients. Nash coefficients at Poses and Paris are generally slightly higher over 1981-2002 validation than on 1985-1991 calibration period. This is an encouraging result since it means that the model has been "robustly" calibrated.

In figure 4.5 are represented observed and simulated discharges at Poses and Paris all along the validation period. Performances of CLSM-LRON are very good.

Validation on the other unit catchment and for the six calibration set is not attached due to lack of space. Routed CLSM does not perform well on all unit catchments, having a Nash coefficient below 0,6 on 9 unit catchments (Yonne, Loing, Grand Morin, Eure, Surmelin, Marne, Petit Morin, Ourcq and Blaise). Many of these unit catchments are upstream catchment (in red in figure 4.6) with deeper sedimentary layers.

	Paris				Poses			
	1985-1991		1981-2002		1985-1991		1981-2002	
	Q [m^3/s]	Nash [-]	Q [m^3/s]	Nash [-]	Q [m^3/s]	Nash [-]	Q [m^3/s]	Nash [-]
Observation	318,36	-	269,76	-	544,21	-	445,38	-
LRON	326,52	0,86	285,09	0,89	506,75	0,86	452,47	0,89
NOLR	300,5	0,85	251,85	0,89	473,73	0,81	411,79	0,86
Stockmin	325,45	0,88	283,6	0,91	513,8	0,85	456,23	0,89
Stockmax	327,71	0,86	287,22	0,89	509,22	0,86	462,77	0,87
Downstream LRON	313,69	0,82	282,56	0,85	473,59	0,85	438,47	0,81
Downstream NOLR	318,3	0,9	276,44	0,91	491,43	0,82	433,88	0,87

Table 4.2: Validation of CLSM performances - SAFRAN 1981-2002: First line gives observed discharges. In the other lines for each calibrated version, simualted discharge and Nash-Sutcliffe coefficients are given at Paris and at Poses on calibration (1985-1991) and validation (1981-2002) periods.

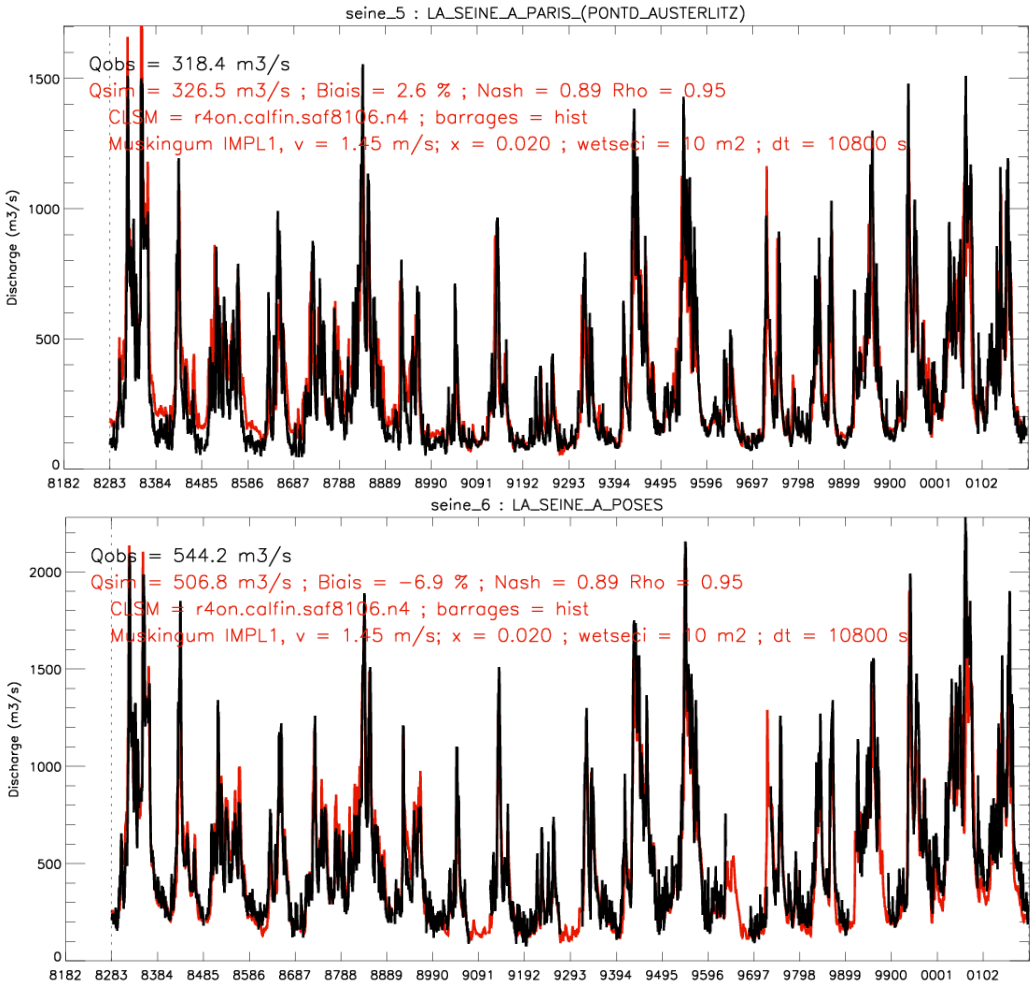

Figure 4.5: Validation of CLSM - LRON version over 1981-2002 at Paris and Poses Black curve represents observed discharge while red curve is SAFRAN with LRON CLSM calibrated run.

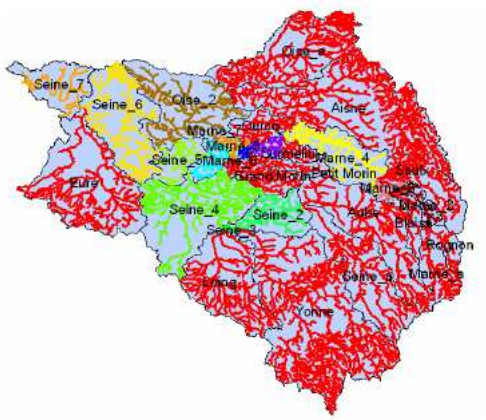

Figure 4.6: Hydrographic network of the Seine river catchment. Red areas are the upstream unit hydrograph which are firstly calibrated. "Seine-5" indicates the Seine at the Paris gauging station.

4.5 Equifinality

There is a open debate in hydrological modeling community on the concept of *equifinality*. A definition of this concept is that there is "equifinality" between models or parameter sets when they all provide similar and acceptable fits to observational data (Beven 2006).

Historically the term equifinality has been used for a long time in geomorphology, indicating that similar landforms might arise as a result of quite different sets of processes and histories. Thus, from the landform alone, without additional evidence, it might be difficult to identify the particular set of causes.

Equifinality was later adopted for environmental modeling also due to the existence of many empirical studies that have where various models were giving good fits to the same data. However many modellers do not fully accept the idea of equifinality in their models. This opposition is probably in relation with a key concept in philosophy: Science, including hydrology, is supposed to be an attempt to work towards a single correct description of reality. It is not supposed to conclude that there are multiple descriptions of reality.

The open debate between hydrologists is wheter one should concentrate on the search of an optimum (in terms of calibration parameter sets) or accept multiple versions (i.e. descriptions of reality) and assess the uncertainties associated to these predictions.

Climate change impact studies are all based on multiple descriptions of what could be reality in the future. This is accomplished trough multi-models and multi-scenarios representations of reality with assessment of the uncertainties and range of variation associated to these scenarios. The REXHYSS project applies this typical multi-model and multi-scenario approach of climate change studies. We describe

fully the multi-scenario assessment in chapter 5. In addition, this thesis applies an "equifinality approach" also on the assessment of the uncertainties in climate change predictions caused by various runs of CLSM. This section is focused on this analysis.

According to Beven (2006), *non uniqueness* indicates the fact that multiple models might give equally acceptable fits to observational data. The six runs of CLSM described in the previous paragraph showed similar performances in simulating observed discharges. In particular their Nash-Sutcliffe coefficients and biases versus observation were very close. It is a typical situation of *non uniqueness* in model identification.

To assess uncertainties due to the choice of the calibrated parameter set, we realised 6 different runs of the SAFRAN observed climate dataset[6] (Quintana-Seguí et al. 2008) over 1981-2002 and of the A1BCONT continuous simulation over 1950-2099. Climate forcings for the A1BCONT simulation have been produced with the variable resolution general circulation model (GCM) Arpege climat version 3+ under A1B GHGs emission scenarios for future time and downscaled with the weather regime approach (described in § 5.1 and 5.4). In the following pages we will refer to the SAFRAN run with CLSM-LR-ON parameters as "SAFRAN run" and and to the A1BCONT run with with CLSM-LR-ON as "A1BCONT run". "A1BCONT run" and "SAFRAN run" are the reference runs for observed present time and for climate change simulations in the next chapter.

The choice has been made to discuss the "equifinality" issue in this chapter rather than in chapter 5, even if we use datasets and methods fully described in that chapter, to follow the "chronological" and logical order of the experimental procedure. First we have tested various runs of CLSM on present (§ 4.5.1) and future time (§ 4.5.2). Then, since the 6 runs did not lead to sensibly different results, assessment of climate change impacts described in chapter 5 has been realised with the LR-ON run only.

4.5.1 SAFRAN annual mean cycle (1982-2000)

Figure 4.7 shows simulated annual mean cycles for the 6 versions of CLSM forced by the same observed and reanalysed climate from SAFRAN dataset. Note that LRON is in the middle of the other runs, which were selected to this purpose. In the numerous parameter sets that were giving similar scores in the calibration exercise at Poses, 6 sets were chosen, based on the modeler's experience, to be representative of contrasted hydrodynamics. As such, they are likely to lead to different climate change impacts, and should provide an interesting sample of the uncertainties related to parameter calibration. Tables 4.3, 4.4 and 4.5 summarise the mean values, biases

[6]Some details on SAFRAN are given in § 5.3.

and impacts and quantify the uncertainties in terms of standard deviation.

The six runs reproduce a very similar **evaporation** since they have a standard deviation of only 0,02 mm/d with a mean value of 1,6 mm/d (table 4.3 and figure 4.7). Range of variation between the different versions is slightly larger in the summer months than in the rest of the year.

Climate dataset	SAFRAN	Arpv3+ - WR				Impact	Rel. Impact
	PT	PT	Bias	Rel. bias	21f	21f - PT	(21f-PT)/PT
	mm/d			%	mm/d		%
	Total runoff						
NO LR	0,54	0,45	-0,09	-17,37	0,2	-0,25	-55,53
LR ON	0,59	0,48	-0,11	-18,36	0,23	-0,25	-52,25
Stockmax	0,6	0,48	-0,12	-19,34	0,22	-0,26	-53,84
Stockmin	0,6	0,49	-0,11	-17,97	0,23	-0,26	-52,73
Downstream - LR on	0,56	0,44	-0,12	-22	0,2	-0,24	-54,41
Downstream – no LR	0,57	0,47	-0,11	-18,53	0,21	-0,25	-54,36
Mean (5 runs)	0,58	0,47	-0,11	-19,21	0,22	-0,25	-53,49
Std dev (5runs)	0,02	0,02			0,01		
	Evaporation						
NO LR	1,63	1,65	0,02	1,19	1,63	-0,02	-1,18
LR ON	1,58	1,61	0,03	1,77	1,61	0,00	0,00
Stockmax	1,58	1,61	0,03	1,93	1,58	-0,03	-1,89
Stockmin	1,58	1,61	0,03	1,76	1,58	-0,03	-1,72
Downstream - LR on	1,62	1,66	0,03	2,06	1,62	-0,03	-2,02
Downstream – no LR	1,60	1,63	0,03	1,73	1,6	-0,03	-1,71
Mean (5 runs)	1,59	1,62	0,03	1,85	1,6	-0,02	-1,47
Std dev (5runs)	0,02	0,02			0,02		

Table 4.3: Mean, biases and impacts of six runs of CLSM - Total runoff and evaporation. For each run, the first column indicates the mean value over 1982-2000 forced by the observed and reanalysed SAFRAN dataset, second column is the value simulated with Arpege version 3+ climate forcings on the same period of time. Bias between Arpv3+ and SAFRAN is given next. Relative bias is in terms of SAFRAN of value. Mean values for 21f time period (2081-2099) are given in the next column, with their impacts in percentage of the 1982-2000 mean value. Last lines give the mean and the standard deviation values of the 5 CLSM runs with linear reservoir

Total runoff too is not very much influenced by the choice of the CLSM run. The six runs have very close mean values (table 4.3) with a std. dev.=0,02 mm/d and mean=0,58 mm/d. Range of variation is larger in high flows (December till March) and in very low flows (June to September).

The **catchment deficit**, the **linear reservoir water content**, **surface runoff** and **baseflow** from linear reservoir all show a distinct behavior between CLSM-noLR and the 5 runs of CLSM-LR (figure 4.7). This is because in CLSM-noLR, total runoff is composed of two fluxes (surface runoff and TOPMODEL's baseflow) while CLSM-LR has a third flux (baseflow from linear reservoir). Thus CLSM-noLR has to subdivide the same runoff on only two fluxes. This implies having a

higher soil catchment deficit (a lower soil moisture content) that produces a greater TOPMODEL's baseflow.

Climate dataset	SAFRAN	Arpv3+ - WR				Impact	Rel. Impact
	PT	PT	Bias	Rel. bias	21f	21f - PT	(21f-PT)/PT
	mm			%	mm		%
	Catchment deficit						
NO LR	266,9	279,63	12,7	4,8	367,9	88,3	31,6
LR ON	145,5	146,69	1,2	0,8	193,0	46,4	31,6
Stockmax	157,9	158,0	0,0	0,0	207,1	49,1	31,1
Stockmin	148,2	149,7	1,4	1,0	197,0	47,3	31,6
Downstream - LR on	182,2	182,9	0,7	0,4	243,4	60,6	33,1
Downstream – no LR	136,0	137,7	1,7	1,2	186,2	48,5	35,2
Mean (5 runs)	154,0	155,0	1,0	0,7	205,3	50,4	32,5
Std dev (5runs)	17,6	17,2			22,6		
	Linear reservoir water content						
NO LR	NO	NO	NO	NO	NO	NO	NO
LR ON	123,2	88,5	-34,7	-28,2	33,0	-55,4	-62,7
Stockmax	182,3	127,1	-55,1	-30,3	45,1	-82,0	-64,5
Stockmin	109,2	74,8	-34,4	-31,5	23,7	-51,1	-68,3
Downstream - LR on	194,0	118,2	-75,8	-39,1	37,6	-80,7	-68,2
Downstream – no LR	100,8	67,7	-33,2	-32,9	20,9	-46,8	-69,1
Mean (5 runs)	141,9	95,3	-46,7	-32,4	32,1	-63,2	-66,6
Std dev (5runs)	43,2	26,3			10,0		

Table 4.4: Mean, biases and impacts of six runs of CLSM - Catchment deficit and linear reservoir water content. For each run, the first column indicates the mean value over 1982-2000 forced by the observed and reanalysed SAFRAN dataset, second column is the value simulated with Arpege version 3+ climate forcings on the same period of time. Bias between Arpv3+ and SAFRAN is given next. Relative bias is in terms of SAFRAN of value. Mean values for 21f time period (2081-2099) are given in the next column, with their impacts in percentage of the 1982-2000 mean value. Last lines give the mean and the standard deviation values of the 5 CLSM runs with linear reservoir

The 5 LR-on runs (concerning the catchment deficit, the linear reservoir water content, surface runoff and baseflow from linear reservoir) show greater differences than on total runoff and evaporation. This shows that the linear reservoir has a greater sensitivity than the rest of CLSM model. The 5 runs can still be considered to give similar representations of these 5 variables since they have relatively little standard deviations values (table 4.4 and 4.5). In particular the SAFRAN LR-ON run is quite close to the mean of the 5 LR-on simulations.

This assessment shows that 6 runs of CLSM (and particularly the 5 runs with a linear reservoir) have a similar behavior (particularly concerning total runoff and evaporation) when forced with SAFRAN observed climate. It means that simulated variables are robusts with respect to the choice of the CLSM run.

In fact, we could have expected this result from the beginning since we are assessing CLSM runs fed with the same climate data used for calibration. It is reassuring

Climate dataset	SAFRAN	Arpv3+ - WR				Impact	Rel. Impact
	PT	PT	Bias	Rel. bias	21f	21f - PT	(21f-PT)/PT
	mm/d			%	mm/d		%
	Surface runoff						
NO LR	0,13	0,11	-0,02	-16,4	0,06	-0,05	-46,6
LR ON	0,09	0,08	-0,01	-13,8	0,04	-0,03	-43,8
Stockmax	0,09	0,07	-0,01	-13,5	0,04	-0,03	-44,0
Stockmin	0,09	0,08	-0,01	-14,3	0,04	-0,04	-44,1
Downstream - LR on	0,08	0,07	-0,01	-14,6	0,04	-0,03	-38,0
Downstream – no LR	0,09	0,07	-0,01	-15,4	0,04	-0,03	-45,7
Mean	0,09	0,08	-0,01	-14,8	0,04	-0,04	-44,0
Std dev	0,02	0,01	0	1,1	0,01	0,01	3,0
	TOPMODEL's baseflow						
NO LR	0,42	0,34	-0,07	-17,67	0,14	-0,20	-58,27
LR ON	0,30	0,26	-0,03	-11,25	0,13	-0,14	-52,17
Stockmax	0,26	0,23	-0,03	-10,50	0,11	-0,12	-52,40
Stockmin	0,31	0,27	-0,04	-12,07	0,13	-0,14	-52,87
Downstream - LR on	0,25	0,22	-0,02	-8,98	0,11	-0,12	-52,30
Downstream – no LR	0,35	0,30	-0,05	-13,35	0,14	-0,16	-53,33
mean	0,29	0,27	-0,02	-6,55	0,12	-0,15	-55,11
std dev	0,04	0,03	0,01	1,64	0,01	0,02	0,48
	LR's Baseflow						
NO LR							
LR ON	0,21	0,14	-0,06	-30,6	0,06	-0,08	-57,1
Stockmax	0,25	0,18	-0,08	-30,3	0,07	-0,11	-59,9
Stockmin	0,19	0,14	-0,06	-29,2	0,06	-0,08	-57,4
Downstream - LR on	0,23	0,14	-0,09	-38,2	0,05	-0,09	-65,4
Downstream – no LR	0,14	0,09	-0,05	-33,2	0,03	-0,06	-64,5
mean	0,21	0,14	-0,07	-32,3	0,05	-0,08	-60,6
std dev	0,04	0,03	0,02	3,6	0,01	0,02	3,9

Table 4.5: Mean, biases and impacts of six runs of CLSM - Surface runoff, Topmodel's baseflow and LR's baseflow For each run, the first column indicates the mean value over 1982-2000 forced by the observed and reanalysed SAFRAN dataset, second column is the value simulated with Arpege version 3+ climate forcings on the same period of time. Bias between Arpv3+ and SAFRAN is given next. Relative bias is in terms of SAFRAN of value. Mean values for 21f time period (2081-2099) are given in the next column, with their impacts in percentage of the 1982-2000 mean value. Last lines give the mean and the standard deviation values of the 5 CLSM runs with linear reservoir

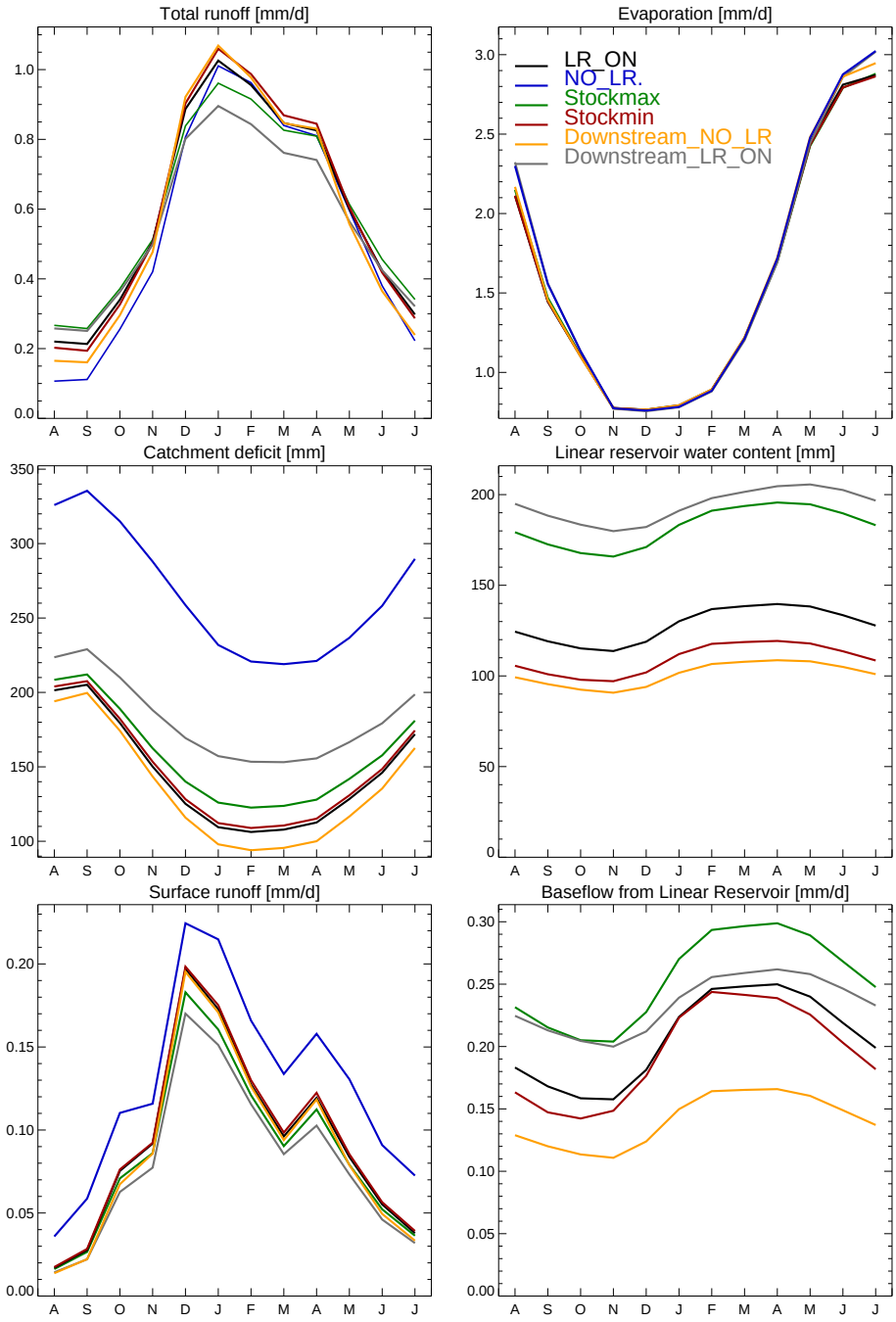

Figure 4.7: Six runs of CLSM - SAFRAN dataset (1981-2002). Mean annual cycle over all the catchment at Poses for total runoff, evaporation, catchment deficit, linear reservoir water content, surface runoff and baseflow from linear reservoir. Black curve represents "SAFRAN run" (CLSM-LRon) which is used in all the simulation of the next chapter as the reference baseline for present time. Blue is CLSM without linear reservoir. Green curves are "stockmax" (dark green) and "stockmin" (light green) runs which were calibrated with the will of having respectively maximum and minimum water content in the linear reservoir. Orange is the "Downstream NO LR" run and grey is the "Downstream LR on" run. These two runs have been calibrated with the same parameters as LRon on upstream unit catchment (in red in figure 4.6) and with the best uniform calibration parameters (respectively withouth LR or with LR) on the downstream unit catchment.

(and quite expectable) that runs that had close values of the Nash coefficient have globally a similar behavior when fed with the same forcings on the same period. The truly exciting question concern how do these 6 runs behave with other climate forcings and on such a long and different time period as the 1950-2099 period. We will discuss this issue in next subsection.

4.5.2 Equifinality in climate change simulation (1950-2099)

In this section we compare 6 runs of CLSM fed with the same climate forcings issued from the ARPEGE Climat v3+ GCM downscaled with the weather regime approach (that is the A1BCONT dataset described in § 5.1). Many expressions of this section recall concepts fully described in nexte chapter. However we chose to place thi section here to justify the choice of realising all the simulation analysed in next chapter with the LR-ON run of CLSM.

Simulated annual mean trends of evaporation and total runoff are very slightly influenced by the choice of the CLSM run (figure 4.8). Impact of climate change on total runoff (defined as the difference between the mean value over 2081-2099 and the 1981-2000 value) is robusts since it is much greater than standard deviation (table 4.3). Mean evaporation remains nearly stable with climate change and this one of the causes of un robust trend on evaporation (mean impacts show smaller values than standard deviation).

The 6 runs show very close simulated mean annual cycle of evaporation and runoff both on 1981-2000 and 2081-2099 time periods (figures 4.9 and 4.10). Seasonal impacts are robusts since uncertainties due to the choice of the run are much smaller than the projected impact.

The catchment deficit is obviously largely influenced by the presence or absence of the linear reservoir. Comparing the 5 runs with linear reservoir, simulated trends on catchment deficit and linear reservoir content (figure 4.8) have a greater range of variation than on runoff and evaporation, however mean impact (reduction of soil moisture content) seems rather robust since they are greater than the standard deviation (table 4.4). In terms of seasonal behavior uncertainties pending on the catchment deficit are much larger in the winter months than in the summer period.

The 5 runs with linear reservoir simulate similar impacts on surface runoff and baseflow too (figures 4.9 and 4.10). These impacts seem quite robusts since greater than the standard deviation (table 4.5).

Generally speaking the selected 6 runs which showed good performances in validation simulate very similar climate change impacts. We have realised all the simulations described in the next chapter with the “LRon” run. This “LRon” run, which is called in next chapter “A1BCONT” for the continuous climate change simulation and “SAFRAN” when fed with the SAFRAN observed dataset, is most of the time within the mean +/- standard deviation curves limits (figure 4.8) and shows a

medium range seasonal behavior (figures 4.9 and 4.10). The main conclusion of the present assessment is that climate change impacts analysed in detail in next chapter are not sensibly driven by the choice of CLSM run.

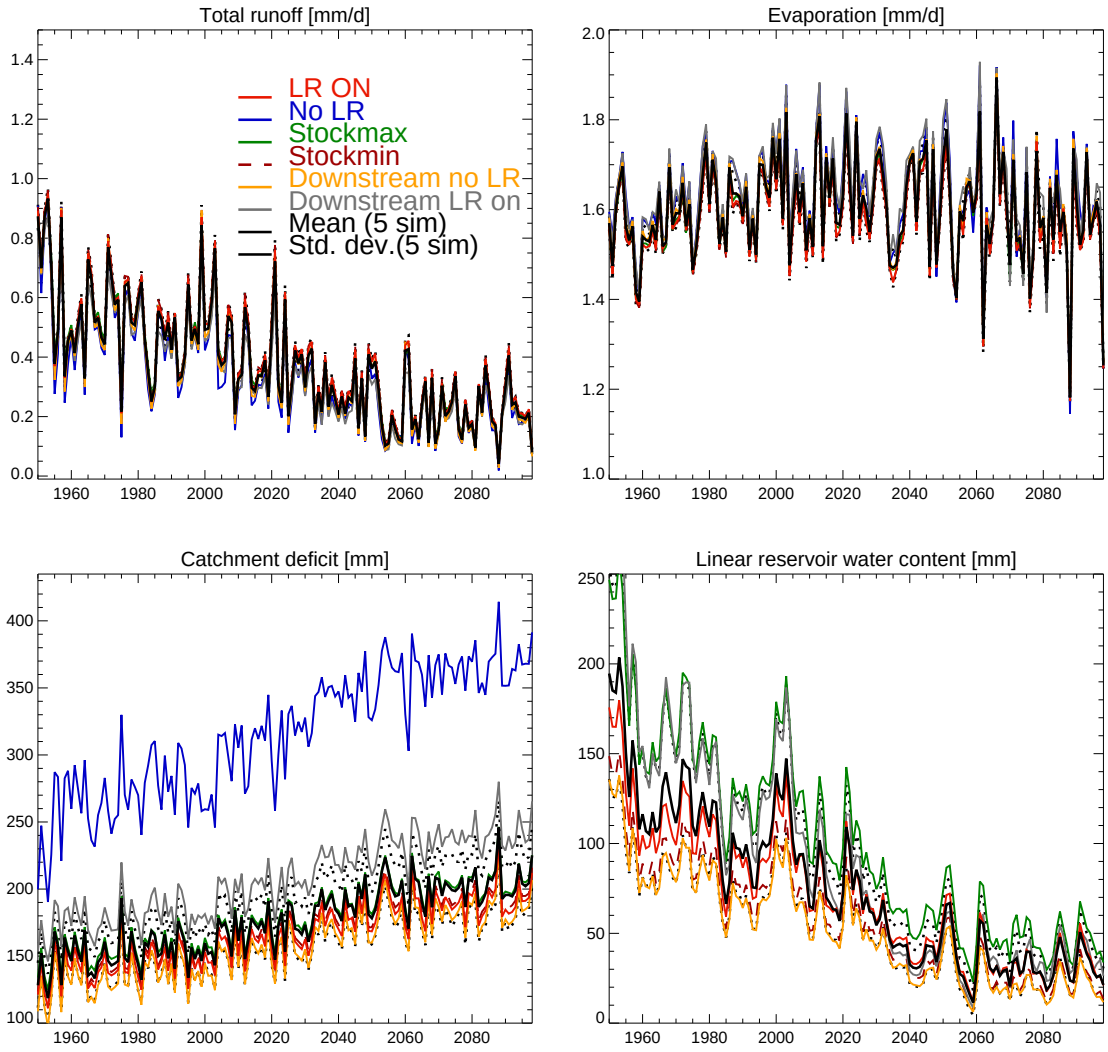

Figure 4.8: Six runs of CLSM - Arpege-v3+ - weather regime approach (1950-2099). Annual mean trends over all the catchment upstream of Poses for total runoff, evaporation, catchment deficit and linear reservoir water content. The curves are different runs, all forced by Arpege version 3+ (under A1B green-house gases emission scenario) downscaled with the weather regime approach. Red is "A1BCONT run" (CLSM-LRon) which is used in the next chapter as the reference simulation for climate change. Dark blue is CLSM without linear reservoir. Green and brick red curves are "stockmax" (dark green) and "stockmin" (dashed brick-red) runs which were calibrated with the will of having respectively maximum and minimum water content in the linear reservoir. Orange is the "Downstream NO LR" run and grey is the "Downstream LR on" run. These two runs have been calibrated with the same parameters as LRon on upstream unit catchment (in red in figure 4.6) and with the best uniform calibration parameters (respectively withouth LR or with LR) on the downstream unit catchment. Black lines are the mean and the standard deviation (dotted) of the 5 runs of CLSM-LR (excluding the CLSM-noLR run).

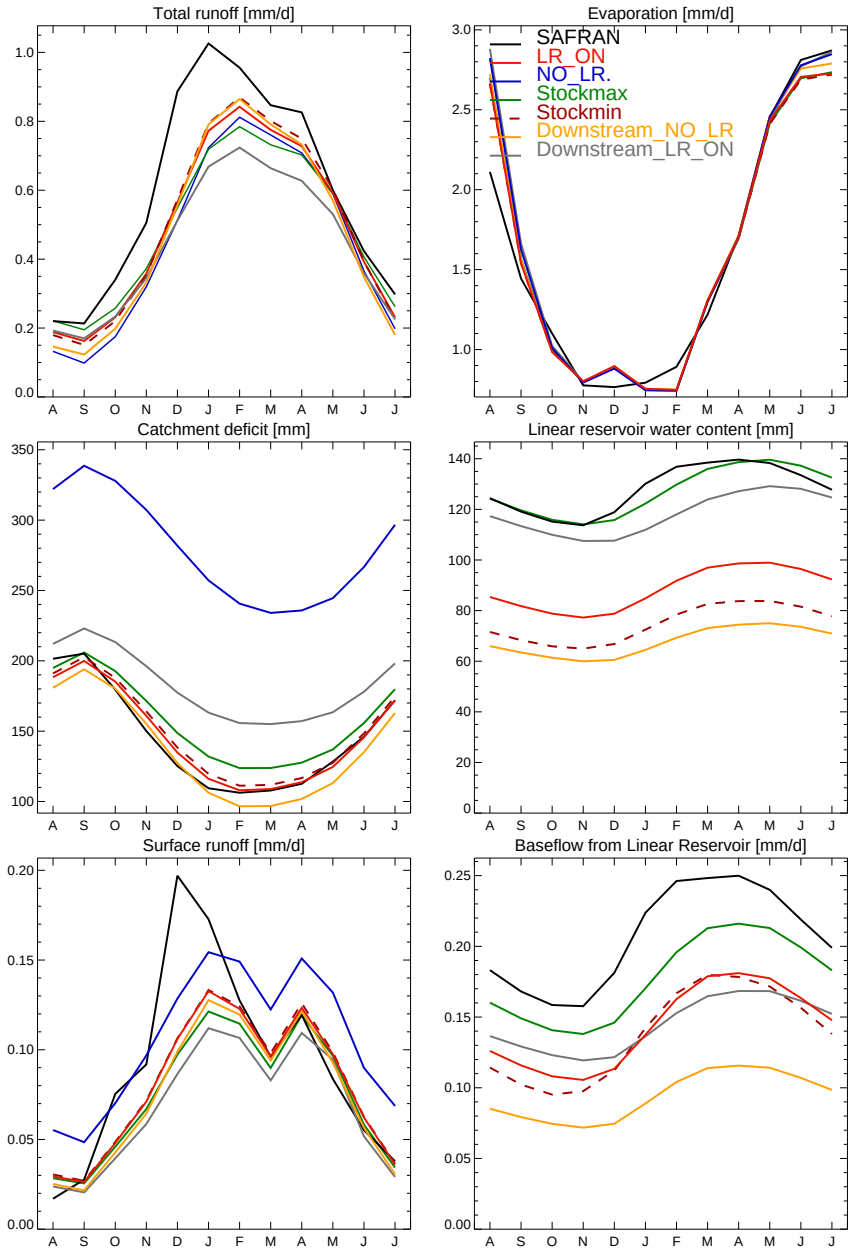

Figure 4.9: Six runs of CLSM - Arpege-v3+ - weather regime approach (1981-2002). Mean annual cycle over all the catchment at Poses for total runoff, evaporation, catchment deficit, linear reservoir water content, surface runoff and baseflow from linear reservoir. Black curve represents "SAFRAN run" (CLSM-LRon) which is used in all the simualtion of the next chapter as the reference baseline for present time. All other curves are different runs, all forced by Arpege version 3+ (under A1B green-house gases emission scenario) downscaled with weather regime approach. Red is "A1BCONT run" (CLSM-LRon) which is used in the next chapter as the reference simulation for climate change. Blue is CLSM without linear reservoir. Green and brick red curves are "stockmax" (dark green) and "stockmin" (dashed brick-red) runs which were calibrated with the will of having respectively maximum and minimum water content in the linear reservoir. Orange is the "Downstream NO LR" run and grey is the "Downstream LR on" run. These two runs have been calibrated with the same parameters as LRon on upstream unit catchment (in red in figure 4.6) and with the best uniform calibration parameters (respectively withouth LR or with LR) on the downstream unit catchment.

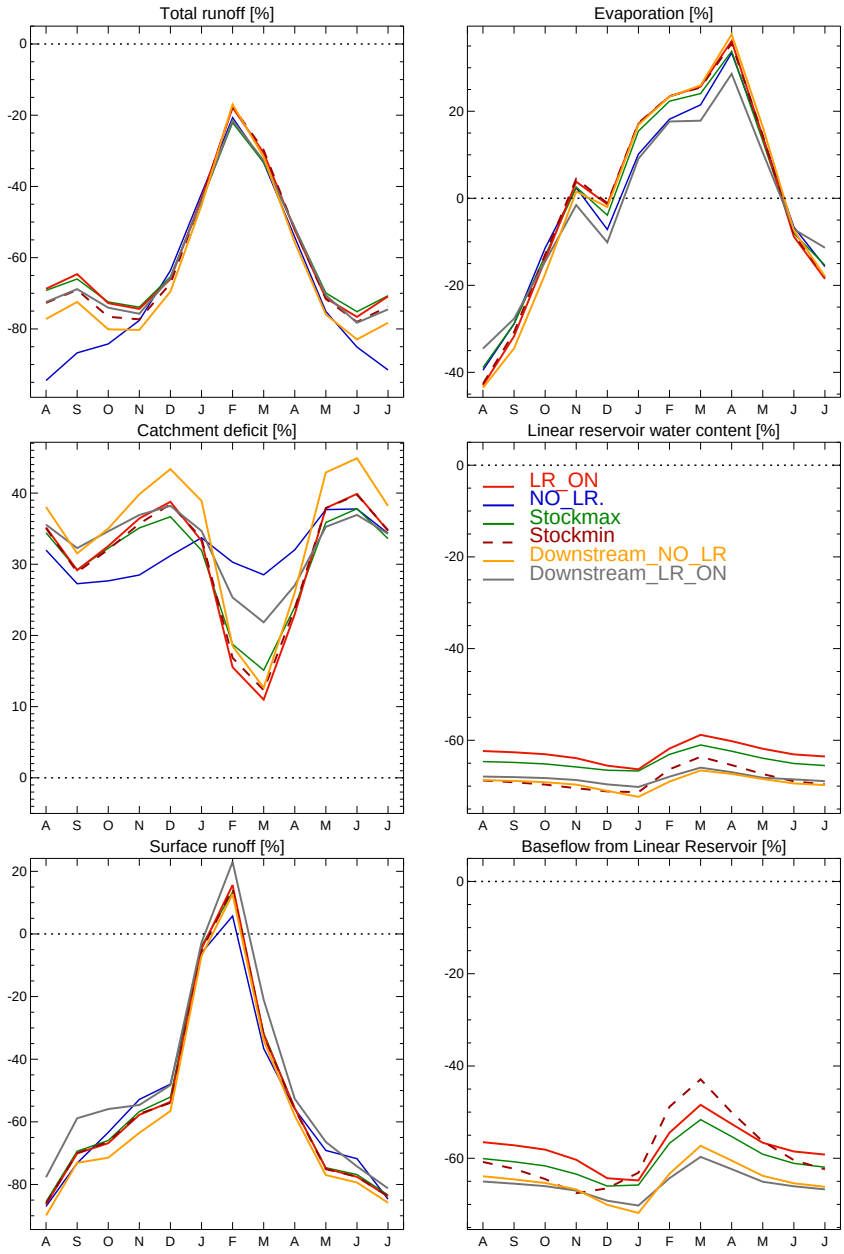

Figure 4.10: Six runs of CLSM - Arpege-v3+ - weather regime approach (2081-2099). Impacts on the mean annual cycle over all the catchment at Poses for total runoff, evaporation, catchment deficit, linear reservoir water content, surface runoff and baseflow from linear reservoir. The curves are various runs over 2081-2099, all forced by Arpege version 3+ (under A1B green-house gases emission scenario) downscaled with weather regime approach. For each simulation impacts are computed as the difference between future time (21f) and present time (PT: 1982-2000) monthly value and expressed in percentage of the present time value (except air temperature which is expressed in °C). Red is "A1BCONT run" (CLSM-LRon) which is used in the next chapter as the reference simulation for climate change. Blue is CLSM without linear reservoir. Green and brick red curves are "stockmax" (dark green) and "stockmin" (dashed brick-red) runs which were calibrated with the will of having respectively maximum and minimum water content in the linear reservoir. Orange is the "Downstream NO LR" run and grey is the "Downstream LR on" run. These two runs have been calibrated with the same parameters as LRon on upstream unit catchment (in red in figure 4.6) and with the best uniform calibration parameters (respectively withouth LR or with LR) on the downstream unit catchment.

Chapter 5

Modeling climate change impacts on hydrology

In chapter 2 we have described the modeling sequence required for producing local scale climate change impact results on hydrology. In chapter 3, we have analysed the catchment based land surface model (CLSM) which is the tool we have been using in this thesis to produce hydrological results from downscaled climate forcings. In chapter 4 we have described the choices made to obtain a good representation of the Seine watershed by the CLSM model particularly in terms of calibration.

All the previous chapters describe and analyse the tools we have directly or undirectly used to produce climate change impacts on the Seine river catchment hydrology. This chapter instead analyses in details the results we have obtained using the previously described tools. It is focused on a full analysis of all the simulations we have conducted to characterise climate change impacts and related uncertainties.

5.1 Set of simulations

5.1.1 Main set of simulations

Climate change scenarios are produced through a complex modeling sequence which has been described in chapter 2. Climate forcings depend from the chosen Green House Gases (GHGs) emission scenarios, the chosen General Circulation Model (GCM) and the chosen downscaling technique (DT). In the framework of the REXHYSS project, the choice has been made to use a great number of climate scenarios for evaluating climate change impacts on the Seine and Somme river basins. In this way it will be possible to test relative uncertainties due to each single element of the modeling sequence.

We have simulated future time hydrological behavior using 10 different climate forcings (table 5.1). Climate change simulations are generally conducted in *time-slices* mode because of high computational cost of longer simulations. However, in the framework of the Rexhyss project a continuous climate scenario is available. This scenario, to which we will refer from now on as the "'continuous"' scenario or as **A1BCONT**, has been produced under A1B emission scenario assumptions[1] with the variable resolution GCM ARPEGE Climat V3+ from the CNRM - Toulouse[2] (Gibelin and Déque 2003) and downscaled with the weather regime (WR) approach (Déque 2007). A1BCONT is a continuous simulation from August 1950 to July 2099. We will assume this simulation to be our **reference climate change simulation** while the other simulations will be used to characterize and quantify uncertainties due to multiple factors: GHGs, GCMs and the downscaling technique.

[1]For future time only.

[2]Centre National de Recherche Meteorologique - Toulouse - Meteo France

Name	GCM	Downscaling	PT	21m	21f
SAFRAN	No	No	Yes	No	No
ERA 40	No	WR	Yes	No	No
A1BCONT	ARPEGE Climat V3+	WR	Yes	A1B	A1B
$ARPV4_{VCM}$	ARPEGE Climat V4	VC	Yes	No	A1B and A2
$ARPV4_{WT}$	ARPEGE Climat V4	WR	Yes	No	A2
IPCC	7 GCMs (IPCC AR4)	WR	Yes	A1B	A1B

Table 5.1: Main set of simulations : for each simulation, the first column indicates the chosen name or abbreviation, in the second column the General Circulation Model's name is given, while the third column expresses the downscaling technique. SAFRAN and ERA 40 are not climate climate change scenarios but observed and reanalysed "present time" meteorological data and obviously no GCM has been used to produce their data. Due to its coarse resolution (2,5°), ERA 40 dataset requires downscaling (the **W**eather **R**egime approach), conversely no downscaling has been used for SAFRAN which has already a resolution of $8km \times 8km$. ARPEGE Climat v4 has been downscaled with both the weather regime approach and the **V**ariable **C**orrection **M**ethod. All the other simulations have been downscaled only with the **W**eather **R**egime approach. The three last columns show for which period of time, each simulation is available. All simulations in **P**resent **T**ime (August 1981 - July 1999) are based on observed GHGs and aerosols concentration. For future time periods (21m from August 2047 to July 2065, and 21f from August 2081 to July 2099) the selected GHGs emission scenario is given in the table: A1B or A2 (SRES 2000). Last line refers to seven simulations which differ only by the chosen GCM (see table 5.2) within the 23 of the IPCC AR4.

Other climate scenarios have been produced in *time-slices* mode. Each climate scenario has its own time-partitioning according to which we have obviously done our simulations. However, for clarity and to permit comparison we have chosen to analyse the results in three different 18 years long periods of time which are common to all the simulations[3](see figure 5.1) : **present time** from August 1981 to July 1999 (**PT**), 21^{st} century **middle future time** from August 2047 to July 2065 (**21m**) and 21^{st} century **future time** from August 2081 to July 2099 (**21f**). Each scenario is available at least on present time (PT) and on future time (21f). A1BCONT and 7 scenarios from the Intergovernmental Panel on Climate Change Fourth's Assessment Report (IPCC AR4) are also available on middle future time (21m).

Analysis realised on A1BCONT simulation (§ 5.4) is made on six 25 years long time periods which are defined in table 5.1.

In climate change research studies it is essential to evaluate representativity of simulated climate parameters versus observed. To that purpose, CLSM simulations forced by climate change simulated datasets are compared to CLSM simulations forced by observed and reanalysed surface meteorological datasets SAFRAN and ERA40 (Quintana-Seguí et al. 2008 and Uppala et al. 2005). Section 5.3 is focused on this issue.

After analysing in detail **A1BCONT** future climate reference simulation (§5.4), given the 11 climate forcing datasets, 3 main simulations intercomparisons will be discussed :

[3]From now on we will refer to these periods as PT, 21m and 21f.

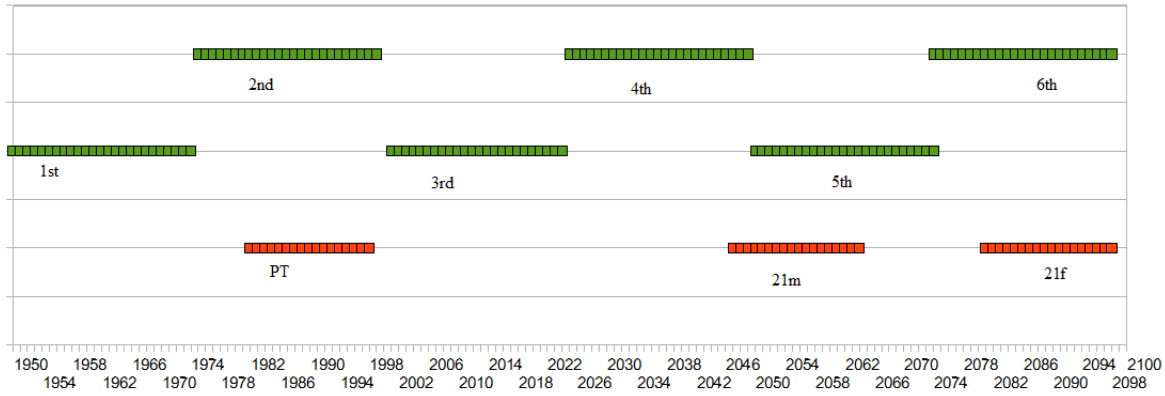

Figure 5.1: **Time partitioning** Red cells refer to 18 years long time periods: Present Time (PT: August 1981 - July 1999), middle future time (21m: August 2047 - July 2065) and future time (21f: August 2081 - July 2099). Green cells refer instead to 25 years long time periods used for A1BCONT continuous simulation analysis (§ 5.4.1 and 5.4.2).

GHGs emission scenario : we will compare **ARPV4-VCM-A2** and **ARPV4-VCM-A1B** simulations on 21f time period (§5.7). These two climate datasets have been both produced using the ARPEGE Climat v4 variable resolution GCM[4] and downscaled with the **V**ariable **C**orrection **M**ethod. Thus the differences between ARPV4-VCM-A2 and ARPV4-VCM-A1B simulations are only due to their GHGs emission assumptions taken from SRES 2000 emission scenarios (Nakinovic and Swart 2000).

General Circulation Models : A1BCONT and 7 simulations issued from 7 GCMs within the IPCC AR4 multimodel intercomparison will be compared (§5.5). Datasets for each one of them have been produced with a different GCM, however all of them have been downscaled with the weather regime approach. The 7 GCMs used in this thesis have been chosen casually, only because they were the first to be downscaled and available in the framework of the Rexhyss project. A few details on these 7 GCMs are given in table 5.2. Full details are given in (Randall et al. 2007). The simulations have been first evaluated on their ability to correctly represent "'present time"' behavior (§ 5.3). Then, a comparison of their results for 21m and 21f time periods under A1B GHGs emission scenario is discussed in section 5.5.

Downscaling techniques : ARPV4-VCM and **ARPV4-WR** simulations will be compared. Climate datasets for both simulations have been realized with

[4]ARPEGE Climat v4 is the newer version of the ARPEGE Climat V3 GCM and has been developed by the Centre National de Recherche Meteorologique (CNRM) - Toulouse within the framework of the european research project ENSEMBLE.

ARPEGE Climat v4 but downscaled with two different techniques : the Variable Correction Method (VCM) (Boé et al. 2006) and the Weather Regime approach (WR) (Déque 2007). The two simulations will be first evaluated on "'present time"' representation (§5.3) and then compared on 21f time period under A2 GHGs emission scenarios (§ 5.6).

Name	IPCC AR4 identifier	Sponsors
CSIROMK30	CSIRO – MK3.0,2001	CSIRO Atmospheric Research, Australia
ECHAM5	ECHAM5 / MPI-OM,2005	Max Planck Institute for Meteorology, Germany
GISS-AOM	GISS - AOM,2004	NASA / GISS, USA
GISS-MODELER	GISS-ER,2004	NASA / GISS, USA
MRI2A	MRI-CGCM2.3.2,2003	Meteorological Research Institute, Japan
CNRM-CM3	CNRM - CM3,2004	Météo-France / CNRM, France
GFDL1	GFDL - CM2.1,2005	U.S. Department of Commerce / NOAA / GFDL, USA

Table 5.2: General Circulation Models from IPCC AR4. First column represent the chosen name within this work. Second column is the model ID in IPCC AR4 (Randall et al. 2007) Last column indicates the name and the country of the sponsoring institution. CSIRO is the Commonwealth Scientific and Industrial Research Organisation. NASA is the National Aeronautics and Space Administration. GISS is the Goddard Institute for Space Studies. CNRM is the Centre National de Recherches Météorologiques. NOAA is the National Oceanic and Atmospheric Administration and GFDL is the Geophysical Fluid Dynamics Laboratory.

5.1.2 Additional simulations

In addition to the simulations described in the previous subsection, two other simulations ensemble have been realised to ascertain two important issues:

- A simulation forced by the same climate forcings as A1BCONT (ARPEGE Climat version 3+ under A1B GHGs emission scenario, downscaled with weather regime approach) with six different runs of CLSM which showed similar performances over historical time was realised to test the "equifinality" of these six runs in predicting climate change impacts. This issue is discussed in § 4.5.

- Other simulations were realised to test the impact of initialisation choices on predicted climate change impacts. The next subsection (§ 5.2) is focused on this issue.

5.2 Testing initialization choices

All of the climate change datasets except one (A1BCONT) are available in "time-slices" mode. This means that the climate scenarios are available on various not continuous time periods. In the Rexhyss project three time periods have been chosen: present time PT (approximately 1980-2000), middle future time 21m (approximately

2045-2065) and future time 21f (2080-2100). Except the Arpv4-VCM-A2, Arpv4-VCM-A1B and Arpv4-WR-A2 scenarios which are available only on present time PT and 21f future time period, all the other "time-slices" scenarios[5] are available on the three time periods PT, 21m and 21f.

How to initialize time slices simulations is an important issue in climate change impacts research. In this thesis, we questioned ourselves on which initial values should we choose for the CLSM parameters such as the catchment deficit, the linear reservoir water content and many others. A classical way to solve this question is to initialize the simulation with a previous simulation who reached spin-up (equilibrium). Practically, a first run of the climate scenario is done and then used as the "restart", i.e. the initial conditions, for a second run which can be the simulation to analyse or that could be used as a restart for a third one and so on.

Since these multiples runs have computational costs, there is a balance to be chosen in the number and in the length of the spin-up runs.

In the framework of this thesis a 4 spin up initialisation has been tested both on present time (on SAFRAN and A1BCONT) and on future time on A1BCONT. Since these tests showed similar results, we will analyse here only the spin-up test on A1BCONT on future time period. We realised this test on 20 years between 2079-2080 and 2098-2099, supposing that A1BCONT simulation had been available only in time-slice mode (while in reality, we had already available A1BCONT results over the continuous time period 1950-2100).

We realised a 4 spin-up sequence: we will refer to these 4 runs as A1BCONT.n1, A1BCONT.n2 and so on. We initialized A1BCONT.n1 first run with values coming from the SAFRAN 1986 year. Successively we initialized A1BCONT.n2 with A1BCONT.n1 2085 values and then A1BCONT.n3 with A1BCONT.n2 2085 values. At the end we obtained A1BCONT.n4, initialized with A1BCONT.n3 2085 values.

Figure 5.2 shows impact of intialisation on total runoff, on catchment deficit and on linear reservoir water content. The test showed that with CLSM model, initial conditions have a very limited impact on most variables (many of them are not shown here due to a lack of space). Only linear reservoir parameters are largely influenced by initialization.

More specifically, for all variables except LR's ones the second run is already sufficiently close to the to 4th one. Moreover, most variables have a very short memory since effect of initialization does not last more than 1 or 2 years.

For LR's reservoir variables such as the linear reservoir linear content (figure 5.2), initialization has some importance. Having started the first run from a very "different" situation (the SAFRAN 1986 datas), 3 runs are necessary to get a stable situation. Influence of initial conditions lasts 12 years for the A1BCONT.n1 run

[5]The 7 scenarios from IPCC AR4, see table 5.2.

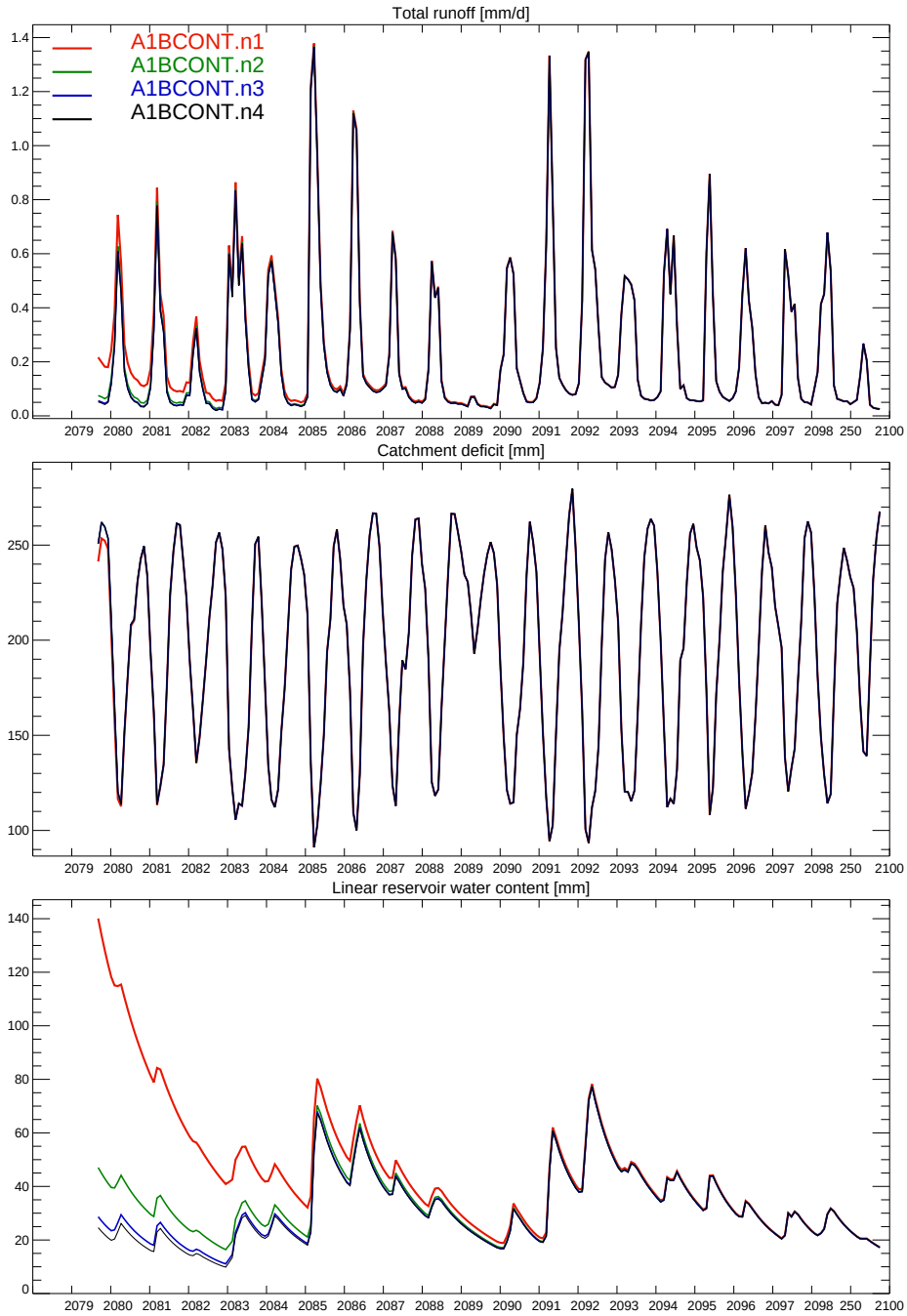

Figure 5.2: Spin up tests on A1BCONT Monthly mean values for the 2079-2099 time period for total runoff, catchment deficit and linear reservoir water content over all the catchment upstream from Poses. Four spin up have been realised labeled A1BCONT.n1, A1BCONT.n2, A1BCONT.n3 and A1BCONT.n4. When red, green and blue curves are not visible, it is because they are under the A1BCONT.n4 black curve.

and 6 years for the three successive runs.

Considering A1BCONT.n1 red curve for all variables, no drift due to the initial conditions is present even if these initial conditions were those of 1986, very different from projected situation in 2079. This is a very reassuring fact. It means that CLSM model gives the same results for the 2090-2100 years no matter how it has been initialized.

Thanks to these tests an initialization strategy has been chosen for all the simulations we have realised in this thesis. For each simulation two runs have been done. For **present time** simulations, an initial 5 years long run, initialized with SAFRAN values, is realised. Then a second run initialized with the first run 5^{th} year value is done. For **future time** simulations, an initial 10 years long run, initialized with A1BCONT continuous simulation values, is realised. Then a second run initialized with the first run 10^{th} year value is done.

5.3 Assessment of simulations in present time observed climate

A first important issue in climate change impact studies is whether the climate models (GCMs and downscaling techniques) used to simulate climate change reproduce a climate comparable to the observed one in *present time*.

It is essential to evaluate representativity of simulated climate parameters versus observed. In other terms, do the climate models (GCMs and downscaling techniques) used to simulate climate change reproduce a climate comparable to the observed one in *present time*? To that purpose, CLSM simulations forced by climate change simulated datasets are compared to CLSM simulations forced by observed and reanalysed surface meteorological datasets SAFRAN and ERA40.

SAFRAN[6] (Quintana-Seguí et al. 2008) is a mesoscale atmospheric analysis system for surface variables. Originally intended for mountainous areas, it was later extended to cover the entire France. The main objective of SAFRAN is to produce an accurate estimation of the variables and downward fluxes required by the Soil Vegetation Atmosphere Transfer (SVAT) models such as CLSM. One of the main features of SAFRAN is that the analysis are performed over climatically homogeneous zones which have irregularly-shaped areas[7] usually smaller than 1000 km^2. SAFRAN produces an interpolated output on a 8 km $\times$ 8 km grid and at a hourly time step. Within the Rexhyss project, SAFRAN's output is available for

[6]Système d'Analyse Fournissant des Renseignements Atmosphériques à la Neige

[7]There are 612 of such zones over France.

the 1982-2005 years and thanks to its fine resolution, SAFRAN's dataset does not require any downscaling.

ERA-40 (Uppala et al. 2005) is a re-analysis of meteorological observations from September 1957 to August 2002 produced by the European Centre for Medium-Range Weather Forecasts (ECMWF) in collaboration with many institutions. ERA-40 is a new, 45-year second-generation re-analysis carried out with the goal of producing the best possible set of analysis, given the changing observing system and the available computational resources. It covers all the planet with a resolution of 2.5°. Within the REXHYSS project, data from the ERA-40 dataset have been downscaled with the weather regime approach.

In **this section** we compare simulated values and observed one for the same period (August 1982 - July 2000) for ERA40, SAFRAN and simulations on present time. We will realize this analysis in two steps: we will firstly (§ 5.3.2) evaluate three scenarios issued from the same general circulation model and downscaled with two different downscaling techniques and then (§ 5.3.3) we will assess 8 different scenarios produced with different General Circulation Models but all downscaled with the weather regime approach. A few details on these GCMs are given in table 5.2.

ARPEGE climat v3+ and v4 versus SAFRAN and ERA-40 is the first intercomparison and we will mainly focus the assessment on the following questions:

- Do A1BCONT, ARPv4-WR and ARPv4-VCM correctly represent SAFRAN and ERA40?
- How do the weather regime approach and the variable correction method perform in terms of accurate representativity of SAFRAN?

A1BCONT and seven IPCC AR4 simulations versus SAFRAN is the second intercomparison where we will discuss these issues:

- What is the range of variation of the 8 simulations? Is this range larger or smaller for a given variable or for a season compared to the others?
- Among the 7 IPCC AR4 + A1BCONT simulations, which ones are the closest and the most different from SAFRAN?
- After computing the mean values of the 8 simulations, how does this "mean simulation" behave?
- Does A1BCONT represents correctly the range of variation of the other simulations? Is A1BCONT close to the mean simulation?

We have already discussed in chapter 4 the choice of analysing our results mostly in Poses which is the last gauging station not being in the estuarine part of the Seine river. Unless stated differently, all results and graphs in this section are referred to of the a spatial average over all the catchment upstream of Poses.

5.3.1 Comparing climate

In order to assess the representativity of simulated versus compared climate, we should first understand and define what do we mean by "comparable" or "similar" climate.

To do that we will shortly introduce the key concept in climate science of the "butterfly effect". It is a famous metaphor developed by the great climate expert, Edward Lorenz in the 60's at Massachusetts Institute of Technology (MIT) within his research on chaos theory. Literally the existence of the "butterfly effect" in a chaotic world implies that a butterfly's wings might create tiny changes in the atmosphere that May ultimately alter the path of a tornado or delay, accelerate or even prevent the occurrence of a tornado in a certain location of the planet.

Going beyond the image, the "butterfly effect" expresses the key concept in chaos theory, that even a small change in a part of a complex system can cause great changes in other parts of the system. According to the chaos theory, climate is a complex system which often is close to a threshold between order and chaos. For example, climate has many regular and periodical or nearly periodical fluctuations such as seasons or El Nino effect. However, in some situations a little perturbation could lead the system to a very instable behavior or worse, to complete chaos.

The butterfly effect means that, since the mean climate is already very close to the chaos domain, initial conditions can massively influence the climate at short timescales. Since initial conditions are generally unknown and can lead to very different results, it is very difficult to correctly simulate the climate at short timescales.

Since the chaos theory applies to meteorology, we do not expect simulated weather to be equal to observations on historical period. We expect climate as a mean state to be simulated correctly but this is not expected, though, on timescales up to annual. On the same basis, future simulated climate is not the actual climate we shall experience. E.g., A1BCONT did not simulate for 2008 the real experienced weather in Paris for the same period. Simulated climate is only a plausible realisation of the complex climate system. When we compare simulations and observations we should keep in mind this issue and think in term of statistical resemblance. In the following section and all along this chapter, we will then use three comparison tools: annual mean values, mean annual cycle (monthly mean values) and empirical probability distributions.

Concerning the **mean annual cycle**, Student's test of the null hypothesis (H_0:"the monthly mean of SAFRAN and A1BCONT are equal") has been conducted on

monthly mean values to test statistical significance of differences between A1BCONT and SAFRAN simulations (at significance level p=0,05).

Regarding **empirical probability distributions** daily values (of discharge, temperature and precipitation) are classified in 100 bins. Each bin is characterised by its central value[8] and by the associated Empirical Relative Frequency (ERF). Over the entire range of values they define the empirical Probability Distribution Function (PDF). For precipitation and for discharge it is more meaningful to plot the central values (runoff or precipitation) versus their associated Complementary Cumulative Distribution Function (CCDF). CCDF expresses the empirical probability distribution of exceedance of the corresponding (discharge or precipitation) values. In such a way we obtain for each discharge and precipitation value its empirical probability function of exceedance, which is an analysis very similar to the *flow duration curve* largely used for discharges in hydrology. This kind of analysis gives some interesting results even if it is not sufficient for very little probability values (rare and very rare heavy rain and flood events or severe droughts). A specific work package within the Rexhyss project is scheduled and will be realized by CEMAGREF[9] - Lyon using a discharge-duration-frequency[10] approach which has been recently developed (Javelle 2001 and Sauquet, Javelle, and Le Clerc 2003).

5.3.2 ARPEGE climat v3+ and v4 versus SAFRAN and ERA-40:

We will firstly compare A1BCONT , ARPV4$_{VCM}$ and ARPV4$_{WR}$ simulated climate to SAFRAN and ERA 40 observed datasets. A1BCONT reference simulation is produced with data from the ARPEGE Climat v3+ general circulation model (GCM), downscaled with the Weather Regime approach. ARPV4$_{WR}$ and ARPV4$_{VCM}$ come from a new version of the same GCM (Arpège Climat v4), they differ from one another only for the downscaling technique: the Weather Regime approach for ARPV4$_{WR}$ and Variable Correction Method for ARPV4$_{VCM}$. SAFRAN reanalysis 8 km × 8 km gridded output does not require downscaling while ERA40 is downscaled with the weather regime approach.

First we will evaluate the climate forcings (particularly air temperature and precipitation). In the second step, we will no more assess the climate forcings only but their result using the CLSM model (§ 5.3.2.2).

[8] A runoff, temperature or precipitation value.

[9] Cemagref is a public research institute that targets results directly usable in land and water management.

[10] Approche Qdf : débits - durée - fréquence.

5.3.2.1 Climate forcings

In this section we will evaluate some of the climate forcings (mainly air temperature and precipitation, and marginally the air humidity) in terms of their representativity of the observed climate.

Air temperature: Simulated and observed annual mean values for air temperature are very close (figure 5.3). Mean, bias with respect to SAFRAN, minimum and maximum values are given in table 5.3. Arp-v4 simulations do not correctly represent the SAFRAN negative minimum value for air temperature.

Mean annual cycles (figure 5.4) for air temperature and air specific humidity show a good similarity too between most simulations. Only the ARPv4$_{VCM}$ has a clearly different behavior with a negative bias on many months both on air temperature and air humidity.

A1BCONT correctly represents SAFRAN mean annual cycle (even if it slightly overestimates maximum temperatures in the summer) and differences between A1BCONT and SAFRAN are not statistically significative[11].

Simulated and observed empirical relative frequency (figure 5.6) are very similar too. Air temperature distribution is quite well simulated. A1BCONT is the closest simulation to the SAFRAN curve.

In literature, there is a general agreement on the fact that temperature is generally correctly represented by general circulation models on a global scale (Terray and Braconnot 2006 and Randall et al. 2007) and through the use of downscaling techniques on a regional and local scale. The assessment of our temperature forcings, with the exception of ARPv4-VCM, confirms this judgment.

Precipitation: Annual mean precipitation values are quite close to SAFRAN observations (figure 5.3). A1BCONT simulation shows a little negative bias (-0.08 mm/d) compared to SAFRAN. On a interannual scale, ARPv4-VCM and ARPv4-WR shows a closer similarity to SAFRAN and a smaller bias than A1BCONT (table 5.4).

The annual mean cycle in figure 5.4 shows that A1BCONT values are representative of SAFRAN and ERA40 observed values in terms of seasonal variations. However A1BCONT simulates weaker seasonality contrasts, as precipitation is underestimated in winter and slightly overestimated in early spring, this is probably due to the version 3+ of ARPEGE Climat. Simulated A1BCONT precipitation is closer to SAFRAN one (with a smaller bias) between February and July than in the

[11]Student's test at significance p=0,05

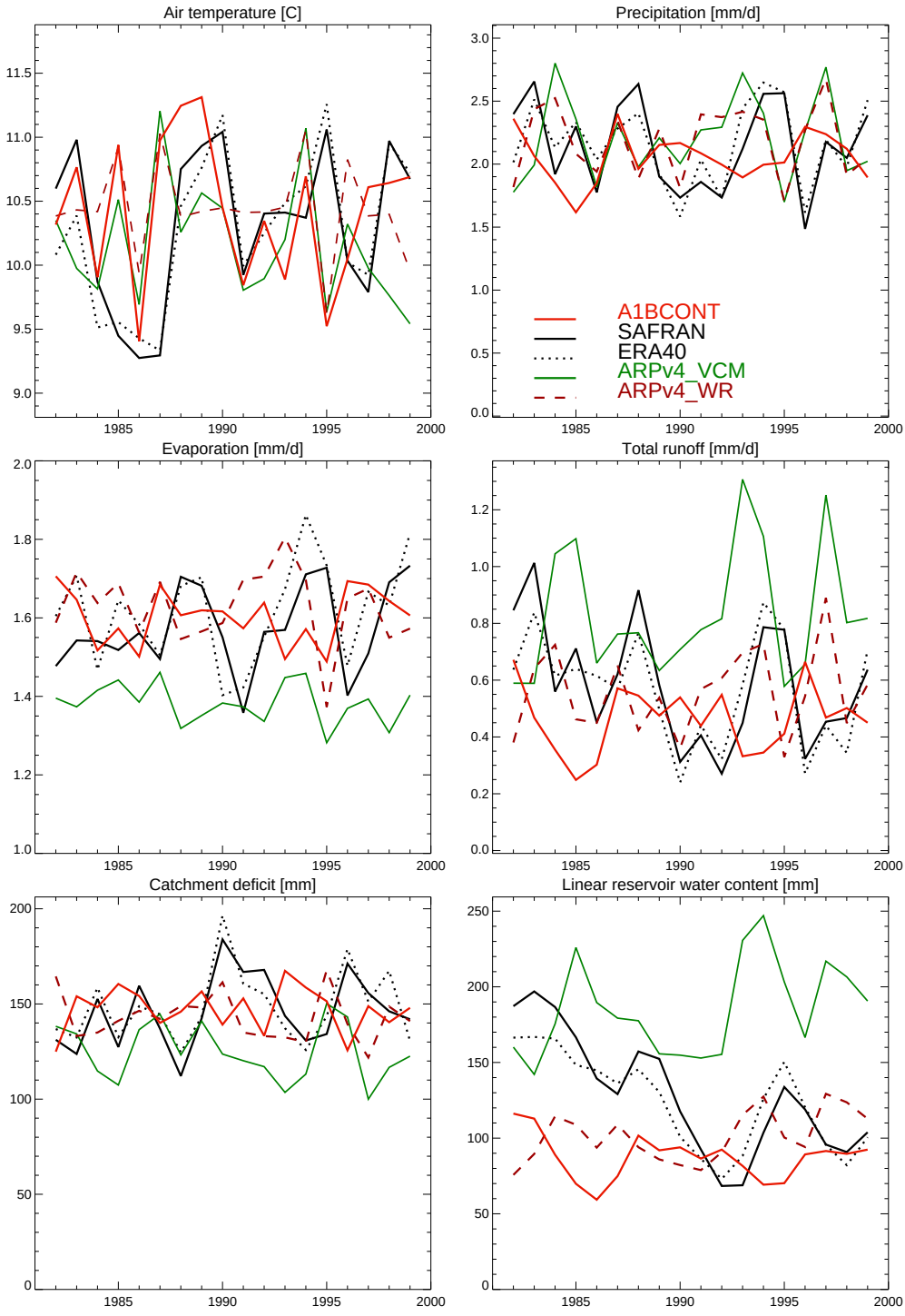

Figure 5.3: Trends on annual mean values (1982-2000) over all the catchment upstream from Poses for precipitation, air temperature, evaporation, catchment deficit and linear reservoir's water content. Black curve represents observed values from SAFRAN (full line), and ERA 40 (dotted). Red curve represents A1BCONT simulation (GCM : ARPEGE climat v3+ downscaled with the weather regime approach). Green and brick-red curves come from the ARPEGE climat v4 GCM downscaled respectively with the weather regime approach (dashed brick-red) or with the variable correction method (green).

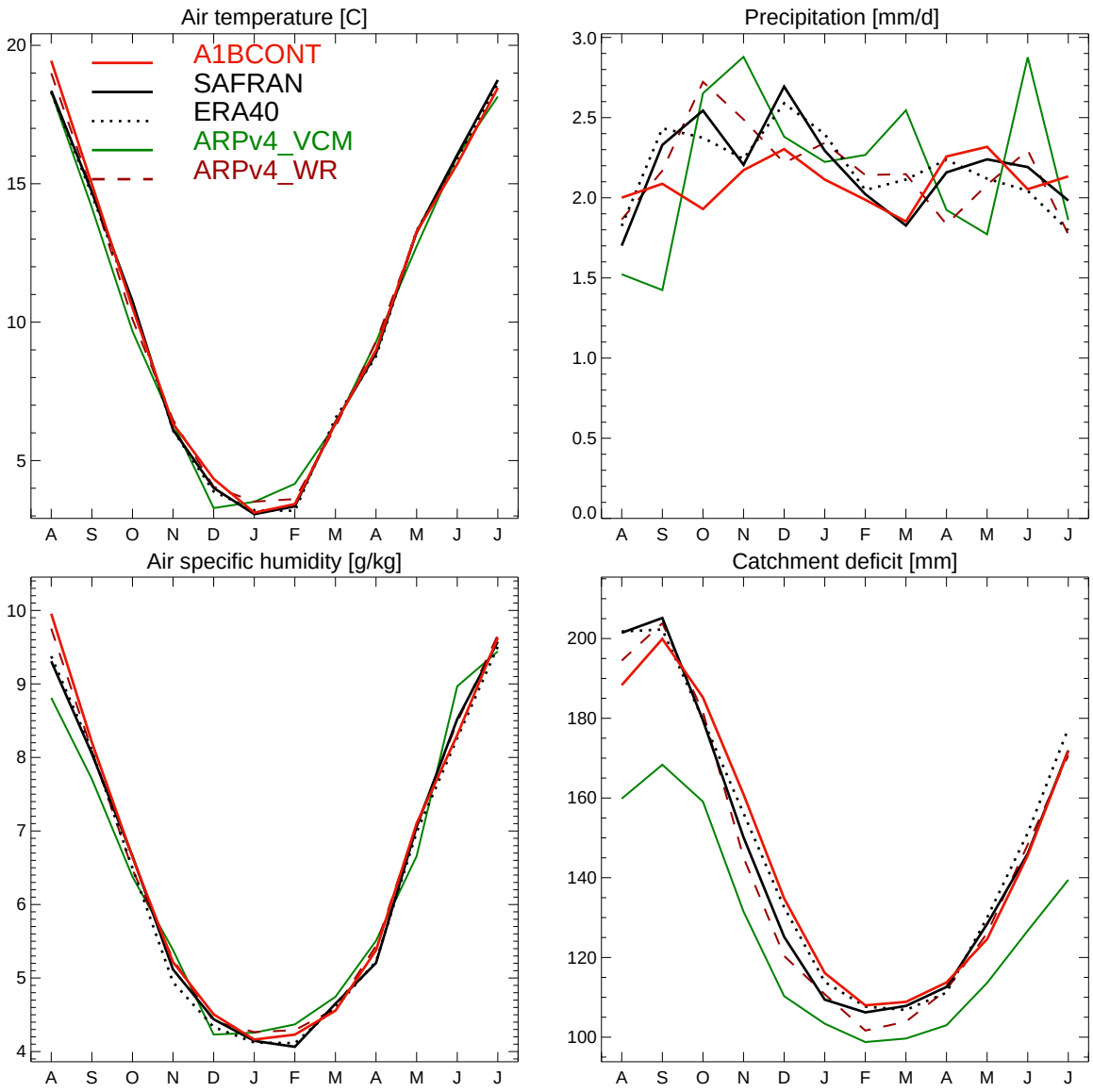

Figure 5.4: Mean annual cycle over all the catchment upstream from Poses for air temperature, precipitation, air humidity and catchment deficit (1982-2000). Black curve represents observed values from SAFRAN (full line), and ERA 40 (dotted). Red curve represents A1BCONT simulation (GCM : ARPEGE climat v3+ downscaled with the weather regime approach). Brick-red and green curves come from the ARPEGE climat v4 GCM downscaled respectively with the weather regime approach (dashed brick-red) or with the variable correction method (green). Student's test of the null hypothesis has been performed on monthly mean values to test statistical significance of differences between A1BCONT and SAFRAN simulations (at significance level p=0,05). It showed no statistical difference for air temperature, precipitation, air humidity and catchment deficit.

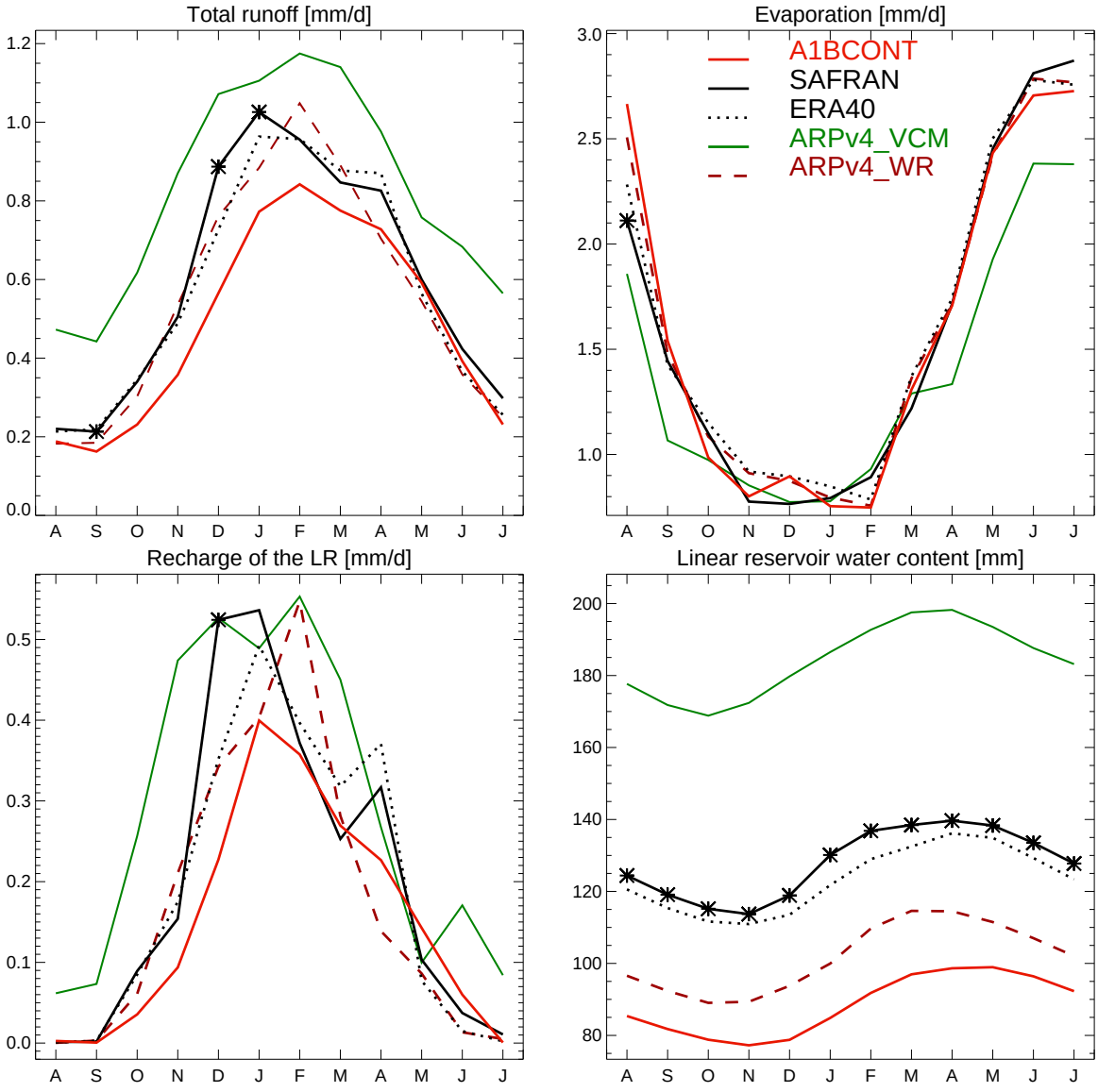

Figure 5.5: Mean annual cycle (1982-2000) over all the catchment upstream from Poses for total runoff, evaporation, recharge flux to the Linear Reservoir and LR's water content. Black curve represents observed values from SAFRAN (full line), and ERA 40 (dotted). Red curve represents A1BCONT simulation (GCM : ARPEGE climat v3+ downscaled with the weather regime approach). Brick-red and green curves come from the ARPEGE climat v4 GCM downscaled respectively with the weather regime approach (dashed brick-red) or with the variable correction method (green). Student's test of the null hypothesis has been conducted on monthly mean values to test statistical significance of differences between A1BCONT and SAFRAN simulations (at significance level p=0,05). Black stars on the graph shows where the test rejected the null hypothesis.

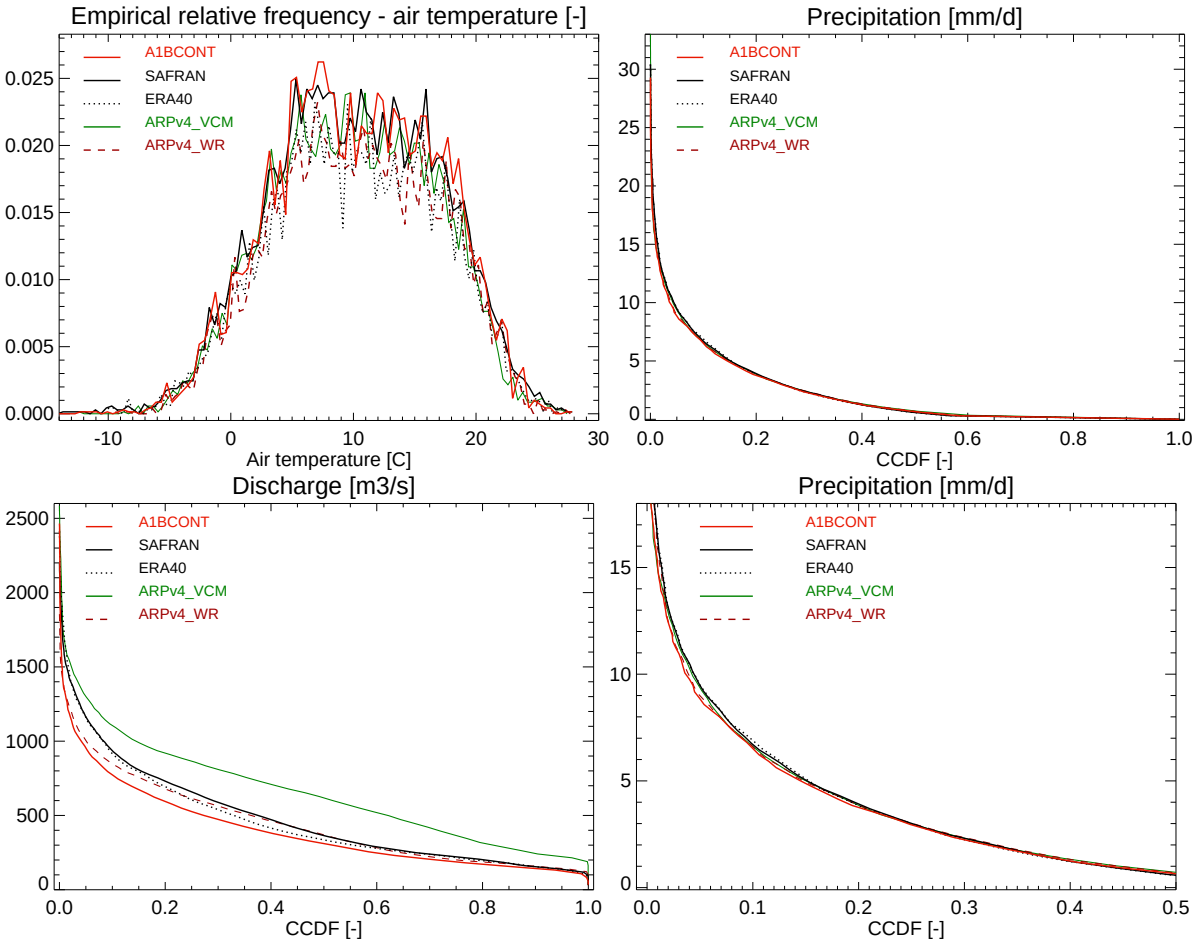

Figure 5.6: Empirical relative frequency for air temperature and Empirical probability of exceedance for precipitation and routed discharge upstream from Poses (1982-2000). Black curve represents observed values from SAFRAN (full line), and ERA 40 (dotted). Red curve represents A1BCONT simulation (GCM : ARPEGE climat v3+ downscaled with the weather regime approach). Brick-red and green curves come from the ARPEGE climat v4 GCM downscaled respectively with the weather regime approach (dashed brick-red) or with the variable correction method (green). The bottom and right graph is a zoom of the above graph (precipitation). Air temperature has been plotted only above the -14°C limit.

Air temperature [°C]				
Simulation 1982-2000	**Mean**	**Bias**	**Min**	**Max**
SAFRAN	10,34	-	-15,9	27,85
ERA40	10,29	-0,05	-10,27	27,41
A1BCONT	10,45	0,11	-15,8	27,83
ARPv4 – VCM	10,18	-0,16	-12,37	27,42
ARPv4 – WR	10,45	0,11	-9,43	27,69
CSIROMK30	10,42	0,08	-15,58	27,06
ECHAM5	10,32	-0,02	-15,7	27,83
GISS-AOM	10,53	0,19	-8,83	26,96
GISS-MODELER	10,37	0,03	-17,87	26,72
MRI2A	10,46	0,12	-15,66	27,55
CNRM-CM3	10,48	0,14	-15,77	27,33
GFDL1	10,47	0,13	-8,99	27,3
Mean 7 IPCC and A1BCONT	10,44	0,10	-	-
Mean + std	10,51	0,17	-	-
Mean - std	10,37	0,03	-	-

Table 5.3: Assessment of present time simulated air temperature over 1982-2000 years. Biases refer to SAFRAN simulation.

Precipitation [mm/d]					
Simulation 1982-2000	**Mean**	**Bias**	**Bias [%]**	**Min**	**Max**
SAFRAN	2,184	-	-	0	30,42
ERA40	2,186	0	0,1	0	30,42
A1BCONT	2,101	-0,08	-3,8	0	29,29
ARPv4 – VCM	2,193	0,01	0,4	0	33,82
ARPv4 – WR	2,173	0,01	0,4	0	30,1
CSIROMK30	2,185	0	0,1	0	29,29
ECHAM5	2,153	-0,03	-1,4	0	29,29
GISS-AOM	2,051	-0,13	-6,1	0	29,29
GISS-MODELER	2,105	-0,08	-3,6	0	30,1
MRI2A	2,091	-0,09	-4,2	0	27,31
CNRM-CM3	2,072	-0,11	-5,1	0	29,29
GFDL1	2,018	-0,17	-7,6	0	30,1
Mean 7 IPCC + A1BCONT	2,097	-0,09	-4,0	-	-
Mean + std	2,150	-0,03	-1,5	-	-
Mean – std	2,044	-0,14	-6,4	-	-

Table 5.4: Assessment of present time simulated precipitation over 1982-2000 years. Biases refer to SAFRAN simulation.

other months of the year. Autumn is the season where precipitations are worse simulated in A1BCONT. The differences between monthly mean values for A1BCONT and SAFRAN are not statistically significative under Student's test (p=0,05).

ARPv4-VCM showed a good performance in term of annual value, however seasonal behavior is different from SAFRAN and other curves showing more variability

at the monthly timescale.The variable correction method leads to an overestimation of precipitation in November, December, February, March and June and to an underestimation in May, August and September. Thus, simulated ARPv4-VCM precipitation is the least representative of the observed SAFRAN values and should be considered with caution.

Empirical relative frequency (probability of exceedance) for precipitation (figure 5.6) shows a rather good similarity between all simulated and observed curves. However probability of exceedance for high and medium precipitation values above 3.5 mm/d (ccdf below 0,2) are slightly underestimated by A1BCONT and other Arpège simulations.

5.3.2.2 CLSM outputs

In this section we will no more assess the climate forcings only but their result using the CLSM model. Thus, we are evaluating the general circulation model and the downscaling techniques combined with a hydrological model which allows to assess discharge widely observed but introduces further errors.

Total runoff - discharge Compared to SAFRAN, A1BCONT total runoff annual mean value (figure 5.3) has a negative bias of -80,71 m^3/s (mean values over all the period are 396 m^3/s for A1BCONT versus 477 m^3/s for SAFRAN). ARPv4-WR is closer than A1BCONT to SAFRAN (bias of -32 m^3/s) while ARPv4-VCM has a large positive bias (+178,9 m^3/s).

Discharge at Poses $[m^3/s]$					
Simulation 1982-2000	**Mean**	**Bias**	**Bias [%]**	**Min**	**Max**
SAFRAN	477,17	-	-	30,28	2197,2
ERA40	458,36	-18,81	-3,9	33,96	2413,4
A1BCONT	396,46	-80,71	-16,9	33,62	2464,8
ARPv4 – VCM	656,07	178,9	37,5	34,58	2584,7
ARPv4 – WR	445,18	-31,99	-6,7	28,99	1855,2
CSIROMK30	463,52	-13,65	-2,9	28,65	2888
ECHAM5	434,8	-42,37	-8,9	28,67	2102,3
GISS-AOM	394,5	-82,67	-17,3	30,06	2185,2
GISS-MODELER	429,35	-47,82	-10,0	28,32	1922,6
MRI2A	418,82	-58,35	-12,2	33,33	2474,4
CNRM-CM3	413,78	-63,39	-13,3	28,16	2548,3
GFDL1	368,88	-108,29	-22,7	31	1999,6
Mean 7 IPCC and A1BCONT	415,01	-62,16	-13,0	-	-
mean + std	443,95	-33,22	-7,0	-	-
Mean – std	386,08	-91,09	-19,1	-	-

Table 5.5: Assessment of the present time simulated total runoff over 1982-2000 years. Bias refer to SAFRAN simulation.

Total runoff annual mean cycle (figure 5.5) shows a negative bias for A1BCONT compared to ERA40 and SAFRAN. This bias is due to the negative bias in precipitation enhanced by CLSM sensitivity. Performed Student's test, between A1BCONT and SAFRAN values, rejects the null hypothesis in the September, December and January months. In these three months simulated runoff will have to be considered with greater caution.

ARPv4-VCM has a large positive bias in all months, conversely ARPv4-WR is very close to the SAFRAN curve and is a good estimation of SAFRAN observed runoff.

Discharge Complementary Cumulative Distribution Function (CCDF) (figure 5.6) confirms that ARPv4-WR is the closest to SAFRAN simulation, A1BCONT underestimates empirical relative frequency while ARPv4-VCM largely overestimates empirical relative frequency. A1BCONT underestimation is larger for medium and high discharge values exceeded less than 40 % of the time (p=0,4).

Catchment deficit Annual mean values of the catchment deficit are mostly similarly simulated using SAFRAN or downscaled GCMs (figure 5.3). Only ARPv4-VCM has a clear negative bias. This means that soil moisture content is overestimated in ARPv4-VCM simulation. This bias is noticeable also in the **mean annual cycle** (figure 5.4). The catchment deficit is largely influenced by precipitation values. We expect to have an underestimated catchment deficit (thus a overestimated soil moisture content) if precipitation is overestimated as simulated in ARPv4-VCM.

Average over all the catchment	**Catchment deficit [mm]**		**Evaporation [mm/d]**	
Simulation 1982-2000	**Mean**	**Bias**	**Mean**	**Bias**
SAFRAN	145,52	-	1,583	-
ERA40	147,78	2,25	1,627	0,044
A1BCONT	146,69	1,16	1,611	0,028
ARPv4 – VCM	126,27	-19,25	1,382	-0,201
ARPv4 – WR	143,43	-2,1	1,627	0,044
CSIROMK30	142,73	-2,79	1,595	0,011
ECHAM5	143,48	-2,05	1,605	0,021
GISS-AOM	149,46	3,93	1,571	-0,012
GISS-MODELER	145,81	0,28	1,565	-0,018
MRI2A	146,56	1,03	1,584	0,000
CNRM-CM3	149,7	4,17	1,558	-0,025
GFDL1	148,35	2,82	1,572	-0,011
Mean 7 IPCC and A1BCONT	146,59	1,07	1,583	-0,001
mean + std	149,16	3,64	1,602	0,018
Mean – std	144,03	-1,5	1,563	-0,020

Table 5.6: Assessment of the present time simulated catchment deficit and evaporation over 1982-2000 years. Bias refers to SAFRAN simulation.

A1BCONT and ARpv4-WR satisfactorily represent SAFRAN mean annual cycle, although they have some bias. The A1BCONT catchment deficit is overestimated compared to SAFRAN curve in the months where precipitation is underestimated (October to February). Conversely it is underestimated from July to September where precipitation is overestimated. Performed Student's test between A1BCONT and SAFRAN did not reject the null hypothesis for any of the monthly values.

Evaporation Evaporation annual mean values (figure 5.3) are rather correctly simulated by A1BCONT and ARPv4-WR with little bias of -0,03 (A1BCONT) and +0,05 (ARPv4-WR). ARPv4-VCM, instead has a large negative bias of -0,20.

A1BCONT and ARPv4-WR correctly represent SAFRAN mean annual cycle of evaporation. Performed Student's test on differences between A1BCONT and SAFRAN values reject the null hypothesis (at significance p=0,05) only in August. This monthly anomaly is due to the overestimation by A1BCONT of August air temperature which enhances evaporative demand, combined to a slightly overestimated precipitation and soil moisture content which allows to fulfill a greater part of the evaporative demand.

Conversely, ARPv4-VCM has a very large negative bias in all months between April and October, during the evaporative season. This is partly due to the underestimated evaporative demand caused by a negative bias on air temperature.

Ground water A1BCONT and ARPv4-WR have negative bias in annual mean values compared to SAFRAN (-39 mm for A1BCONT and -26 mm for ARPv4-WR). This bias is larger in the 1982-1992 years than in 1992-2000 (figure 5.3). In terms of annual mean cycles (figure 5.5), A1BCONT and ARPv4-WR show a similar underestimation. Performed Student's test (p=0,05) between A1BCONT and SAFRAN values rejects the null hypothesis in all months.

The causes of these differences have to be found in the recharge flux to the LR which is underestimated in most months of the year. LR's recharge flux underestimation is due to the catchment deficit overestimation (underestimation of soil moisture content).

In contrast, ARPv4$_VCM$ LR's water content has a large positive bias (+56 mm) which is noticeable both in terms of annual mean value (figure 5.3) and in all months of the mean annual cycle (figure 5.13). This is due to the underestimated catchment deficit values which allows overestimated recharge flux to the linear reservoir.

In general, ground water parameters such as the recharge flux to the linear reservoir (LR) or the LR's water content show large bias with respect to SAFRAN values. The LR's sensitivity amplifies the existing bias on the climate forcings and other CLSM variables such as the catchment deficit leading to relatively large bias

Average over all the catchment	Recharge flux to the LR [mm/d]		Water content in the LR [mm]	
Simulation 1982-2000	**Mean**	**Bias**	**Mean**	**Bias**
SAFRAN	0,200	0,000	127,94	0
ERA40	0,190	-0,010	123,2	-4,74
A1BCONT	0,150	-0,049	88,47	-39,48
ARPv4 – VCM	0,291	0,091	184,1	56,15
ARPv4 – WR	0,173	-0,027	101,65	-26,29
CSIROMK30	0,190	-0,009	109,25	-18,69
ECHAM5	0,167	-0,032	101,69	-26,25
GISS-AOM	0,146	-0,054	89,58	-38,36
GISS-MODELER	0,166	-0,034	97,38	-30,56
MRI2A	0,156	-0,043	99,78	-28,17
CNRM-CM3	0,167	-0,033	95,93	-32,01
GFDL1	0,126	-0,074	79,86	-48,08
Mean 7 IPCC and A1BCONT	0,159	-0,041	95,243	-32,7
mean + std	0,177	-0,022	104,328	-23,61
Mean – std	0,140	-0,060	86,157	-41,79

Table 5.7: Assessment of the present time simulated recharge flux to the Linear Reservoir and LR's content over 1982-2000 years. Bias refers to SAFRAN simulation.

on LR's variables. This means that the change simulated by CLSM can be more extreme than using other models.

5.3.3 A1BCONT and seven IPCC AR4 simulations versus SAFRAN

We are assessing now, with respect to SAFRAN observed values, A1BCONT and 7 simulations from various GCMs of the IPCC AR4 (Randall et al. 2007), all downscaled with the weather regime approach. A few details on these GCMs are given in table 5.2.

5.3.3.1 Climate forcings

Air temperature: Observed air temperature is quite well represented by the 8 considered simulations both in terms of annual mean values (figure 5.7) and of mean annual cycle (figure 5.8). ECHAM5, GISS-MODELER, and CSIROMK30 have the smallest bias (-0,02 ; +0,03 ; +0,08 °C) with respect to SAFRAN values (**table 5.3**). GISS-AOM, CNRM-CM3 and GFDL1 have the highest bias (+0,19 ; +0,14 ; +0,13 °C). A1BCONT has an intermediate bias value (+0,11 °C). These performances are confirmed on a monthly base (figure 5.8). Empirical relative frequency (figure 5.10) shows that ECHAM5 and CSIROMK30 best reproduce the SAFRAN distribution of daily temperature values. It also confirms that GISS-AOM and GFDL1 worse represents SAFRAN. A1BCONT and the 3 other simulations are in an intermediate position (i.e. they are neither the best neither the worse representation of SAFRAN).

The "mean simulation" has a bias of +0,10 °C (with a standard deviation of 0,07 °C). The air temperature range of variation of the 8 simulations is very narrow

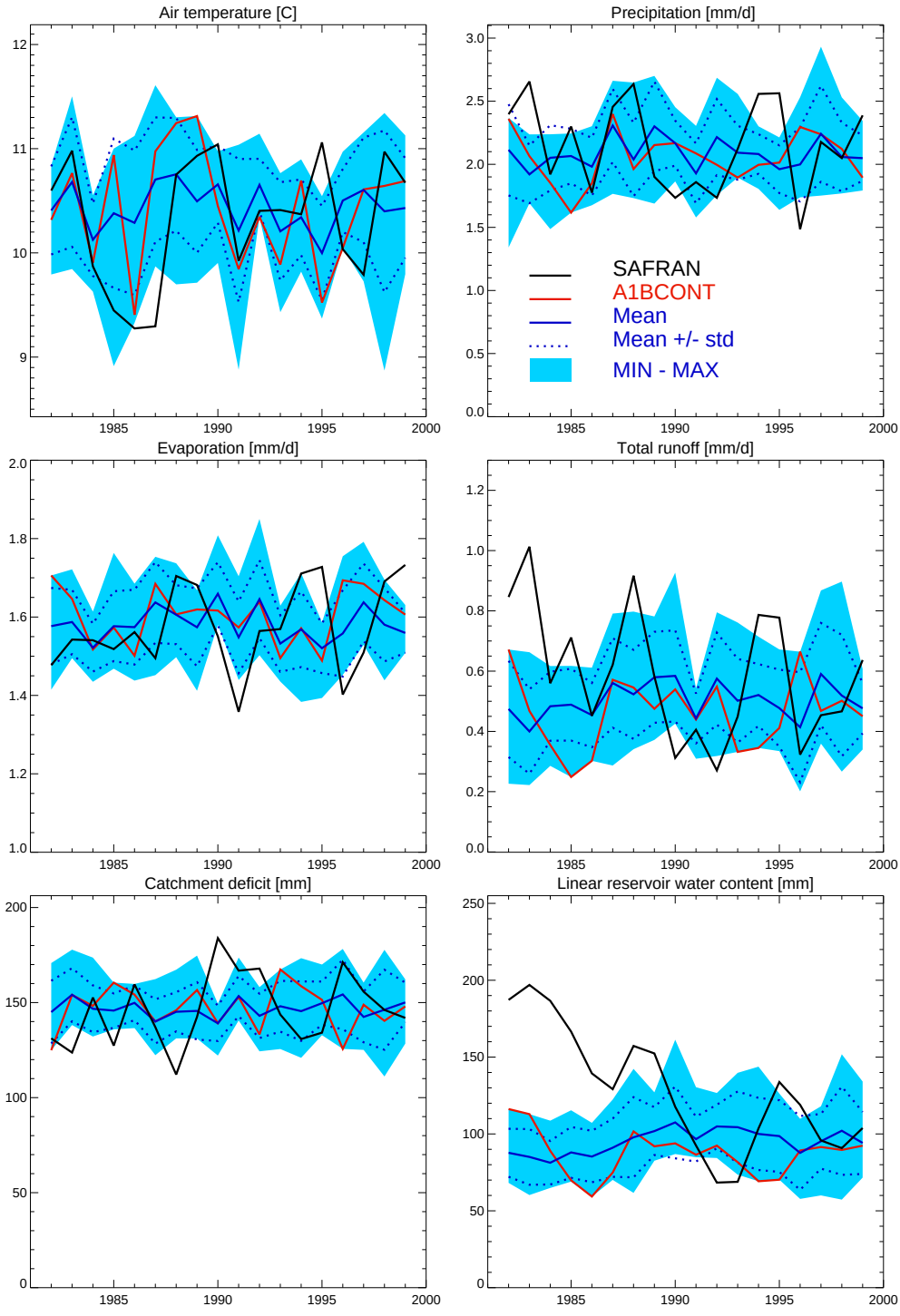

Figure 5.7: Trends on annual mean values (1982-2000) over all the catchment upstream from Poses for precipitation, air temperature, evaporation, catchment deficit and linear reservoir's water content. Black curve represents SAFRAN observed values. Red curve represents A1BCONT simulation (GCM : ARPEGE climat v3+ downscaled with the weather regime approach). Blue curve is the mean between 8 simulations (A1BCONT and 7 simulations from IPCC AR4). Dotted blue curves are the standard deviation of this mean curve. The cyan shaded area indicates the whole spread of values of the 8 simulations.

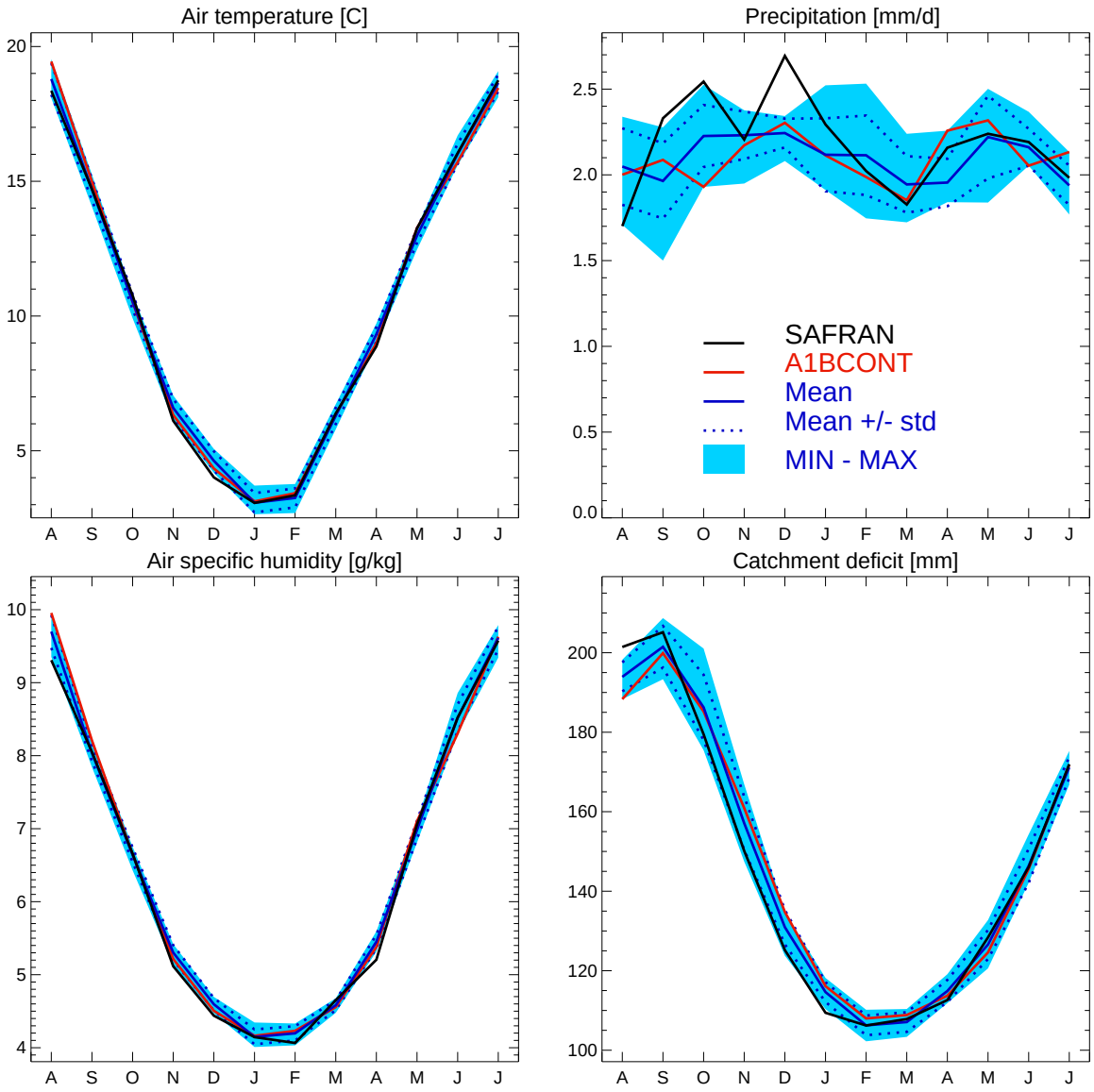

Figure 5.8: Mean annual cycle over all the catchment upstream from Poses for air temperature, precipitation, air humidity and catchment deficit (1982-2000). Black curve represents SAFRAN observed values. Red curve represents A1BCONT simulation (GCM : ARPEGE climat v3+ downscaled with the weather regime approach). Blue curve is the mean between 8 simulations (A1BCONT and 7 simulations from IPCC AR4). Dotted blue curves are the standard deviation of this mean curve. The cyan shaded area indicates the whole spread of values of the 8 simulations.

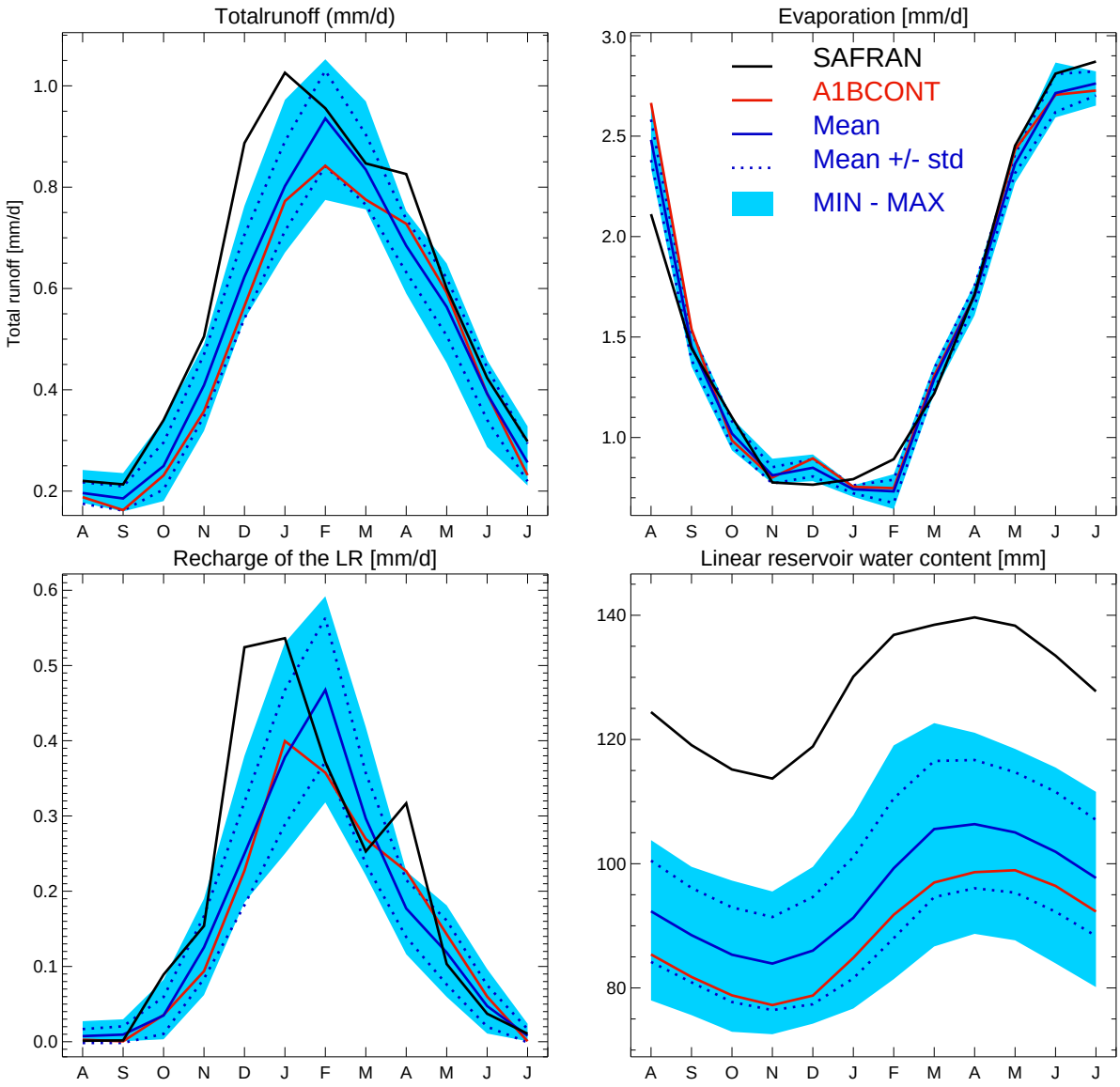

Figure 5.9: Mean annual cycle over all the catchment upstream from Poses for air temperature, precipitation, air humidity and catchment deficit (1982-2000). Black curve represents SAFRAN observed values. Red curve represents A1BCONT simulation (GCM : ARPEGE climat v3+ downscaled with the weather regime approach). Blue curve is the mean between 8 simulations (A1BCONT and 7 simulations from IPCC AR4). Dotted blue curves are the standard deviation of this mean curve. The cyan shaded area indicates the whole spread of values of the 8 simulations.

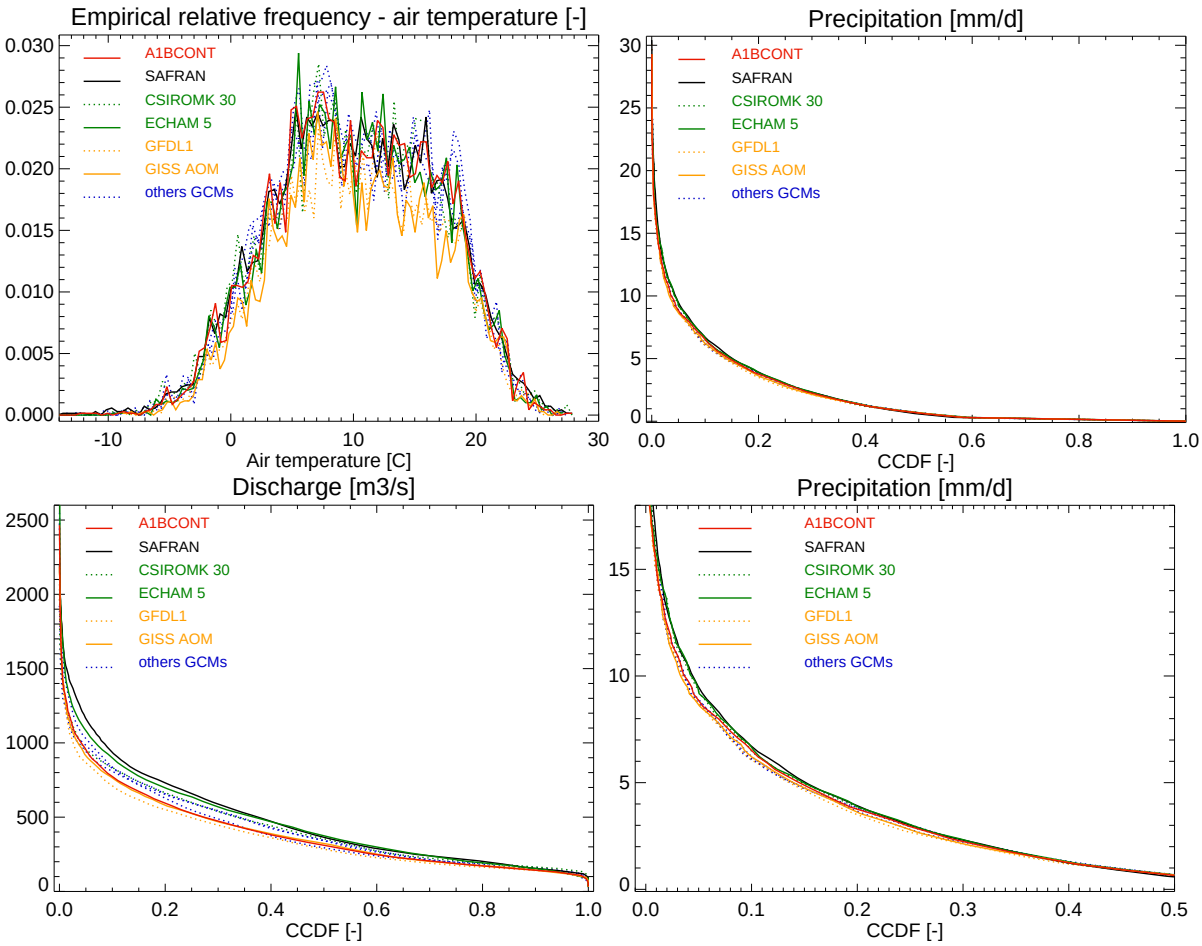

Figure 5.10: Empirical relative frequency for air temperature and empirical probability of exceedance for precipitation and routed discharge upstream from Poses (1982-2000). Black curve represents SAFRAN observed values. Red curve represents A1BCONT simulation (GCM : ARPEGE climat v3+ downscaled with the weather regime approach). Green curves represent the two closest to SAFRAN GCMs from IPCC AR4: CSIROMK30 (dotted) and ECHAM5 (full line). Orange curves are the two simulations from IPCC AR4 with poorest results with respect to SAFRAN: GFDL1 in full line and GISS AOM in dotted line. The three blue dotted curves represents the three other IPCC AR4 GCMs: CNRM-CM3, GISS-MODELER and MRI2A which have performances between orange and green curves in terms of similarity to SAFRAN.The bottom and right graph is a zoom of the above graph (precipitation). Air temperature has been plotted only above the -14°C limit.

compared to the other variables. There is a slightly larger range of variation for air temperature and air humidity on December to February values; this means that slightly larger uncertainties are pending on these monthly values.

A1BCONT has a bias (+0,11 °C) comparable to the "mean simulation" one (+0,10°C). Although it overestimates summer temperature, it shows a good representativity of the 7 other simulations ensemble in terms of mean annual cycle (figure 5.8).

Precipitation: Most simulations have a negative bias on precipitation (table 5.4). GISS-AOM and GFDL1 have the largest bias, ECHAM5 and CSIROMK30 have the smallest. A1BCONT has an intermediate bias value (-0,08 mm/d). These performances are confirmed on a monthly basis but not shown here due to a lack of space. Empirical probability of exceedance (figure 5.10) confirm that ECHAM5 and CSIROMK30 best reproduce SAFRAN. It also shows that GISS-AOM and GFDL1 gave the poorest representation of SAFRAN. A1BCONT and the 3 other simulations are in an intermediate position (i.e. they are neither the best neither the worse representation of SAFRAN).

The "mean simulation" has a bias of -0,09 mm/d (with a standard deviation of 0,053 mm/d). In terms of mean annual cycle, the range of variation of precipitation is much larger than air temperature one. As for air temperature and air humidity, the range of variation is particularly large on winter precipitations. Larger uncertainties are pending on the behavior of these months.

A1BCONT has a bias (-0,08 mm/d) comparable to the "mean simulation". Being most of the times within the standard deviation dotted line limits, it shows a good representativity of the 7 other simulations ensemble in terms of mean annual cycle (figure 5.7) and of mean annual values (figure 5.8).

5.3.3.2 CLSM outputs

Total runoff - Discharge: The 8 simulations have all a negative bias on discharge as on precipitation (table 5.5 and figure 5.7). As for precipitation, CSIROMK 30 and ECHAM 5 have the smallest bias while GFDL1 and GISS-AOM have the largest. Despite the negative bias, many scenarios overestimate the maximum discharge. This is striking for maximum discharge simulated by CSIROMK (2800 m^3/s instead of 2197 m^3/s of SAFRAN). Figure 5.9 shows an important bug of the modeling sequence (GCM + Weather Regime + CLSM): monthly maximum value is one month forward (in January) in simulated scenarios than in SAFRAN (in December). This due to the fact that GCMs do not simulate the precipitation maximum in December.

Referring to the discharge versus empirical probability of exceedance graph(figure 5.10), medium discharge values (for $0.1 < ccdf < 0.5$) are underestimated by most

scenarios. As for the mean values, CSIROMK 30 and ECHAM 5 are the closer to SAFRAN while GFDL1 and GISS-AOM have the greater underestimation of SAFRAN. A1BCONT underestimates all discharge values which are exceeded between 10 and 80 % of the time. Compared to CSIROMK 30 and ECHAM 5 and many other IPCC scenarios, A1BCONT does not represent very well the discharge empirical probability of exceedance as it has a greater underestimation.

The "mean simulation" has a bias of -62 m^3/s (with a standard deviation of 28,93 m^3/s). A1BCONT has a larger bias (-80 m^3/s) and it simulates values below the "mean simulation" and below SAFRAN nearly for all months of the year (figure 5.9). However A1BCONT can still be considered a not so bad representation of the 8 scenarios ensemble since it is most of the time within the standard deviation dotted line limits both in the annual mean values and in the mean annual cycle graphs.

The range of variation is much more important for the December to March values than for the other months of the year. This is largely due to the larger discharge values in winter. Conversely range of variation is much smaller in the summer months : there are much lower uncertainties pending on summer values.

Catchment deficit and evaporation: The catchment deficit is well represented with little bias by most simulations (table 5.6). The "mean simulation" and A1BCont both have little positive bias: they both slightly underestimate the soil moisture content. Mean annual cycle is correctly represented (figure 5.8).

Evaporation is correctly represented with little bias (table 5.6). Annual mean (figure 5.7) and mean annual cycle curves (5.9) show a good similarity between A1BCONT, the mean simulation and SAFRAN. The "mean simulation" and A1BCONT behave similarly in most months, with an overestimated value in August and an underestimated one in June and July. As described in the previous section for A1BCONT, this is due to the combined bias in air temperature and precipitation: e.g., in August a positive bias in precipitation and air temperature allows an overestimation of the evaporation rate whereas the underestimated air temperature in June and July explain the underestimated evaporation.

Catchment deficit and evaporation results appear quite robusts since the range of variation is relatively small in the mean annual cycle graphs. In both graphs A1BCONT behaves similarly to the mean simulation and is mostly within the dotted lines standard deviation limits, thus the catchment deficit and evaporation simulated by A1BCONT are a good representation of the 8 scenarios ensembles.

Ground water Both the mean recharge flux and the mean water content of the deep linear reservoir (LR) show an important bias (table 5.7 and figure 5.7) probably due to the bias in precipitation. This is striking in terms of mean annual cycle (figure 5.9):

- The recharge flux is underestimated in all months and especially in its peak value.

- The LR's water content is largely underestimated: both the mean simulation and A1BCONT have a large downshift.

- The range of variation is very large for both variables showing great uncertainties.

- A1BCONT is close to the "mean simulation". They both have large negative bias, not representing correctly SAFRAN's behavior. All the same, A1BCONT can still be considered an acceptable representative of the 8 scenarios since it is most of the time within the limits of the dotted standard deviation lines

In general, ground water parameters such as the recharge flux to the linear reservoir (LR) or the LR's water content show large bias with respect to SAFRAN values and a larger range of variation. The LR's sensitivity amplifies the existing bias on the climate forcings and other CLSM variables such as the catchment deficit leading to relatively large bias and ranges of variation on LR's variables.

5.3.4 Main results

Present time air temperature is correctly represented in most scenarios. Precipitation is affected by larger biases. Both climate forcings are worse represented in the winter months than in other seasons.

The variable correction method produces a scenario (Arpv4-VCM) very different from the weather regime ones and with larger biases on most variables.

A1BCONT shows some negative biases and it is not the best representation for many variables (for example A1BCONT has a negative bias on runoff annual mean cycle where ARPv4-WR seems to better represent the SAFRAN simulation (figure 5.5). CSIROMK and ECHAM5 are "good scenarios" showing very little biases. A1BCONT is less representative of SAFRAN observed climate than the mean of 8 simulation downscaled with the WR approach. However A1BCONT can still be considered an acceptable representation of the 8 simulation ensemble since differences between A1BCONT and the "mean simulation" are generally lower than the standard deviation of the 8 simulations.

The variable correction method does not simulates correctly SAFRAN observed values, with a positive bias on precipitation, runoff, soil moisture and linear reservoir water content. In other words, the VCM scenarios describes a much "wetter" present time climate than SAFRAN observations.

5.4 Climate change reference simulation

In the framework of the Rexhyss project a continuous climate scenario (A1BCONT) is available. Even if the A1BCONT scenario is not the closest to present time climate as represented by the SAFRAN analysis (subsection 5.3.1), continuity from 1950 to 2100 makes it very interesting to assess the dynamics of the changes in climate and hydrology.

A1BCONT simulation has been realised using climate forcings produced with the variable resolution GCM ARPEGE Climat v3+ (Gibelin and Déque 2003), downscaled with the weather regime approach (Boé et al. 2006). In the 1950-2000 period the GCM has been fed with observed Green House Gases and aerosols concentrations while future time (after the year 2000), has been simulated under A1B GHGs emission scenario.

In this section we will discuss in detail all the results of the reference simulation (A1BCONT) while in sections 5.7, 5.5 and 5.6 we will analyse the range of uncertainties caused respectively by emission scenarios, GCMs and downscaling techniques. A synthesis of all the results will be given in §6.2.

In the next subsections, we will firstly analyse our results in terms of mean annual cycle (§ 5.4.1), then in terms of empirical distribution (§ 5.4.2) and finally in terms of mean annual values and trends. These analysis are conducted on six 25 years long sliding time periods previously defined in figure 5.1.

5.4.1 Changes in mean annual cycle

In this section we will analyse the main changes in the mean annual hydrological cycle. Assessing changes in seasonality is a key issue in climate change impact studies. Furthermore, the aim of the REXHYSS project is to evaluate the impact of climate change on extreme hydrological events. Analysing seasonal behavior is the first but essential step.

Air temperature and precipitation: Air temperature (figure 5.11) and air humidity (not shown here due to lack of space) show a net and clear increase in all seasons. Warming is slightly larger in winter (December, January, February) than in other months.

Precipitation curves (figure 5.11) show a clear reduction in spring and summer (from April to September). Winter precipitation (DJF months) tends to increase but this is less evident than the reduction of summer precipitations.

A possible reason for this change in precipitation has been found by Giorgi, Bi, and Pal (2004) who identified under climate change enhanced anticyclonic circulation in summer over the north-eastern Atlantic, which induces a ridge over western Europe. This structure would deflect storms northward causing a substantial and

widespread decrease of precipitation (up to 30-45 %) over the Mediterranean basin as well as western and central Europe. Giorgi, Bi, and Pal found also that increased cyclonic activity in DJF leads ro enhanced precipitation over much of western, northern and central Europe (Bates et al. 2008).

The most striking change is that monthly precipitation is very homogeneous in present time, in agreement with SAFRAN, whereas it exhibits seasonal contrasts by the end of the century with wetter winters than summers. The precipitation curves shows also a change in seasonality. In present time (black curve) monthly maxima happen in spring (April and May) and fall (November and December) while in simulated future climate (red curve) January and February would have the monthly maximum values.

Evaporation and soil moisture: Evaporation (figure 5.11) is enhanced in winter and early spring (December to April) and reduced in summer and fall (May to October).

The catchment deficit and the areal fraction below wilting point (figure 5.12) increase with climate change in all seasons, meaning lower soil moisture content. However, this trend is particularly striking in summer and to a lower extent in spring and fall. Only winter (DJF) does not show a remarkable reduction.

It is classical in hydrology, to describe actual evaporation rate as ruled by a "supply and demand" mechanism. If there is enough water supply, evaporation sticks to the evaporative demand. Conversely, actual evaporation rate can be much below potential evapotranspiration if water supply is not large enough.

Thus, the winter and early spring increase in evaporation (up to nearly +40% in April) is demand-driven: due to higher temperature and higher incident radiation, evaporative demand is enhanced. The soil moisture content is relatively high in those months (i.e. the catchment deficit is relatively low) and actual evaporative rate can satisfy to a large extent the evaporative demand.

Conversely, the evaporation reduction in summer (up to nearly -40% in August) is caused by a lack of supply: due to a very low soil moisture content (very high catchment deficit, high wilting areal fraction), actual evaporation cannot respond to the high evaporative demand.

These opposite seasonal-specific changes in evaporation (summer reduction and a winter and early spring increase), give an explanation for the stability of the annual mean evaporation rate described in section 5.4.3: the two opposite seasonal trends combine together into a rather stable mean annual value. As a result, the decrease in soil moisture (increase in the catchment deficit) is mostly driven by the decrease in precipitation.

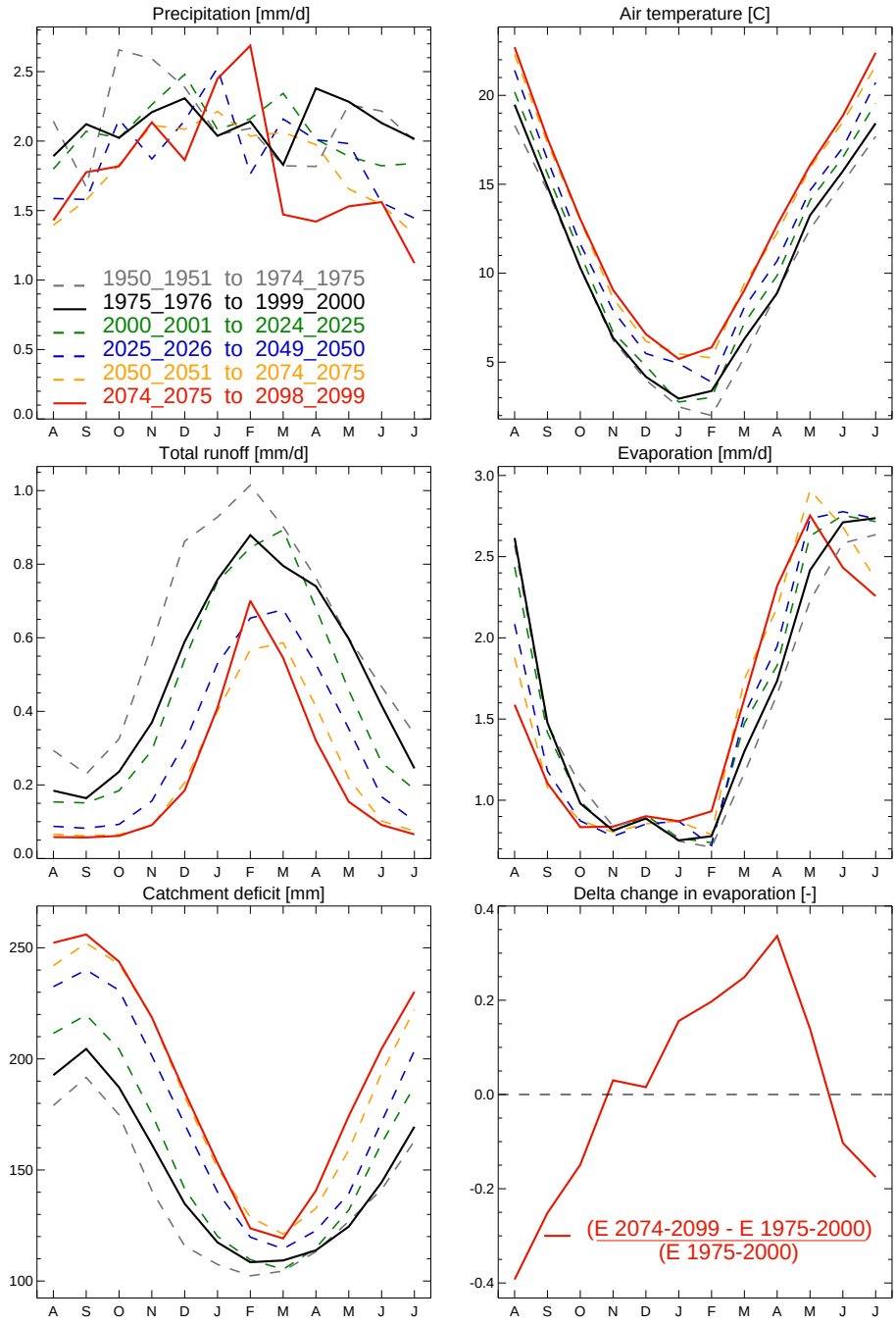

Figure 5.11: Monthly mean values (A1BCONT simulation) over the entire watershed upstream of Poses for precipitation, air temperature, total runoff, evaporation and catchment deficit. Months order is typical of a hydrological year (August to July). A1BCONT 150 years long simulation has been divided into six 25 years long "sliding" periods of time. Each curve represents the monthly mean values over a specific period of time. Last period of time and present time period of time are laid out as red and black full lines while other periods of time are plotted as dash lines of various colors accordingly to the legend. Precipitation, runoff and evaporation values are given in mm/d, air temperature in [°c] and the catchment deficit in mm. Last box (at the bottom on the left) is the relative anomaly between climate change and present time monthly mean value expressed in terms of present time monthly mean value.

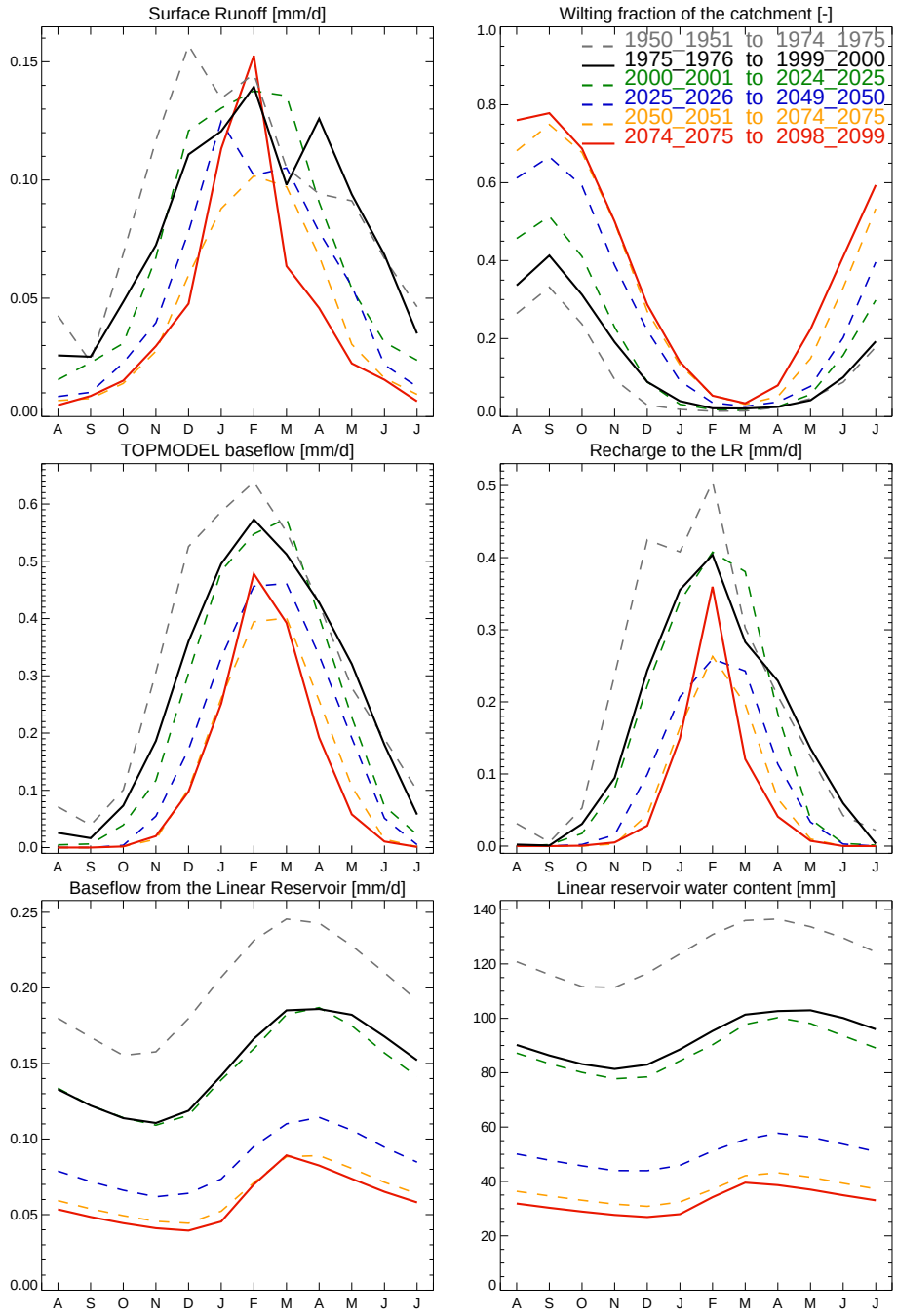

Figure 5.12: **Monthly mean values (A1BCONT simulation) over the entire watershed upstream of Poses for surface runoff, wilting areal fraction, TOPMODEL's baseflow, LR's baseflow, recharge flux to the LR, and LR's water content.** Months order is typical of a hydrological year (August to July). A1BCONT 150 years long simulation has been divided into six 25 years long "sliding" periods of time. Each curve represents the monthly mean values over a specific period of time. Last period of time and present time period of time are laid out as red and black full lines while other periods of time are plotted as dash lines of various colors accordingly to the legend. The specific linear reservoir water content is expressed in mm, all other variables (except the wilting areal fraction) are given in mm/d.

Runoff and groundwater: Total runoff goes down all along the year. This reduction is particularly strong in spring and summer when present time value is nearly quartered due to little precipitation and low soil moisture content.

In classical hydrological terms, surface runoff (overland flow) is described as the fraction of *net precipitation* [12] which cannot infiltrate into the soil. In a simple and traditional formulation, as the *rational method* overland flow is often expressed as a fraction of precipitation through the use of a runoff coefficient [13].

Then, it is not surprising at all that the surface runoff modified seasonality (figure 5.12) reflects the seasonal changes in precipitation. There is a clear decreasing trend in all non-winter months (especially form April to October and a weak increase or stability in December to February values.

Directly influenced by the catchment deficit M_D, TOPMODEL's baseflow and Linear Reservoir's recharge flux go down in all months and strikingly in the summer tightening the bell-shaped width.

Since LR's recharge flux nearly shuts down in the summer months, LR's water content is strongly reduced with climate change in all seasons. Being not fed with enough water (due to a lower soil moisture content), the Linear Reservoir's ability in sustaining total runoff goes down. As LR's water content, LR's baseflow curve is shifted down and nearly shuts off in winter. With climate change, deep groundwater Linear Reservoir's importance is much lower, which explains most of the decrease in total runoff in summer.

Results from GICC-Seine project: Similar results were obtained previously for both evaporation and soil moisture content in the same watershed within the GICC-Seine project (Ducharne et al. 2007 and Ducharne et al. 2004). In that project, however, summer precipitation was not projected to decrease so badly, thus simulated summer reduction in soil moisture content and evaporation rate was not as striking as in the present result

Concerning runoff, results within the GICC-Seine project showed already a reduction in summer runoff, but of a much smaller amplitude. Those previous results showed also (with a lower level of certainty) an increase in February to April flows. This is clearly not the case in our study : due to the greater reduction in precipitation projected in A1BCONT climate scenario compared to scenarios used within the GICC-Seine project, there is no increase of winter monthly runoff values.

[12] Net precipitation is precipitation minus the loss of water due to evapotranspiration.

[13] which depends on watershed land use.

5.4.2 Changes in probability distribution functions

In the previous section we have analysed A1BCONT simulation in terms of mean annual cycle behavior. The present section deals instead with changes in empirical probability distributions.

5.4.2.1 Daily air temperature

Empirical relative frequency (or Probability Distribution Function) for air temperature (figure 5.13) in future time is clearly shifted of approximately 3°C to the right: it means that the air temperature value associated to a given frequency is 3°C higher at the end of the 21^{st} century than in the reference baseline. Climate change induces also a change in the shape with increased frequency for the higher temperatures and decreased frequencies for the values lower or equal to the median.

In future time, temperature below 20°C (and especially temperature below 8°C) are much less frequent, conversely relatively high daily temperature values above 20°C appear to become much more probable with climate change. The most frequent temperature values are in the 7 to 12 °C range in future time while they are in the 3 to 7°C range in reference baseline and the corresponding frequencies are lower under climate change.

5.4.2.2 Daily precipitation and discharge

Empirical Complementary Cumulative Distribution Function (CCDF) for precipitation and discharge (figure 5.13) are continuously and progressively shifted down with climate change. Given a CCDF value, values for the present time period (black curve) are higher than the last time period ones (red curve).

Precipitation empirical CCDF shows a general reduction of all the values corresponding to probability of exceedance values in the 0,05 to 0,6 range. Our analysis is not sufficient for rare and very rare events with exceedance probability below 0,05. Taking a probability of exceedance, it associated precipitation goes down with time. For example, the precipitation daily value exceeded 50% of the time is 0,55 mm/d in present time versus 0,27 mm/d in last future time period. Conversely, given a daily precipitation value, its associated probability of exceedance is reduced with time. This is the case, for example for the 4 mm/d daily precipitation value which is exceeded 19 % of the time in reference period versus 14.5% of the time in future time period.

Changes in **discharge** empirical probability of exceedance are even larger than changes on precipitation CCDF. A striking change is already present for the 2025-2050 time period (gray curve) which is very close future. Mediane discharge for p = 0.5 is a significative value since it it is the discharge exceeded 50% of time on daily basis over 24 years period. At p = 0.5, discharge for 2025-2050 (blue curve) (110

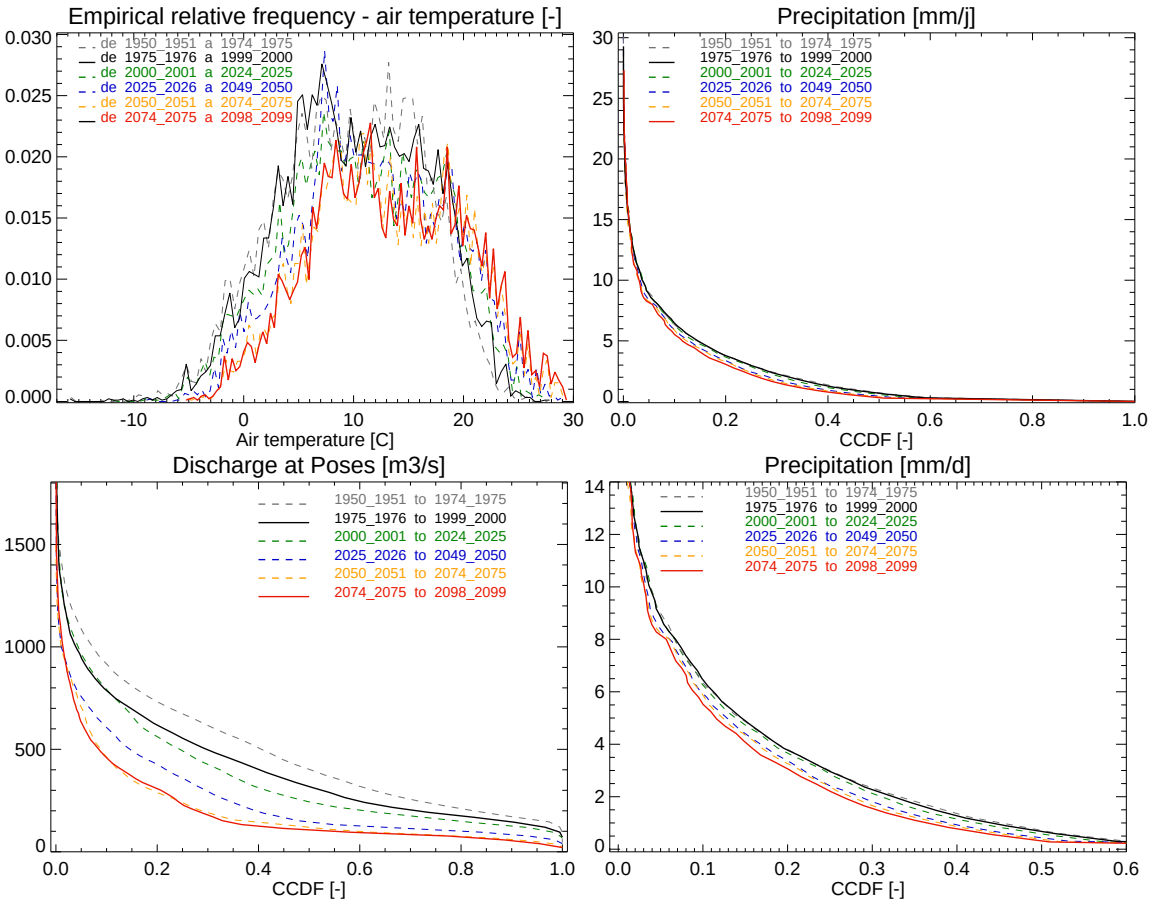

Figure 5.13: Changes in probability distribution functions for A1BCONT simulation. Plotted curves refer to 18 years long periods of time from 1950 to 2099 and to spatially averaged values over all the catchment upstream from Poses. Black curve is our "reference" present time, while red curve is the last simulated future time. Starting from the top and from the left side, first graph represents the empirical probability distribution for daily air temperature. Second graph is the Complementary Cumulative Distribution Function (or empirical probability of exceedance) for precipitation. The third graph is a zoom of the previous one. The last graph represents the empirical probability of exceedance for routed discharges. The bottom and right graph is a zoom of the above graph (precipitation). Air temperature has been plotted only above the -14°C limit.

m^3/s) is already one third than 1975-2000 one (310 m^3/s, black curve). Median discharge for 2050-2075 is nearly equal to the value for 2075-2100 (110 m^3/s).

Consider now, how a daily discharge value changes its probability of exceedance. Consider for example the 650 m^3/s discharge value, in 1975-2000 it was exceeded nearly 20% of the time ($CCDF \approx 0.19$), while in 2075-2100 it will be exceeded only 5% of the time. Or consider the 400 m^3/s discharge value, in 1975-2000 it was exceeded 40% of the time ($cdf \approx 0.55$), while in 2075-2100 it will be exceeded only 13% of the time.

For high or very high flows, the change is even bigger, i.e. consider the 800 m^3/s value, in 1975-2000 it had the probability of being exceeded nearly 1% of the time

(*ccdf* ≈ 0.012, 3 days per year as an average), while in 2075-2100 it will have the probability to be exceeded only 0,3% of the time (1 day per year as an average). There are very big changes concerning low flows too: the 200 m^3/s discharge is exceeded 70% of the time in baseline while it is exceeded only 30% of the time in future time (2075-2100). The minimum discharge value (the discharge exceeded 100 % of the time was 71 m^3/s in present time and would be 20 m^3/s in future time. These changes in the frequency of severe low and high flows are nearly changes in the magnitude scale. On a first analysis, this would mean that flood events will be less frequent or of a smaller intensity and that severe droughts will be much more common. However we must be very careful not to give a hasty conclusion. For very little probability values (rare and very rare heavy rain and flood events or severe droughts not realized every year on average), the above analysis is not sufficient. As already written, a specific work package within the Rexhyss project is scheduled and will be realized by CEMAGREF - Lyon.

5.4.3 Trends in annual mean values

After having analysed A1BCONT simulation in terms of seasonal and extreme values behavior, we will give in the present subsection a few descriptions on trends in annual mean values. We will refer to "present" (PT), "middle future" (21m) and "future" (21f) time periods defined in figure 5.1.

A first and general comment is that climate forcings and CLSM outputs in the middle of the 21^{st} century (21m period) are already very different from present time forcings and much more similar to the situation of the end of 21^{st} century (21f). Values are summarized in table 5.8. This means that projected climate change would have some large impacts on hydrology and water resources already in close future. This result should encourage the adoption with no delay of determined mitigation and adaptation policies.

Precipitation and air temperature: Mean annual values for precipitation P and air temperature T_{air}, two of the most important climate parameters for Land Surface Models, over all the Seine river basin upstream from Poses, are given in figure 5.14. They show that A1BCONT simulates correctly *present time* observed climate as the behavior of A1BCONT, SAFRAN and ERA 40 is similar. This issue has already been discussed in section 5.3. The present section is focused instead on the analysis of the A1BCONT simulation red curve.

Mean AIR TEMPERATURE increases strikingly from 10.5 °C to 13.4 °C with an intermediate value of 12.8 °C in 21^{st} century *middle time* (21m). This trend (+2.9 between PT and 21f) is consistent with projected global mean surface temperature increase of 3°C under A1B green house gases emission scenario (IPCC-AR4 2007).

Mean PRECIPITATION decreases from 2.09 mm/d in *present time* (PT) to 1.81 mm/d in 21^{st} century *middle time* (21m) and 1.76 mm/d in 21^{st} century *future time* (21f).

		PT	**21m**	**21f**	Δ_{21mPT}	Δ_{21f21m}	Δ_{21fPT}
		1982-2000	2047-2065	2081-2099			
Precipitation	[mm/j]	2,09	1,81	1,76	-13,4	-2,4	-15,8
Air temperature	[°C]	10,40	13,00	13,60	2,6	0,6	3,2
Air humidity	[kg /kg]	6,5E-03	7,2E-03	7,4E-03	11,4	2,0	13,5
Wind	[m/s]	2,82	2,65	2,62	-6,1	-1,1	-7,2
Longwawe radiation	[W/m2]	309,91	318,69	320,73	2,8	0,7	3,5
Shortwawe radiation	[W/m2]	139,93	128,23	132,05	-8,4	2,7	-5,6
Evaporation	[mm/j]	1,61	1,58	1,53	-1,9	-3,1	-5,0
Total runoff	[m^3/s]	403,60	211,50	197,00	-47,6	-3,6	-51,3
	[mm/j]	0,47	0,25	0,23	-47,6	-3,7	-51,3
Surface runoff	[mm/j]	0,08	0,04	0,04	-42,0	-0,5	-42,5
TOPMODEL'baseflow	[mm/j]	0,26	0,14	0,13	-45,5	-5,2	-50,7
LR's baseflow	[mm/j]	0,14	0,07	0,06	-48,2	-9,0	-57,1
Catchment deficit	[mm]	147,90	187,60	193,00	26,8	3,7	30,5
Recharge to the LR	[mm/j]	0,14	0,07	0,06	-48,2	-9,0	-57,1
LR's water content	[mm]	86,70	41,70	33,00	-51,9	-10,0	-61,9
Wilting areal fraction	[-]	0,15	0,35	0,39	135,1	27,7	162,8
Unsaturated areal fraction	[-]	0,82	0,63	0,59	-23,2	-4,9	-28,0
Saturated areal fraction	[-]	0,04	0,02	0,02	-36,1	-2,8	-38,9

Table 5.8: A1BCONT mean values comparison for 21m, PT and 21f time periods. Δ_{21mPT}, Δ_{21f21m} and Δ_{21fPT} values are expressed in percentage of PT values.

Total runoff: There is a striking decreasing trend in the annual mean total runoff at Poses that is on average 403.6 m^3/s in present time, 211.5 m^3/s in middle time and 197.2 m^3/s in future time (figure 5.14). Total runoff value is more than halved from PT to 21f. It is consistent with precipitation change, described above, which puts the Seine river basin in the "Southern part" of Europe.

The **catchment deficit** (figure 5.15) increases up to 193 mm in 21f (+30%). An increase in catchment deficit means in fact a decrease in catchment soil moisture and a lower water table (see §3.2.3.2 for futher details). Likewise, the areal fraction of the catchement below wilting point is much higher (0.389) in future time (21f) than in present time (0.148). Clearly, higher catchment deficit and higher wilting areal fraction are caused by precipitation's reduction. Higher catchment deficit and wilting areal fraction imply enhanced soil moisture stress.

In our results, mean annual **evaporation rate** remains nearly stable with a mean value of 1.6 mm/d (figure 5.14). The reason of this stability has been explained previously in section 5.4.1.

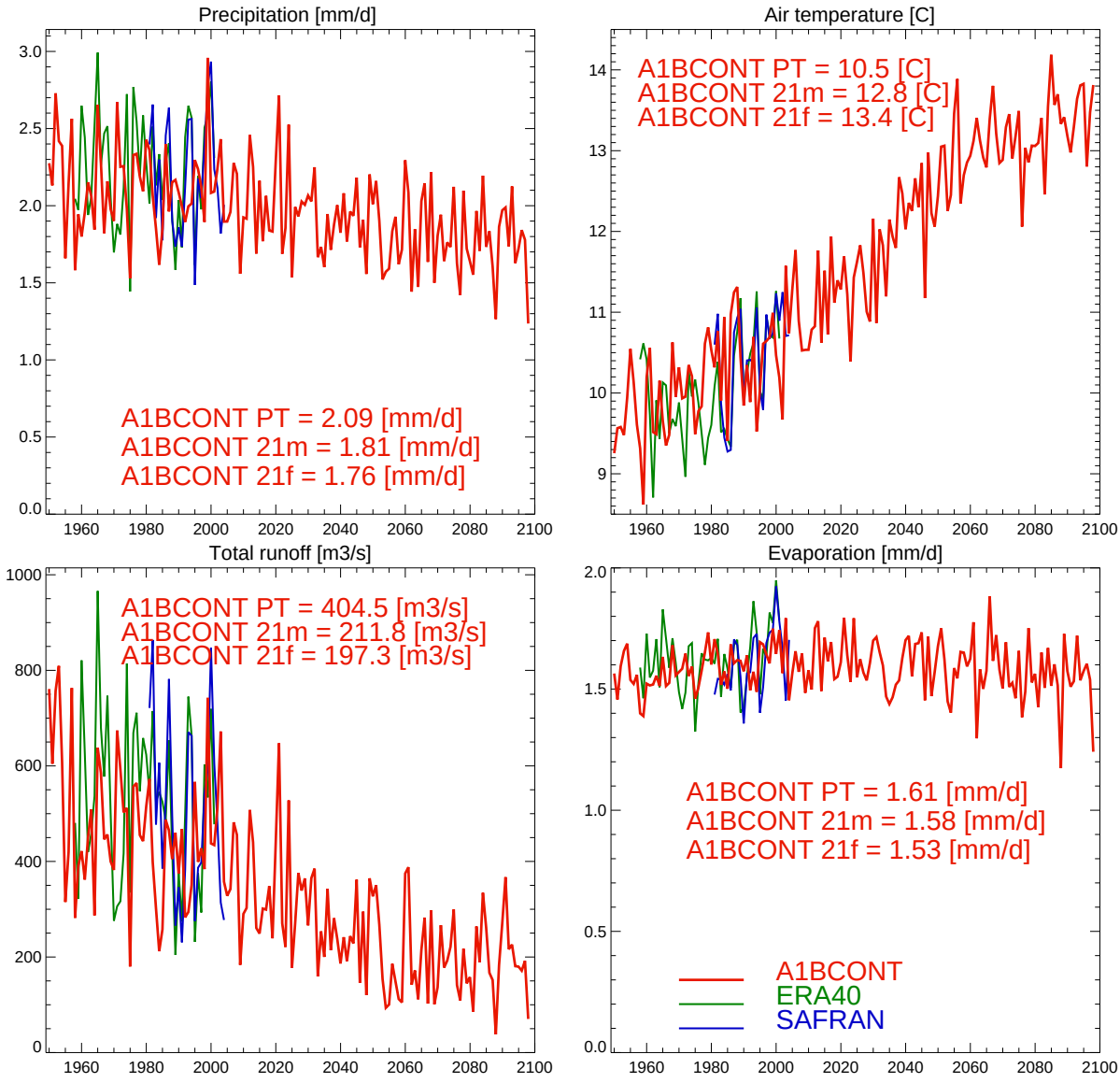

Figure 5.14: Trends on annual mean values over all the catchment upstream from Poses for precipitation, air temperature, total runoff and evaporation. Red curve represent A1BCONT reference simulation, while blue and green are SAFRAN and ERA 40 simulations, fed with observed and reanalysed meteorological data. Values given in red are mean values over 18 years long periods in present time PT (aug 1982 - July 2000), middle future time 21m (aug 2046 - July 2065) and future time 21f (aug 2081 - July 2099).

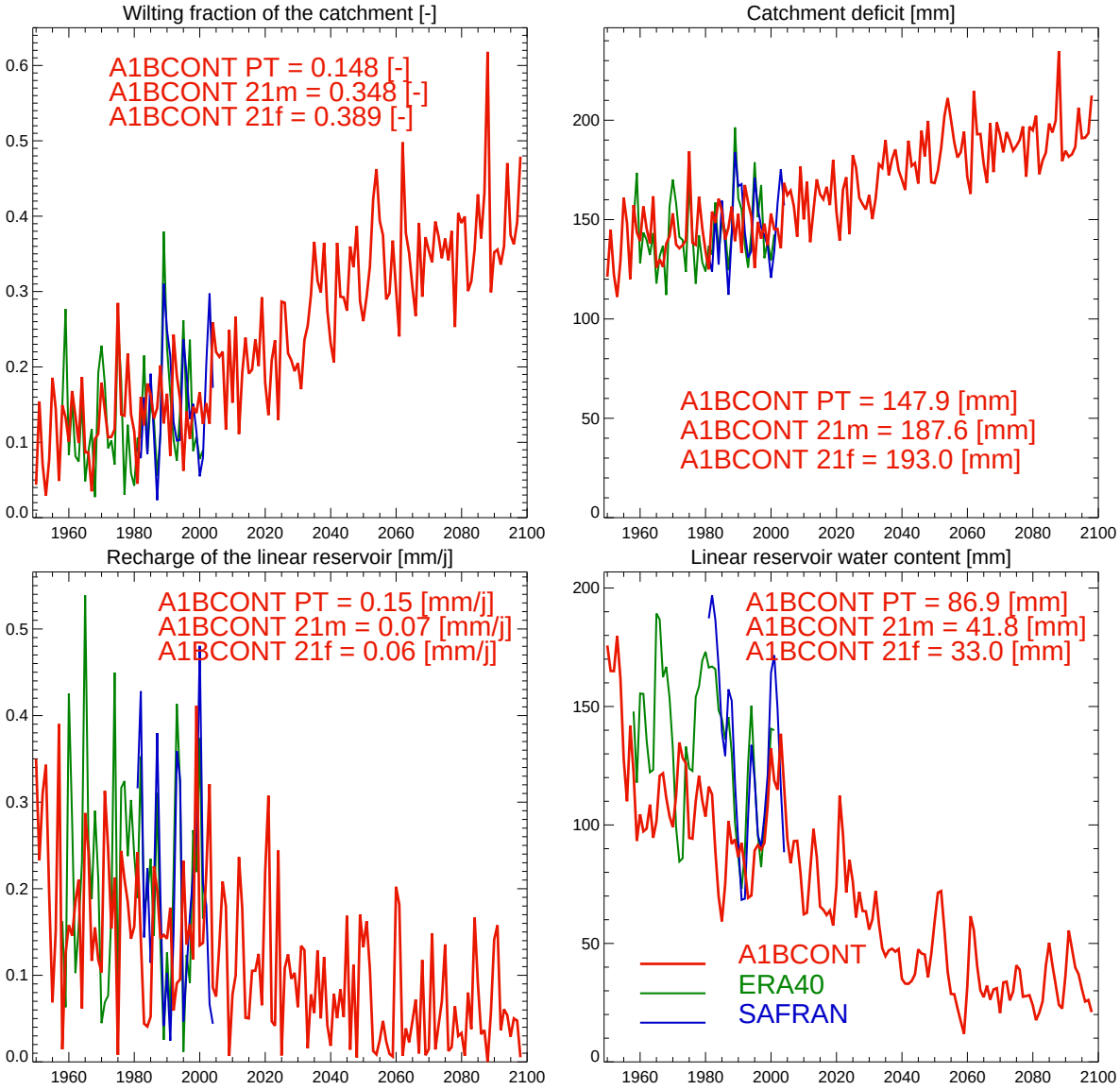

Figure 5.15: Trends on annual mean values over all the catchment for wilting areal fraction, catchment deficit, recharge to the linear reservoir and linear reservoir content. Red curve represent A1BCONT reference simulation, while blue and green are SAFRAN and ERA 40 simulations, fed with observed and reanalysed metereological data. Values given in red are mean values over 18 years long periods in present time PT (aug 1982 - July 2000), middle future time 21m (aug 2046 - July 2065) and future time 21f (aug 2081 - July 2099).

Runoff and groundwater: CLSM LR model[14] computes total runoff[15] as the sum of surface runoff, TOPMODEL's baseflow and linear reservoir's baseflow deep component called *base flow from LR*. Figure 5.16 shows the composition of A1BCONT total runoff at Poses. All the components contributing to total runoff decline with time as summarized also in table 5.8. Lower precipitation and thus, higher catchment deficit are the cause of the reduction in both TOPMODEL's and LR's baseflow. TOPMODEL's baseflow is directly driven by the catchment deficit M_D through equation 3.12.

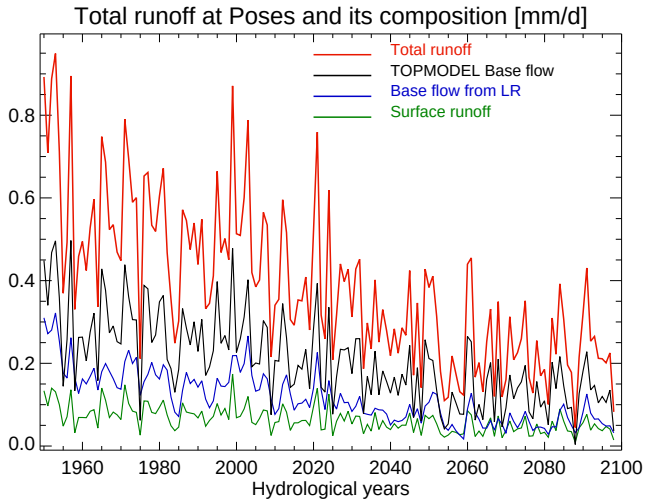

Figure 5.16: Mean annual runoff, overland flow and base flow at Poses for A1BCONT simulation. Green curve is overland flow (surface runoff). Total baseflow is the sum of TOPMODEL's baseflow (black) and baseflow from the linear reservoir (blue). Total runoff (red) is the sum of the 3 other curves.

The catchment deficit regulates indirectly the LR's baseflow too in the following way:

- Higher catchment deficit implies reduced recharge to the linear reservoir (equation 3.15). Recharge flux q_r to the LR shuts down from 0.14 mm/d in present time to 0.06 mm/d in 21f time (figure 5.15).
- With lower recharge, LR's water content is nearly divided by 3 in future time: 33 mm in 21f versus 86.7 mm in PT.
- LR's baseflow is driven by the water content in the deep linear reservoir through equation 3.18 and thus indirectly is regulated by the catchment deficit.

[14]Catchment Land Surface model with Linear Reservoir.

[15]see §3.3

LR's base flow goes down from 0.14 mm/d PT value to 0.06 mm/d 21f value. Note the equilibrium between the input and the output from the LR.

The difference between 21f and PT values is nearly of -60 % for LR's parameters while it is of -50% for total runoff and for TOPMODEL's baseflow. Thus, climate change reduces the importance of the deep LR of CLSM in producing total runoff (see table 5.8).

5.5 General Circulation Model related uncertainties

In climate change research, it is classical to use a multi-model approach to characterize future climate and impacts. We have already discussed in section 5.3 how large are the differences between the climate scenarios produced by various GCMs and the observed climate on historical time. The 8 scenarios, already assessed on present time (7 GCMs[16] from IPCC AR4 (Randall et al. 2007) and A1BCONT[17]) are all downscaled with the weather regime approach and based for future time on the A1B GHGs emission scenario from the IPCC SRES 2000. Thus, each of these 8 scenarios differs from one another for the General Circulation Model only. These specific 7 GCMs have been used in this thesis because they were the only one to be already downscaled by CERFACS at the time of this study.

In this section we will analyse and quantify the range of variations in climate change hydrological impacts caused by differences between these GCMs as a mean to assess the related uncertainties. In this way we will determine whether the climate change scenarios and impacts are robust or not with respect to the sampled GCM uncertainties.

5.5.1 Climate forcings

Table 5.9 summarizes the mean values of air temperature and precipitation (and runoff) for present time (PT), middle future time (21m) and future time (21f). It also reports the climate change impact of those variables. A "mean simulation" which is an average of the 8 climate change simulations has been computed.

Mean simulation impact on **air temperature** under climate change is robust since its absolute value (+2,5 °C) is three times the associated standard deviation (0,64 °C). This impacts is robust too in terms of mean annual cycle (figure 5.17 and

[16]A few details on these GCMs are given in table 5.2

[17]A1BCONT scenario issued from the variable resolution GCM ARPEGE v3+

	PT : 1982-2000			21m : 2047-2065			21f : 2081-2099			Impact 21f-PT		
	T	**P**	**R**	**T**	**P**	**R**	**T**	**P**	**R**	**T**	**P**	**R**
	°C	mm/d		°C	mm/d		°C	mm/d		°C	mm/d	
SAFRAN	10,35	2,18	0,59	-	-	-	-	-	-	-	-	-
A1BCONT	10,45	2,10	0,48	12,85	1,81	0,25	13,42	1,76	0,23	2,97	-0,34	-0,25
CSIROMK30	10,42	2,19	0,57	11,48	1,98	0,36	11,9	2,12	0,43	1,48	-0,07	-0,14
ECHAM5	10,32	2,15	0,54	12,46	2,16	0,41	13,72	2	0,26	3,4	-0,15	-0,27
GISS-AOM	10,53	2,05	0,48	12,15	1,83	0,25	12,23	1,82	0,26	1,7	-0,23	-0,22
GISS-MOD.	10,37	2,11	0,53	12,11	2,04	0,36	12,56	2,15	0,43	2,19	0,04	-0,1
MRI2A	10,46	2,09	0,51	12,35	2,04	0,35	13,07	1,99	0,31	2,61	-0,1	-0,21
CNRM-CM3	10,48	2,07	0,51	12,76	1,8	0,24	13,38	1,69	0,18	2,9	-0,38	-0,33
GFDL1	10,47	2,02	0,45	11,98	1,93	0,37	13,23	1,87	0,29	2,76	-0,15	-0,16
Mean	10,44	2,10	0,51	12,27	1,95	0,33	12,94	1,92	0,3	**2,5**	**-0,17**	**-0,21**
Std dev.	0,07	0,05	0,04	0,44	0,13	0,07	**0,64**	**0,17**	**0,09**	-	-	-

Table 5.9: Assessment of GCMs related uncertainties: precipitation (P), air temperature (T) and total runoff (R). For each variable are given the SAFRAN observed reference values on 1982-2000, the 8 climate change scenarios on present time PT, middle future time 21m and future time 21f. The mean value of the 8 scenarios and its standard deviation is given too. Last column quantify the maximum impact as the difference between 21f and present time value.

5.18) since their range of variation is smaller than their impact. Empirical relative frequency for air temperature confirm the robustness of the impact since the future time curves (figure 5.19) are clearly distincts from the present time ones (figure 5.10).

In contrast the mean impact on **precipitation** is not as robust since it is not above the standard deviation. The reduction is systematic on an annual mean basis (table 5.9). The magnitude however of this reduction is largely uncertain. Climate change impact on the mean precipitation annual cycle (figures 5.17 and 5.18) does not show a clear signal since the range of inter-model variations shows uncertainty even on the sign of the impact. The complementary cumulative distribution function for precipitation confirms that future time (figure 5.19) is not so clearly distinct from present time (figure 5.10).

While air temperature is correctly represented by most climate model, there are still large uncertainties pending on climate model simulated precipitation. At a first glimpse, this is not consistent with global scale climate multi-model ensembles projections that show an increase in globally averaged precipitation over the 21^{st} century ((Bates et al. 2008)). However, precipitation is very largely impacted by regional and local scale factors. On a continental scale, for all scenarios within IPCC AR4, projected mean annual precipitation increases in northern Europe and decreases further south (Bates et al. 2008). The Seine river basin is at the limit between Norther and Southern areas and would be in the southern part according to our scenarios. Furthermore, there is an area in western and central Europe where where even the sign of the precipitation change is not certain through IPCC multi-model intercomparisons and the Seine river catchment is in that area. Due to this large uncertainty pending on precipitation values, we need to consider as many climate scenarios as possible to gain insight on the most likely trends.

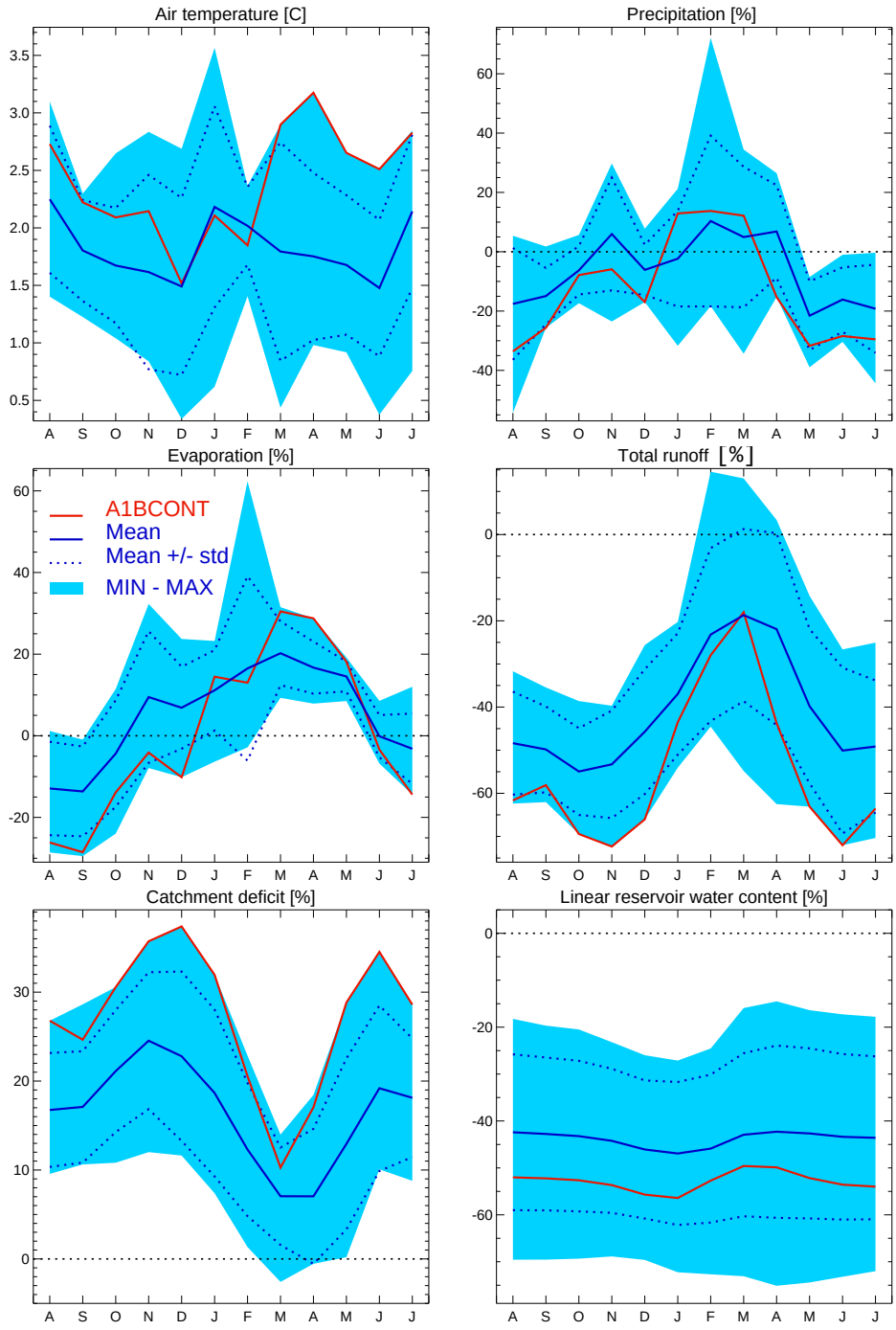

Figure 5.17: Assessment of GCMs related uncertainties on 2047-2065 (21m) impacts on the mean annual cycle. Monthly impacts over all the catchment upstream from Poses for air temperature, precipitation, evaporation, total runoff, catchment deficit and linear reservoir water content. For each simulation impacts are computed as the difference between future time (21m) and present time (PT: 1982-2000) monthly value and expressed in percentage of the present time value (except air temperature which is expressed in °C). Red curve represents A1BCONT simulation (GCM : ARPEGE climat v3+ downscaled with the weather regime approach). Blue curve is the mean between 8 simulations (A1BCONT and 7 simulations from IPCC AR4). Dotted blue curves are the standard deviation of this mean curve. The cyan shaded area indicates the whole spread of values of the 8 simulations.

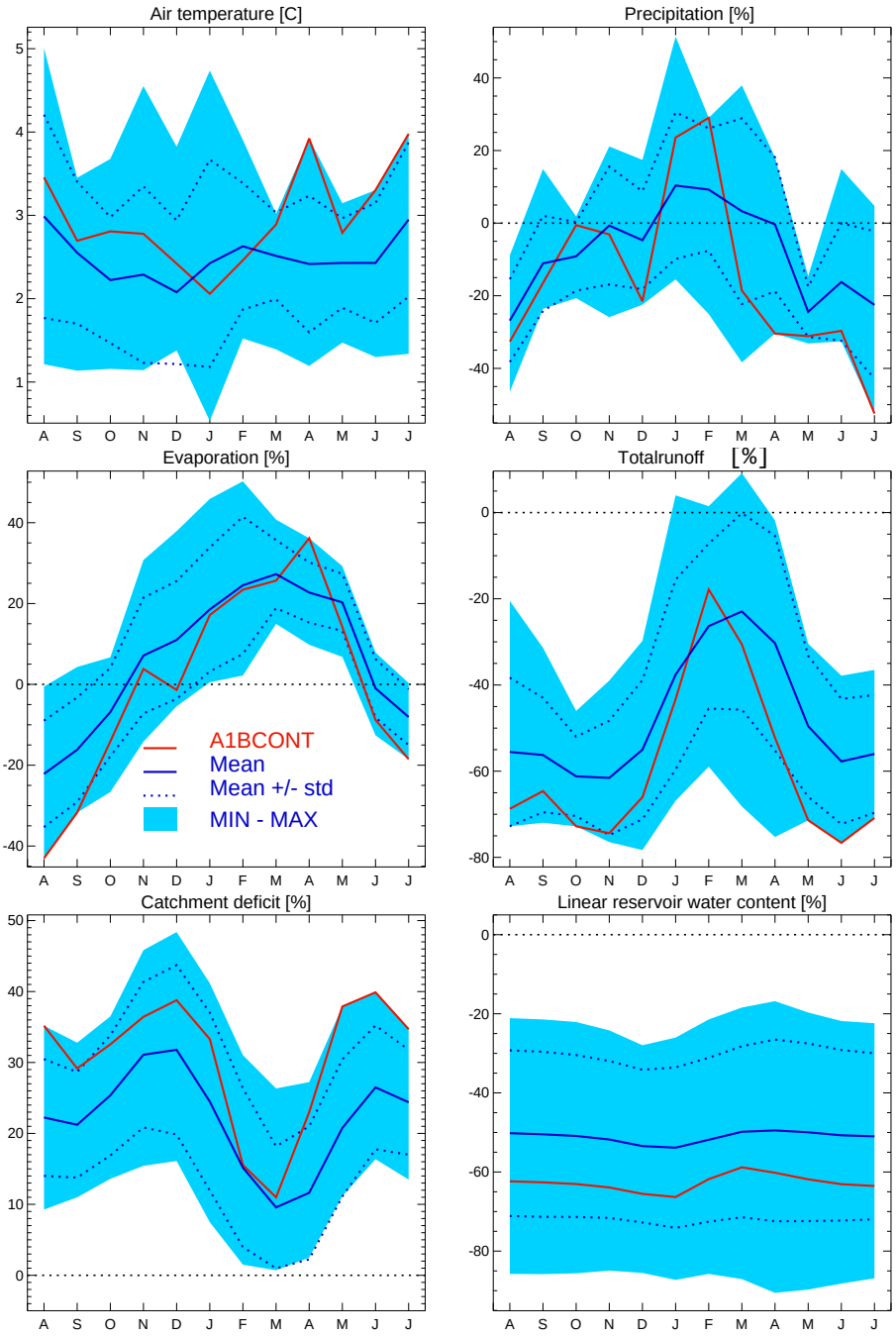

Figure 5.18: Assessment of GCMs related uncertainties on 2081-2099 (21f) impacts on the mean annual cycle. Monthly impacts over all the catchment upstream from Poses for air temperature, precipitation, evaporation, total runoff, catchment deficit and linear reservoir water content. For each simulation impacts are computed as the difference between future time (21f) and present time (PT: 1982-2000) monthly value and expressed in percentage of the present time value (except air temperature which is expressed in °C). Red curve represents A1BCONT simulation (GCM : ARPEGE climat v3+ downscaled with the weather regime approach). Blue curve is the mean between 8 simulations (A1BCONT and 7 simulations from IPCC AR4). Dotted blue curves are the standard deviation of this mean curve. The cyan shaded area indicates the whole spread of values of the 8 simulations.

Our reference climate change simulation A1BCONT overestimates the impact on air temperature warming and underestimates the impact on precipitation with respect to the mean scenario.In terms of mean annual cycle too, A1BCONT is "warmer" and "drier" than the mean of the 8 scenarios.

5.5.2 Impacts on hydrology

The "Mean simulation" impact on total **runoff** is a robust result even if it results from the reduction of precipitation, the magnitude of which is very uncertain. Actually the impact's absolute value (0,21 mm/d) is well above the associated standard deviation (0,09 mm/d). Impact is robust too in terms of mean annual cycle (figure 5.17 and 5.18) on most months (except January to March). Discharge empirical probability of exceedance (figure 5.10) expresses a robust impact of climate change. Discharge exceedance probabilities are much lower in all 21f scenarios (figure 5.19) with respect to their own present time baseline (figure 5.10).

Continental scale results reported in Alcamo et al. (2007) are that "annual average runoff is projected to increase in Northern Europe (north of 47°N)" and "to decrease in southern Europe (south of 47°N)" Alcamo, Flörke, and Märker 2007. Given the Seine watershed latitude, (48 degrees 52' N in Paris), our trend is not consistent with the cited continental scale result. Though, the edge position found by Alcamo, Flörke, and Märker varies greatly with the chosen general circulation model, i.e. the Seine river catchment is in the southern region where annual mean runoff decreases in Echam4 simulation while it is in the northern one in HadCM3 simulation. As discussed for precipitation (§, regarding runoff too, the Seine river catchment is located in an area of uncertainty, close to a climate divide.

In the 21f mean annual cycle graph (figure 5.18), our reference climate change simulation, A1BCONT, is most of the time within the standard deviation dotted line limits, meaning that it can still be considered representative of the 8 scenarios ensemble. However, A1BCONT is one of the 8 climate change scenarios that most underestimates the runoff.

Mean impact on **evaporation**, on the contrary, is not robust. Their absolute value (0,05 mm/d) is nearly half of the standard deviation of the 21f period (0,09 mm/d) (table 5.10). Referring to the mean annual cycle in figures 5.17 and 5.18, climate change curves merge with SAFRAN reference in most months. Only the enhanced evaporation rate in the spring months is a robust signal.

A1BCONT mean interannual impacts on evaporation, are not representative of the "mean scenario" since they have even a different sign compared to the "mean simulation". A1BCONT underestimates evaporation in all months between May and October due to the higher catchment deficit (lower soil moisture content).

Mean impacts for the **catchment deficit** Md and the **LR's water content** are rather robusts since they are largely above their respective standard deviation.

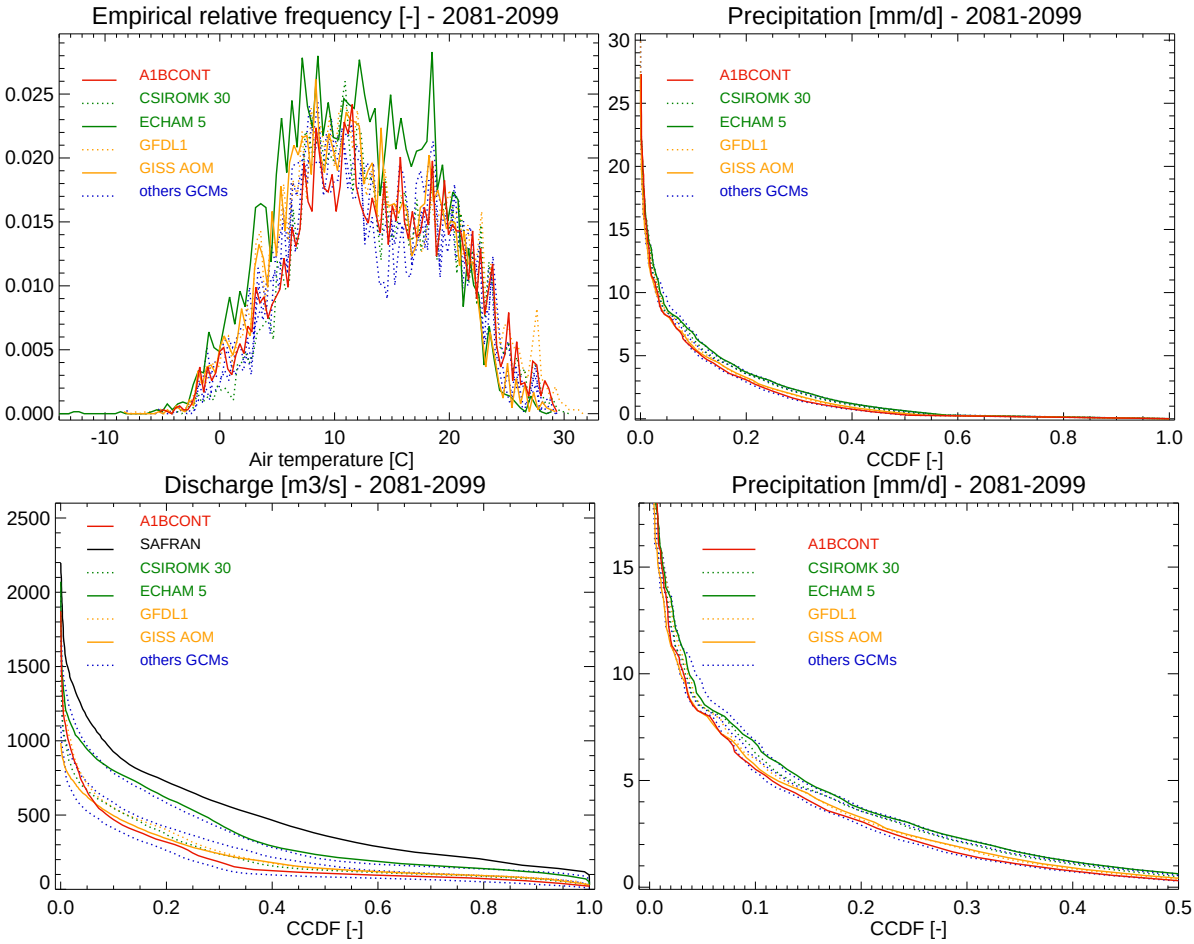

Figure 5.19: Empirical relative frequency for air temperature and empirical probability of exceedance for precipitation and routed discharge at Poses (2081-2099). Red curve represents A1BCONT simulation (GCM : ARPEGE climat v3+ downscaled with the weather regime approach). Green curves represent the two closest to SAFRAN GCMs from IPCC AR4 (see § 5.3.3): CSIROMK30 (dotted) and ECHAM5 (full line). Orange curves are the two simulations from IPCC AR4 with poorest results with respect to SAFRAN (see § 5.3.3): GFDL1 in full line and GISS AOM in dotted line. The three blue dotted curves represents the three other IPCC AR4 GCMs: CNRM-CM3, GISS-MODELER and MRI2A which have performances between orange and green curves in terms of similarity to SAFRAN in present time. The bottom and right graph is a zoom of the above graph (precipitation). Air temperature has been plotted only above the -14°C limit. Each curve has to be compared to its own baseline in present time (figure 5.10).

	PT : 1982-2000			21m : 2047-2065			21f : 2081-2099			Impact: 21f-PT		
	E	**Md**	**LR**	E	Md	LR	**E**	**Md**	**LR**	**E**	**Md**	**LR**
	mm/d	mm		mm/d	mm		mm/d	mm		mm/d	mm	
SAFRAN	1,58	145,5	127,9	-	-	-	-	-	-	-	-	-
A1BCONT	1,61	146,7	88,5	1,58	187,6	41,8	1,53	193,0	33,0	-0,08	46,4	-55,4
CSIROMK30	1,59	142,7	109,3	1,61	164,0	64,2	1,69	160,7	81,0	0,09	18,0	-28,3
ECHAM5	1,60	143,5	101,7	1,74	160,7	71,9	1,74	184,0	39,1	0,13	40,5	-62,6
GISS-AOM	1,57	149,5	89,6	1,58	176,7	37,2	1,58	174,1	39,5	0,01	24,6	-50,1
GISS-MOD.	1,57	145,8	97,4	1,67	165,9	60,2	1,72	168,7	76,2	0,15	22,9	-21,2
MRI2A	1,58	146,6	99,8	1,7	162,3	61,0	1,69	174,4	51,1	0,11	27,9	-48,7
CNRM-CM3	1,56	149,7	95,9	1,56	182,9	31,6	1,5	197,2	18,0	-0,06	47,5	-78,0
GFDL1	1,57	148,3	79,9	1,57	173,0	64,0	1,59	186,5	44,0	0,02	38,2	-35,9
Mean	1,58	146,6	95,2	1,63	171,6	54,0	1,63	179,8	47,7	**0,05**	**33,2**	**-47,5**
Std dev.	0,02	2,6	9,1	0,07	10,0	14,8	**0,09**	**12,5**	**21,3**	-	-	-

Table 5.10: Assessment of GCMs related uncertainties: evaporation (E), catchment deficit (MD) and LR's water content (LR). For each variable are given the SAFRAN observed reference values on 1982-2000, the 8 climate change scenarios on present time PT, middle future time 21m and future time 21f. The mean value of the 8 scenarios and its standard deviation is given too. Last column quantifies the maximum impact as the difference between 21f and present time value.

The mean annual cycle for those two variables (figures 5.17 and 5.18) shows their robustness for most months.

Clearly in all scenarios and in all months, the soil moisture content declines with climate change (i.e. the catchment deficit increases). A1BCONT is one of the scenarios which simulates the largest impacts of climate change on the catchment deficit and on the LR's water content.

5.5.3 Main results

The increase in temperature is a robust forcing not much sensitive to the choice of the general circulation model while precipitation's decline is an uncertain signal. The subsequent impacts, however are robusts: decline of total runoff, enhanced catchment deficit (i.e. a decline in soil moisture content) and decline of LR's reservoir water content. As for the change in evaporation, the sign is uncertain but it is small in any case.

In general, A1BCONT and CNRM-CM3, which are two scenarios issued from the ARPEGE model family[18], predict the largest impacts (largest warming, greatest reduction concerning precipitation, runoff and evaporation). They are the only two scenarios to predict a reduction of mean evaporation.

For all impact variables uncertainties increase with time: standard deviation and the range of variation are much larger in 21f than in 21m and PT time periods. Furthermore, for most variables, A1BCONT curve is closer to the "mean simulation"

[18]The main difference between the two scenarios is that A1BCONT is issued from a variable resolution uncoupled GCM and CNRM-CM3 from a classical coupled GCM with a coarse resolution

curve in the 21f than in the 21m time period. In other words, A1BCONT scenario is most of the time more representative of the "mean simulation" in 21f time period than in 21m time period: this means that A1BCONT scenario simulates a climate change signal greater than the mean scenario on 21m period but then starts to converge to that mean scenario by the end of the 21st century (threshold effect).

5.6 Downscaling techniques related uncertainties

Climate forcings generated by General Circulation Models have a coarse resolution of approximately 300 km × 300 km. Even when a regional model or a variable resolution GCM is used, the scale resolution is generally not finer than 50 km × 50 km. Hydrological local impact models require instead a much finer resolution. Downscaling techniques are used to solve this scale mismatch problem.

In the framework of this thesis we used 9 scenarios downscaled with the weather regime approach and 2 scenarios downscaled with the variable correction method. A few detail on these two downscaling techniques have been given in chapter 2. In this section we will compare Arp-v4-WR-A2 and Arp-v4-VCM-A2 scenarios. These two scenarios have been both produced with the variable resolution ARPEGE Climat version 4 under A2 GHGs emission scenario for future time. They differ only for the downscaling technique.

The differences between simulated impacts by these two simulations will allow us to assess the importance of the downscaling technique, the impact of which has already been showed to be very large on present time scenarios (§5.3.2).

5.6.1 Climate forcings

Differences on simulated mean air temperature over 21f time period between the two downscaling schemes are very little. However, the Variable Correction Method simulates larger seasonal contrasts (figure 5.20) with larger increase on air temperature values in summer and smaller increase on air temperature values in winter. The empirical relative frequency graph (figure 5.21) shows that the variable correction method leads to more extreme values at both tails of the distribution.

The annual mean reduction in precipitation is slightly greater with the variable correction method than with the weather regime approach. As in present time, the VCM scheme simulates higher contrasts with low reduction of precipitation in fall and winter and a massive decline in summer. In terms of empirical probability distribution, with respect to the weather regime approach, the VCM scenario underestimates medium daily precipitation exceeded more than 10% of the time and less than 40% of the time and overestimates high precipitation values exceeded less than 10%.

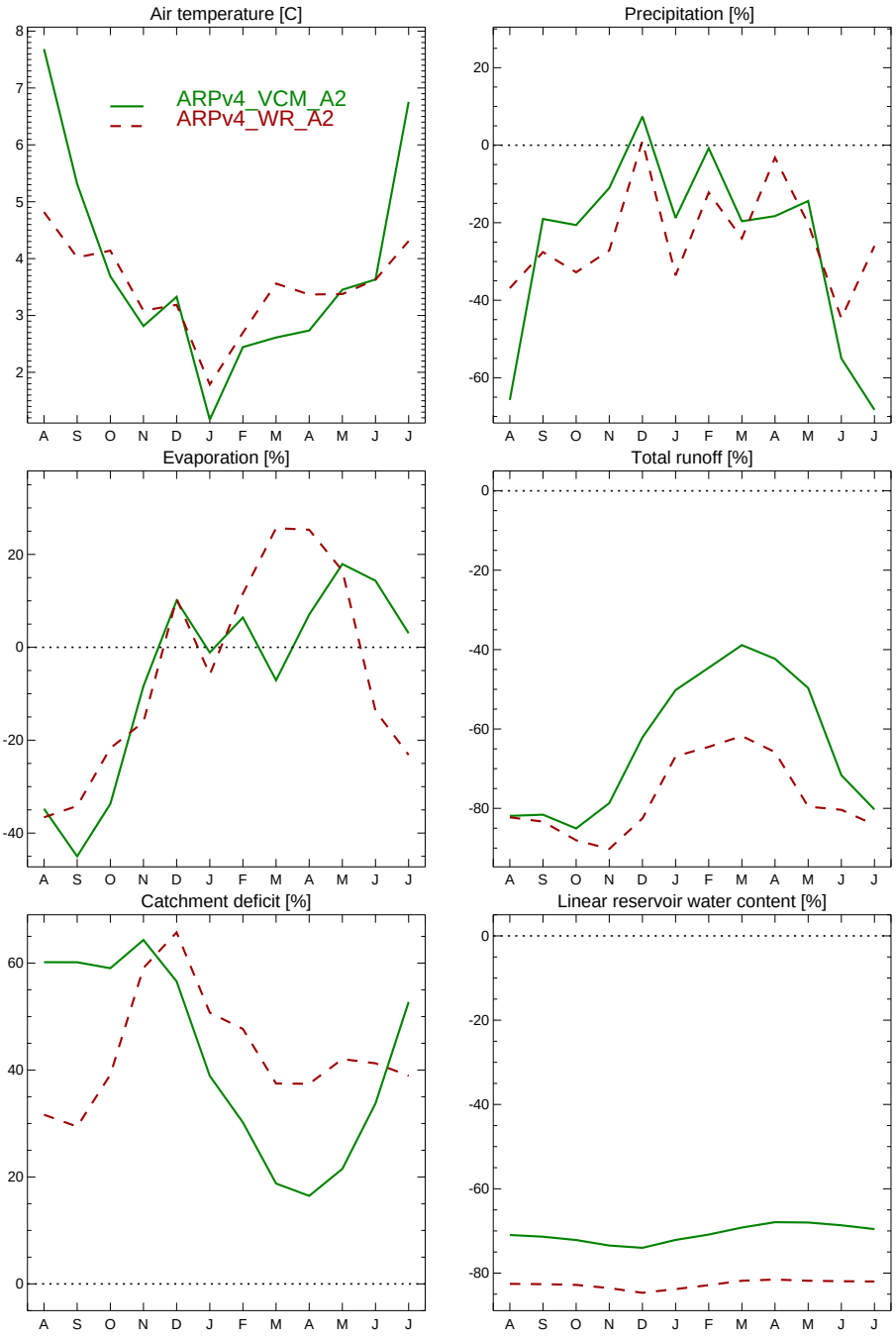

Figure 5.20: Assessment of downscaling techniques related uncertainties on 2081-2099 impacts on the mean annual cycle. Monthly impacts over all the catchment upstream from Poses for air temperature, precipitation, evaporation, total runoff, catchment deficit and linear reservoir water content. For each simulation impacts are computed as the difference between future time (21f) and present time (PT: 1982-2000) monthly value and expressed in percentage of the present time value (except air temperature which is expressed in °C). Green curve comes from the ARPEGE climat v4 GCM downscaled with the variable correction method. Brick-red curve comes from the ARPEGE climat v4 GCM downscaled with the weather regime approach.

Simulation name	PT : 1982-2000			21f : 2081-2099			Impact 21f-PT		
	T	P	R	T	P	R	T	P	R
	°C	mm/d		°C	mm/d		°C	mm/d	
SAFRAN	10,35	2,18	0,59	-	-	-	-	-	-
A1BCONT	10,45	2,10	0,48	13,42	1,76	0,23	2,97	-0,34	-0,25
Arpv4-WR-A2	**10,45**	**2,17**	**0,55**	**13,96**	**1,66**	**0,14**	**3,51**	**-0,51**	**-0,41**
Arpv4-VCM-A2	**10,18**	**2,19**	**0,82**	**14**	**1,64**	**0,33**	**3,82**	**-0,55**	**-0,49**
Mean (11 simulations)	10,39	2,13	0,57	13,14	1,86	0,3	2,75	-0,26	-0,27
St. dev. (11 simulations)	0,12	0,06	0,13	0,68	0,18	0,1	-	-	-
Difference WR – VCM	0,27	-0,02	-0,27	-0,05	0,02	-0,19	-	-	-

Table 5.11: Assessment of downscaling techniques related uncertainties: precipitation (P), air temperature (T) and total runoff (R). For each variable are given the SAFRAN observed reference values on 1982-2000, A1BCONT, Arpv4-VCM and Arpv4-WR simulations on present time PT and future time 21f (under A2 scenario). The mean value of the 11 scenarios (A1BCONT, Arpv4-WR-A2, Arpv4-VCM-A2, Arpv4-VCM-A1B and 7 scenarios from IPCC-AR4) and its standard deviation are given too. Last column quantifies the maximum impact as the difference between 21f and present time value. Last line gives the difference between WR and VCM simulated values.

In other terms, it seems that the variable correction method predicts more frequent extreme climate forcings such as high temperatures and large precipitation events. There is the need for further investigations within the work package 3 of the Rexhyss project (§ 1.2).

5.6.2 Impacts on hydrology

All hydrological variables (except evaporation and the catchment deficit) shown in tables 5.11 and 5.12 undergo a larger mean reduction with the VCM scenario than with the WR one.

Simulation Name	PT : 1982-2000			21f : 2081-2099			Impact 21f-PT		
	E	Md	LR	E	Md	LR	E	Md	LR
	mm/d	mm		mm/d	mm		mm/d	mm	
SAFRAN	1,58	145,5	127,9	-	-	-	-	-	-
A1BCONT	1,61	146,7	88,5	1,53	193,0	33,0	-0,08	46,4	-55,4
Arpv4-WR-A2	**1,627**	**143,4**	**101,6**	**1,5**	**203,8**	**17,7**	**-0,13**	**60,4**	**-84,0**
Arpv4-VCM-A2	**1,382**	**126,3**	**184,1**	**1,33**	**183,5**	**54,1**	**-0,05**	**57,2**	**-130,0**
Mean (11 simulations)	1,55	142,9	113,3	1,57	181,5	48,3	0,02	38,6	-65,0
St. dev. (11 simulations)	0,09	8,4	36,5	0,14	13,2	22,4	-	-	-
Difference WR – VCM	0,25	17,2	-82,4	0,17	20,3	-36,4	-	-	-

Table 5.12: Assessment of downscaling techniques related uncertainties: evaporation (E), catchment deficit (Md) and LR's water content (LR). For each variable are given the SAFRAN observed reference values on 1982-2000, A1BCONT, Arpv4-VCM and Arpv4-WR simulations on present time PT and future time 21f (under A2 scenario). The mean value of the 11 scenarios (A1BCONT, Arpv4-WR-A2, Arpv4-VCM-A2, Arpv4-VCM-A1B and 7 scenarios from IPCC-AR4) and its standard deviation are given too. Last column quantifies the maximum impact as the difference between 21f and present time value. Last line gives the difference between WR and VCM simulated values.

Observing the mean annual cycle (figure 5.20), simulation downscaled with the VCM approach describes a less impacted scenario than the WR one (higher runoff, lower catchment deficit, higher LR's water content) for all variables (except evaporation). It has to be reminded that the variable correction method showed large

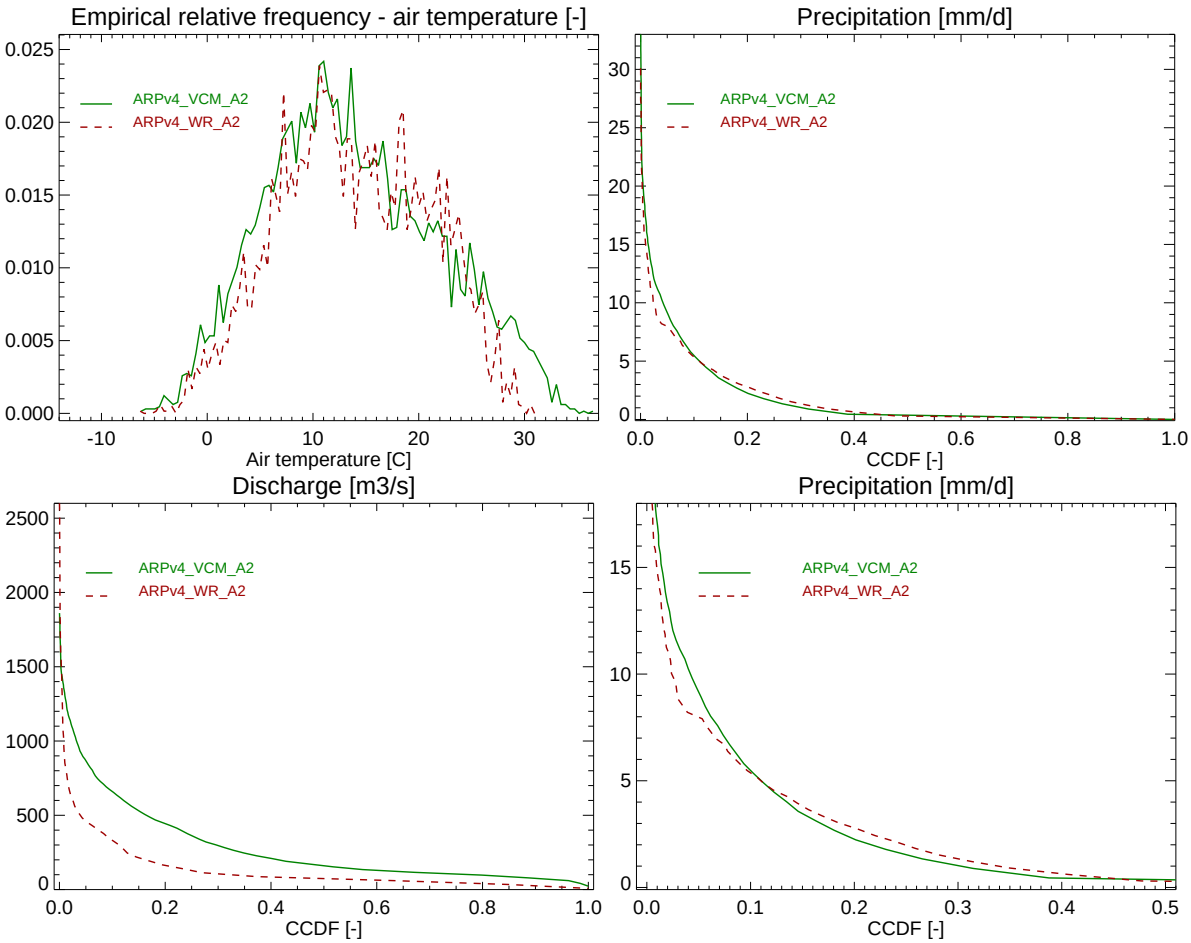

Figure 5.21: Empirical relative frequency for air temperature and Empirical probability of exceedance for precipitation and routed discharge upstream from Poses (2081-2099) - daily values. Green curve comes from the ARPEGE climat v4 GCM downscaled with the variable correction method. Brick-red curve comes from the ARPEGE climat v4 GCM downscaled with the weather regime approach. The bottom and right graph is a zoom of the above graph (precipitation). The bottom and right graph is a zoom of the above graph (precipitation). Air temperature has been plotted only above the -14°C limit.

biases versus SAFRAN on present time assessment (§ 5.3.2).

Total runoff undergoes a lower decline with the VCM scenario than with the WR one (particularly in the winter months). Thus, discharge values have larger probability of exceedance with the VCM downscaling than with the WR approach. However, it has to be considered also that the VCM method showed a large overestimation of exceedance probabilities for daily discharge values in present time assessment (§ 5.3.2.2). The same differences exist between the methods at present time (PT) and in the future (21f). Specifically, as SAFRAN was between the two methods in PT, one can suspect that the impact of climate change simulated by the variable correction method is a bit less severe than the one predicted by the weather regime approach.

The seasonal impacts on the catchment deficit shows a different behavior between VCM and WR scenario (because of the deficit in precipitation) with an enhanced catchment deficit in the summer months under VCM scenario. Evaporation rate seasonal behavior is clearly supply-driven by the catchment deficit. Differences between the VCM and the WR in the catchment deficit explain the differences in evaporation between the two simulations.

The LR's water content is less impacted in VCM scenario than in WR one for all months of the year. The reason is that the recharge occurs in winter when the catchment deficit is larger with the variable correction method.

Generally speaking, even if the differences between the weather regime approach and the variable correction method are not negligible, table 5.12 shows that they are much smaller than the climate change impact, what fosters our confidence on our results.

5.6.3 Main results

The previous paragraphs show that the Weather Regime downscaling technique induces greater impacts on most variables than the Variable Correction Method. However the VCM downscaling showed large biases versus SAFRAN on present time assessment (§ 5.3.2).

The differences between WR and VCM scenarios given in tables 5.11 and 5.12 are all smaller than the projected mean impact of the 11 climate change simulations (except evaporation). Differences in precipitation and temperature are lower than the standard deviation too, meaning that uncertainties on these climate forcings are more due to the general circulation models and emission scenario than to the downscaling technique. Concerning runoff, catchment deficit and LR's water content, the choice of the downscaling technique seems to influence a great part of the uncertainties since the differences between the WR and VCM scenarios are larger than the standard deviation of the 11 simulations on these 3 variables.

This analysis shows that the choice of the downscaling technique is an important issue in climate change impact studies. Validity of a downscaling scheme can unfortunately be assessed only versus historical observation. In present time assessment, the weather regime approach showed little biases and a good representativity of present climate while the variable correction method had large biases on many variables. A1BCONT, our climate change "reference simulation", and most of the scenarios used in this work have been downscaled with the weather regime approach in which we have more confidence.

5.7 Emission scenarios related uncertainties

In the modeling sequence which is used to produce climate scenarios, the first step is the choice of a green house gas and aerosols emission scenario. Special emission report on emission scenarios (IPCC SRES 2000) characterises various emission scenarios depending on future economic, environmental and demographic choices. In the framework of this thesis we used 9 climate change simulations based on the A1B scenario and 2 on the A2 scenario.

The A1B scenario describes a world of very rapid economic growth, global population that peaks in mid-century and declines thereafter, rapid introduction of new and more efficient technologies, convergence among regions and reduction in regional differences in per capita income. A1B scenario is distinguished by a "balanced" energy related technological change which means *not relying too heavily on one particular energy source, with similar improvement rates applied to all energy supply and end use technologies* (SRES, Nakinovic and Swart 2000).

The A2 scenario describes a very heterogeneous world where self-reliance and preservation of local identities are predominant. There is a continuously increasing global population. Economic development is mainly regional. Economic growth and technological change is slower and more fragmented than in other storylines.

A1B scenario assumes much lower GHGs emissions in 2100 than A2 (approximatively 55 Gt CO_2-eq. per year in A1B scenario versus 130 Gt CO_2-eq. per year in A2, Nakinovic and Swart 2000). In IPCC multi model simulations A1B scenario leads to an average global warming of 2.8°C versus 3.4 °C for A2 (IPCC AR4, 2007).

In this section we will mainly compare ARPv4-VCM-A1B and ARPv4-VCM-A2 simulations which are both issued from the ARPEGE Climat v4 variable resolution GCM and downscaled with the variable correction method. These two simulations have a common present time based on observed GHGs. On the future time period they differ only for the GHGs emission scenario. The differences between simulated impacts by these two simulations will allow us to assess the importance of the GHGs emission scenario compared to the other parts of the modeling sequence (the general circulation model and the downscaling technique). However, the uncertainty related

to GHG forcing cannot be fully assessed as GHGs emissions depend on human decisions which cannot in any case be predicted.

An important preliminary comment is that the assessment of GHGs emission scenario related uncertainties presented in the forthcoming section has to deal with two important limiting factors:ting factors:

- The variable correction method (VCM), which we use for this comparison, has shown some large biases in the assessment versus present time observed climate (§ 5.3.2).
- Comparing only two simulations is not enough for giving a clear result on the importance of the emission scenario.

To realize the assessment of the importance of the GHGs emission, it would have been preferable to dispose of more paired simulation datasets differing only for the GHGs emission scenario. Particularly it would have been interesting to have A1B version of the ARPv4-WR simulation (downscaled with the weather regime approach which shown better results in terms representativity of the present climate).

Other datasets are not available in the framework of the Rexhyss project at the moment. We are aware of the limits of the comparison realised in the present section, however we think that this assessment, can still give some interesting preliminary indications and be valuable as an example of the multi-scenario assessment methodology largely use in climate change impact studies.

5.7.1 Climate forcings

Mean climate change impacts of A1BCONT, ARPv4-VCM-A1B and ARPv4-VCM-A2 simulations are given in table 5.13. It shows that warming and precipitation reduction are larger in A2 scenario than in A1B scenario as expected. Mean impacts of climate change on air temperature are within the range of global mean values found in IPCC AR4.

Empirical probability distributions are shown in figure 5.23. The air temperature graph confirms that A2 scenario simulates higher frequencies for higher temperature values. The precipitation probability of exceedance graph shows a higher reduction in A2 scenario for medium value precipitation which are exceeded between 10 and 50% of the time while it shows a lower reduction trend for higher precipitation values exceeded less that 10% of the time. However, as already discussed, our analysis is not sufficient for rare precipitation values.

The mean annual cycles given in figure 5.22 confirm these results. The impacts on air temperature are larger for the A2 scenario than for A1B in most months. As for the impacts on precipitation, they are not very different between the two scenarios but the summer reduction is larger in A2 scenario.

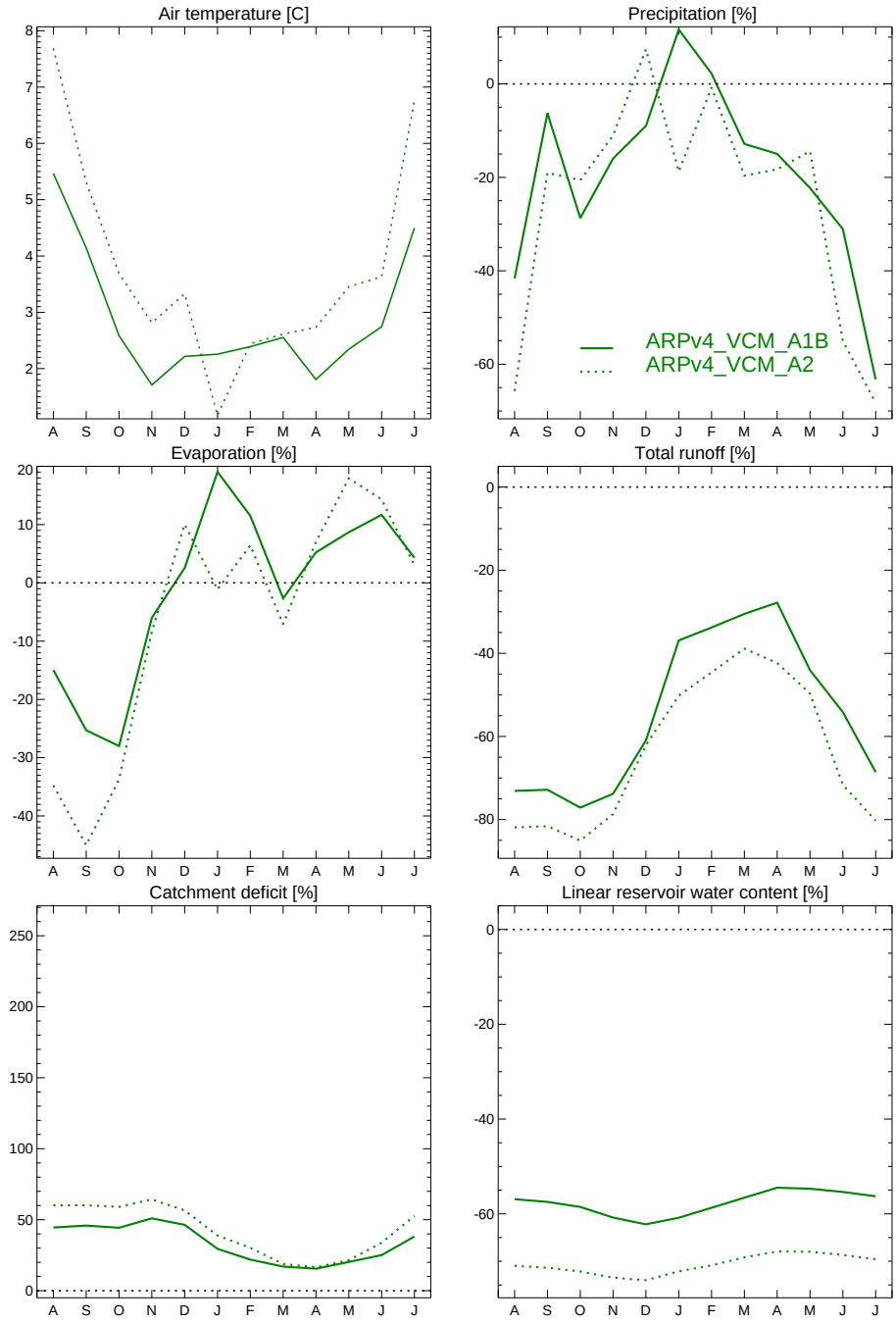

Figure 5.22: Assessment of GCMs related uncertainties on 2081-2099 impacts on the mean annual cycle. Monthly impacts over all the catchment upstream from Poses for air temperature, precipitation, evaporation, total runoff, catchment deficit and linear reservoir water content. For each simulation impacts are computed as the difference between future time (21f) and present time (PT: 1982-2000) monthly value and expressed in percentage of the present time value (except air temperature which is expressed in °C). Green curves come from the ARPEGE climat v4 GCM downscaled with the variable correction method under A1B (full line) and A2 (dotted line) GHGs emission scenarios.

Simulation name	PT : 1982-2000			21f : 2081-2099			Impact 21f-PT		
	T	**P**	**R**	**T**	**P**	**R**	**T**	**P**	**R**
	°C	mm/d	mm/d	°C	mm/d	mm/d	°C	mm/d	mm/d
SAFRAN	10,35	2,18	0,59	-	-	-	-	-	-
A1BCONT	10,45	2,10	0,48	13,42	1,76	0,23	2,97	-0,34	-0,25
Arpv4-VCM-A1B	**10,18**	**2,193**	**0,821**	**13,09**	**1,78**	**0,41**	**2,91**	**-0,41**	**-0,41**
Arpv4-VCM-A2	**10,18**	**2,193**	**0,821**	**14**	**1,66**	**0,33**	**3,82**	**-0,53**	**-0,49**
Mean (11 simulations)	10,39	2,13	0,57	13,14	1,86	0,3	2,75	-0,26	-0,27
St. dev. (11 simulations)	0,12	0,06	0,13	0,68	0,18	0,1	-	-	-
A2-A1B	-	-	-	0,91	-0,12	-0,08	-	-	-

Table 5.13: Assessment of GHGs emission scenarios related uncertainties: precipitation (P), air temperature (T) and total runoff (R). For each variable are given the SAFRAN observed reference values on 1982-2000, A1BCONT, Arpv4-VCM-A1B and Arpv4-VCM-A1B simulations on present time PT and future time 21f. The mean value of the 11 scenarios and its standard deviation are given too. Last column quantifies the maximum impact as the difference between 21f and present time value. Last line gives the difference between A2 and A1B simulated values.

5.7.2 Impacts on hydrology

All hydrologic variables (except evaporation) shown in tables 5.13 and 5.14 undergo a larger mean reduction under A2 than A1B.

	PT : 1982-2000			21f : 2081-2099			Impact 21f-PT		
	E	**Md**	**LR**	**E**	**Md**	**LR**	**E**	**Md**	**LR**
	mm/d	mm	mm	mm/d	mm	mm	mm/d	mm	mm
SAFRAN	1,58	145,5	127,9	-	-	-	-	-	-
A1BCONT	1,61	146,7	88,5	1,53	193,0	33,0	-0,08	46,36	-55,43
Arpv4-VCM-A1B	**1,382**	**126,27**	**184,1**	**1,38**	**170,58**	**77,91**	**-0,002**	**44,3**	**-106,18**
Arpv4-VCM-A2	**1,382**	**126,27**	**184,1**	**1,33**	**183,5**	**54,09**	**-0,05**	**57,23**	**-130,01**
Mean (11 simulations)	1,55	142,85	113,31	1,57	181,5	48,32	0,02	38,65	-64,99
St. dev. (11 simulations)	0,09	8,41	36,51	0,14	13,17	22,44	-	-	-
A2-A1B	-	-	-	-0,05	12,92	-23,82	-	-	-

Table 5.14: Assessment of GHGs emission scenarios related uncertainties: evaporation (E), catchment deficit (MD) and LR's water content (LR). For each variable are given the SAFRAN observed reference values on 1982-2000, A1BCONT, Arpv4-VCM-A1B and Arpv4-VCM-A1B simulations on present time PT and future time 21f. The mean value of the 11 scenarios and its standard deviation are given too. Last column quantifies the maximum impact as the difference between 21f and present time value. Last line gives the difference between A2 and A1B simulated values.

In terms of mean annual cycle (figure 5.22), A2 scenario simulates more dramatic impacts in terms of water resources availability. The increase in the catchment deficit (i.e. decline in soil moisture content) is larger for A2 than for A1B scenario, particularly in the summer months. Total runoff in A2 scenario is much lower than in A1B, particularly in the summer months. LR's water content undergo a greater reduction under A2 scenario. These three impacts are all unanimous in describing a large degradation of water resources availability in both GHGs scenario but larger in A2. Evaporation mean annual cycle does not show great differences between the two GHGs scenarios because of a small difference in the catchment deficit.

Complementary cumulative distribution function (figure 5.23) shows lower probability of exceedance under A2 scenario for all **discharge** values.

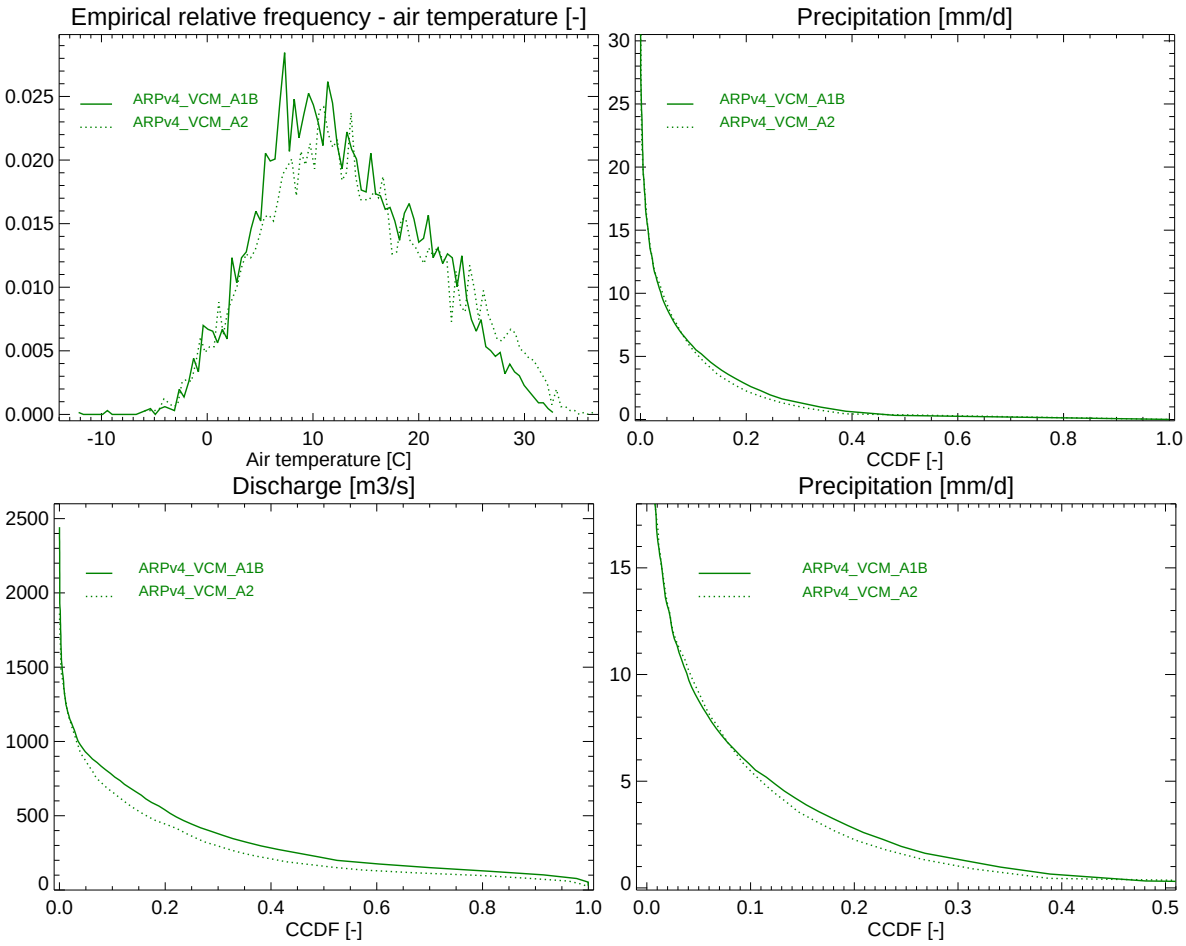

Figure 5.23: Empirical relative frequency for air temperature and Empirical probability of exceedance for precipitation and routed discharge at Poses (2081-2099) - daily values. Green curves come from the ARPEGE climat v4 GCM downscaled with the variable correction method under A1B (full line) and A2 (dotted line) GHGs emission scenarios. The bottom and right graph is a zoom of the above graph (precipitation). Air temperature has been plotted only above the -14°C limit.

5.7.3 Main results

The previous paragraphs show that the A2 scenario simulates greater impacts on most variables. This analysis implies that assuming a GHGs emission reduction policy on a global scale could limit the impacts on the Seine river basin's hydrology. This is particularly evident on runoff (figure 5.23).

The differences between A2 and A1B scenario given in tables 5.13 and 5.14 are all lower than the projected mean impact of the 11 climate change simulations. Most of them (except air temperature) are lower than the standard deviation too.

Differences on **climate forcings** (precipitation and air temperature) between the two different downscaling techniques are lower than differences caused by the two GHGs emission scenarios. The opposite is true for simulated impacts on **hydrologic variables** (runoff, catchment deficit, LR's content). This would mean that the chosen GHGs emission scenario induce more uncertainties on climate than the downscaling technique, while the uncertainties pending on hydrologic impacts depend more on the downscaling than on the GHGS emission scenario. However, confidence in this conclusion is not very high since two GHGs scenarios are not enough to cover the related uncertainties.

The sampled uncertainties on GHGs emission do not cast doubt on the results obtained with A1B scenarios since A2 leads to larger impacts.

Chapter 6

Conclusion

Within this thesis, a detailed analysis of main impacts of climate change on the hydrology of the Seine river basin has been accomplished using CLSM model. A synthesis of these results is given in section 6.2. Next section 6.1 summarises instead the overall approach

6.1 Overall approach

This master's thesis has been realised in the framework of the Rexhyss project (see § 1.2). To characterise climate change impacts a multi-scenario approach classical in climate change impact studies has been used to feed a hydrological distributed and physically based land surface model (Catchment Based Land Surface Model : CLSM). The modeling sequence used to produce the available climate scenarios has been described in chapter 2. State of the art on Land Surface Models and CLSM model have been analysed in chapter 3 with reference to a recent version of CLSM with a linear reservoir.

The field of study of the present thesis is the Seine river catchment upstream from Poses, it has been shortly described in chapter 4. In the same chapter a validation of six different runs of CLSM showed good performances of the model in representing observed discharges. Thus, "equifinality" of these six runs has been tested and discussed on present time and future time. Differences between the six runs were little both on present time values and on future time impacts. Climate change impacts are not sensibly driven by the choice of the CLSM run. Thus a medium range run has been chosen and applied to all the simulations analysed in chapter 5 and summarised in the next section.

6.2 Synthesis of climate change impacts

6.2.1 Climate Forcings

All the 11 simulations mostly agree in the trends on air temperature and precipitation (figure 6.2). A mean of the 11 simulations has been computed and is given in table 6.1, we will refer to this mean as the "mean simulation". It shows mean impacts in future time[1] of +2.75°C on air temperature and -0,26 mm/d on precipitation. These impacts can be considered rather robusts since they are well above the standard deviation of the 11 simulations.

[1]Mean impacts on future time are defined as the difference between the mean value of future time 21f and the mean value of present time PT

We have already discussed that climate models and downscaling techniques simulate quite well air temperature and with much greater uncertainties precipitation. This is the case also with the 11 climate change simulations compared in this thesis. **Air temperature** monthly mean increases robustly in all months of the year (figure 6.1). **Precipitation** has a much less robust signal since the range of variation of the 11 simulations is very large. In fact, large uncertainties due to the modeling sequence (GHGs emission scenarios, GCMs and downscaling techniques) are still pending on the precipitation signal. However, the reduction in the summer months appears to be quite robust since it is confirmed by most models. Winter enhanced precipitation is much more uncertain.

A1BCONT, our reference simulation under climate change, appear to be not so close to the mean of the other simulations ("mean simulation") in present time and future time. A1BCONT simulates larger climate change signal both in terms of warming and of precipitation's reduction. Furthermore, in A1BCONT simulation, 21m middle time (2047-2065) is already very close in terms of climate forcings to the end of the 21st century.

	PT : 1982-2000			**21m : 2047-2065**			**21f : 2081-2099**			**Impact 21f-PT**		
	T	**P**	**R**	**T**	**P**	**R**	**T**	**P**	**R**	**T**	**P**	**R**
	[°C]	[mm/d]		[°C]	[mm/d]		[°C]	[mm/d]		[°C]	[mm/d]	
SAFRAN	10,35	2,18	0,59	-	-	-	-	-	-	-	-	-
A1BCONT	10,45	2,10	0,48	12,85	1,81	0,25	13,42	1,76	0,23	2,97	-0,34	-0,25
Mean 8 sim	10,44	2,10	0,51	12,27	1,95	0,33	12,94	1,92	0,30	2,50	-0,17	-0,21
Std. dev. 8 sim	0,07	0,05	0,04	0,44	0,13	0,07	0,64	0,17	0,09	-	-	-
Arpv4-WR-A2	10,45	2,17	0,55	-	-	-	13,96	1,66	0,14	3,51	-0,51	-0,41
Arpv4-VCM-A1B	10,18	2,19	0,82	-	-	-	13,09	1,78	0,41	2,91	-0,41	-0,41
Arpv4-VCM-A2	10,18	2,19	0,82	-	-	-	14,00	1,64	0,33	3,82	-0,55	-0,49
Mean 11 sim	10,39	2,13	0,57	-	-	-	13,14	1,86	0,30	2,75	-0,26	-0,27
Std. dev. 11 sim)	0,12	0,06	0,13	-	-	-	0,68	0,18	0,10	-	-	-
Downscaling	0,27	-0,02	-0,27	-	-	-	-0,05	0,02	-0,19	-	-	-
Emission scenario	-	-	-	-	-	-	0,92	-0,14	-0,08	-	-	-

Table 6.1: Climate change impacts on precipitation (P), air temperature (T) and total runoff (R). For each variable are given the SAFRAN observed reference values on 1982-2000, A1BCONT (ARPEGE version 3+, downscaled with the weather regime approach), ARPEGE v4 downscaled with the variable correction method (ARPv4-VCM) and with the weather regime (ARPv4-WR). ARPv4-VCM is available for future time under the two GHGs emission scenarios A1B and A2. The mean of 8 climate change scenarios (A1BCONT and 7 IPCC) and of the 11 scenarios and their standard deviation is given too. Last column quantifies the maximum impact as the difference between 21f and present time value. Last two lines quantify the differences between the two downscaling techniques and between the two emission scenarios.

Air temperature forcing is influenced to a relatively important extent by the GHGs emission scenario since difference between A1B and A2 scenarios in future time is of 0,92 °C, larger than the 11 simulations standard deviation. Precipitation, instead, is less largely driven by the green house gases emission scenario and more by the general circulation model and the downscaling technique.

6.2.2 CLSM outputs

The **catchment deficit** is greatly enhanced by the end of the century, meaning that the **soil moisture content** is greatly reduced with climate change (figure

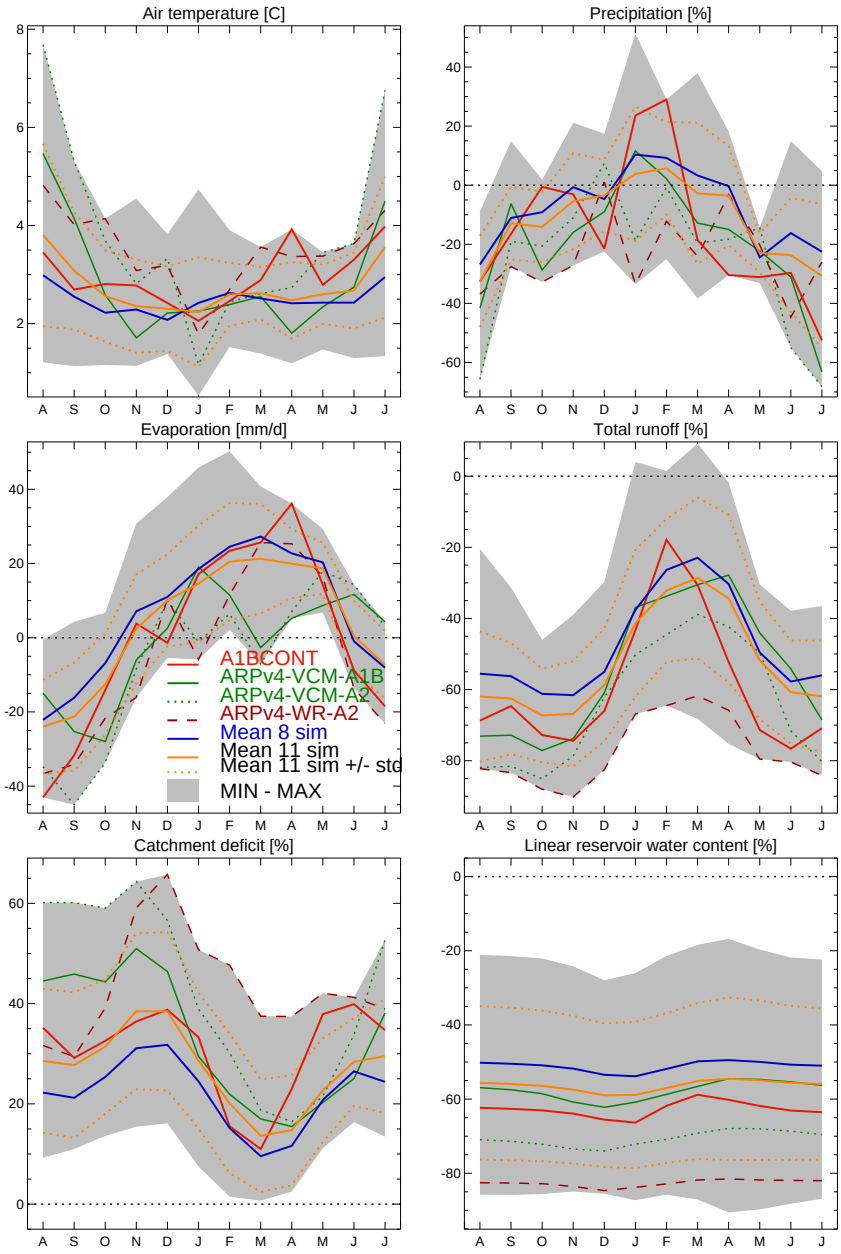

Figure 6.1: Main results on 2081-2099 impacts on the mean annual cycle. Monthly impacts over all the catchment upstream from Poses for air temperature, precipitation, evaporation, total runoff, catchment deficit and linear reservoir water content. For each simulation impacts are computed as the difference between future time (21f) and present time (PT: 1982-2000) monthly value and expressed in percentage of the present time value (except air temperature which is expressed in °C). Red curve represents A1BCONT simulation (GCM : ARPEGE climat v3+ downscaled with the weather regime approach). Dark green curves come from the ARPEGE climat v4 GCM downscaled with the variable correction method under A2 (dotted line) and A1B GHGs emission scenario (full line). Dashed brick-red curve represent the ARPEGE climat v4 GCM downscaled with the variable correction method under A2 GHGs emission scenario. Blue curve is the mean between 8 simulations (A1BCONT and 7 simulations from IPCC AR4). Orange curve is the mean between the 11 simulations. Dotted orange curves are the standard deviation of this mean curve. The grey shaded area indicates the whole spread of values of the 11 simulations. On 21m time period, only 8 simulations are available (A1BCONT and 7 simulations from IPCC AR4): the mean (full blue line), the associated standard deviation curves (dotted blue lines) and the range of variation (shaded cyan) of these 8 simulations are given.

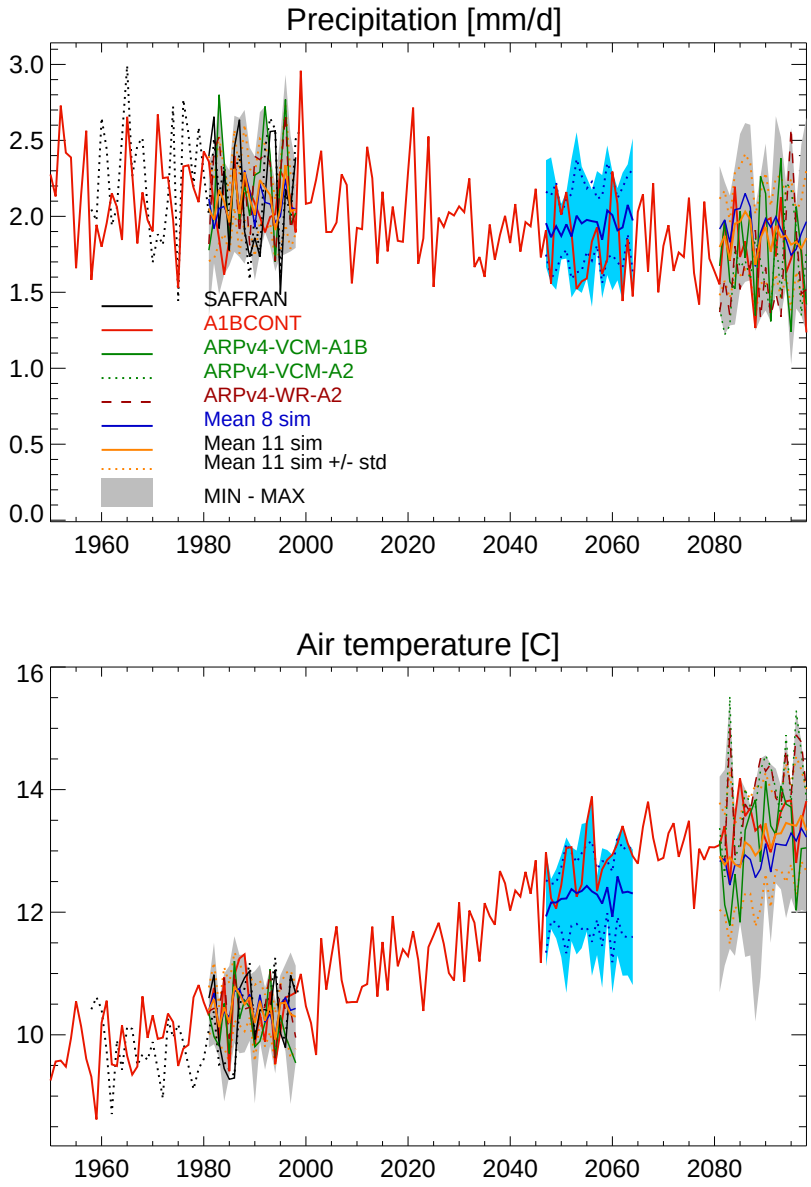

Figure 6.2: Trend on annual mean values for the 11 simulation ensemble over all the catchment at Poses for air temperature and precipitation. Black curve represents SAFRAN present time (1982-2000) observed values. All the other curves are climate change simulations for the 2081-2099 years ("future time" - 21m). Red curve represents A1BCONT simulation (GCM : ARPEGE climat v3+ downscaled with the weather regime approach). Dark green curves come from the ARPEGE climat v4 GCM downscaled with the variable correction method under A2 (dotted line) and A1B GHGs emission scenario (full line). Dashed brick-red curve represent the ARPEGE climat v4 GCM downscaled with the variable correction method under A2 GHGs emission scenario. Blue curve is the mean between 8 simulations (A1BCONT and 7 simulations from IPCC AR4). Orange curve is the mean between the 11 simulations. Dotted orange curves are the standard deviation of this mean curve. The grey shaded area indicates the whole spread of values of the 11 simulations. On 21m time period, only 8 simulations are available (A1BCONT and 7 simulations from IPCC AR4): the mean (full blue line), the associated standard deviation curves (dotted blue lines) and the range of variation (shaded cyan) of these 8 simulations are given.

6.4). Since the **recharge flux** to the deep linear reservoir is mostly driven by the catchment deficit, **linear reservoir water content** is greatly reduced too. These two impacts are rather robusts since their absolute value is much greater than the 11 simulations standard deviation (table 6.2).

The catchment deficit is particularly enhanced in the summer months due to the great reduction in summer precipitations (figure 6.1). Higher catchment deficit means lower soil moisture content. Lower soil moisture content in the summer months explains the evaporation behavior. **Evaporation** remains nearly stable on a mean annual basis (figure 6.3 and table 6.2). Mean impact on evaporation is rather unrobust. In terms of mean annual cycle, evaporation becomes clearly "supply driven"[2] in the May to October months under climate change: due to lower soil moisture content in the summer(i.e. higher catchment deficit), evaporation rate cannot satisfy the evaporative demand (which is enhanced due to higher air temperature values).

Total runoff undergoes a massive decline, it is nearly halved by the end of the 21^{st} century. All scenarios confirm this trend (figure 6.3). The 4 scenarios from the ARPEGE GCM family[3] all predict a larger reduction than the mean result. This is due not only to the general circulation model, but also to the different downscaling technique (Arp-v4-VCM-A1B) or to the different GHG's emission scenario (Arpv4-VCM-A2, Arpv4-WR-A2). The downscaling technique appears to influence runoff uncertainties since difference between Arpv4-VCM-A2 and Arpv4-WR-A2 are greater than the standard deviation of the 11 simulations. However, we must take into account that the variable correction method had shown large biases on present time assessment (§ 5.3).

In terms of seasonal behavior, total runoff is greatly reduced in the May to October months. This is a robust result since the range of variation is relatively small in these months and the impacts are greater than the standard deviation. On the other months of the year, there is a general reduction too, but this trend is surrounded by a larger range of variation and greater uncertainties.

Generally speaking, simualted impacts are nearly fully accomplished already by the middle of the century (21m). This is partly due to the fact that 9 of the 11 scenarios are issued from A1B GHGs emission scenario which simulates the peak of GHGs emission in the middle of the 21st century (see figure 2.4).

[2]In present time instead, there is enough soil moisture content over the Seine river catchment and evaporation is most of the time demand driven.

[3]A1BCONT which comes from the ARPEGE climat version 3+ and the three other scenarios from the ARPEGE climat version 4

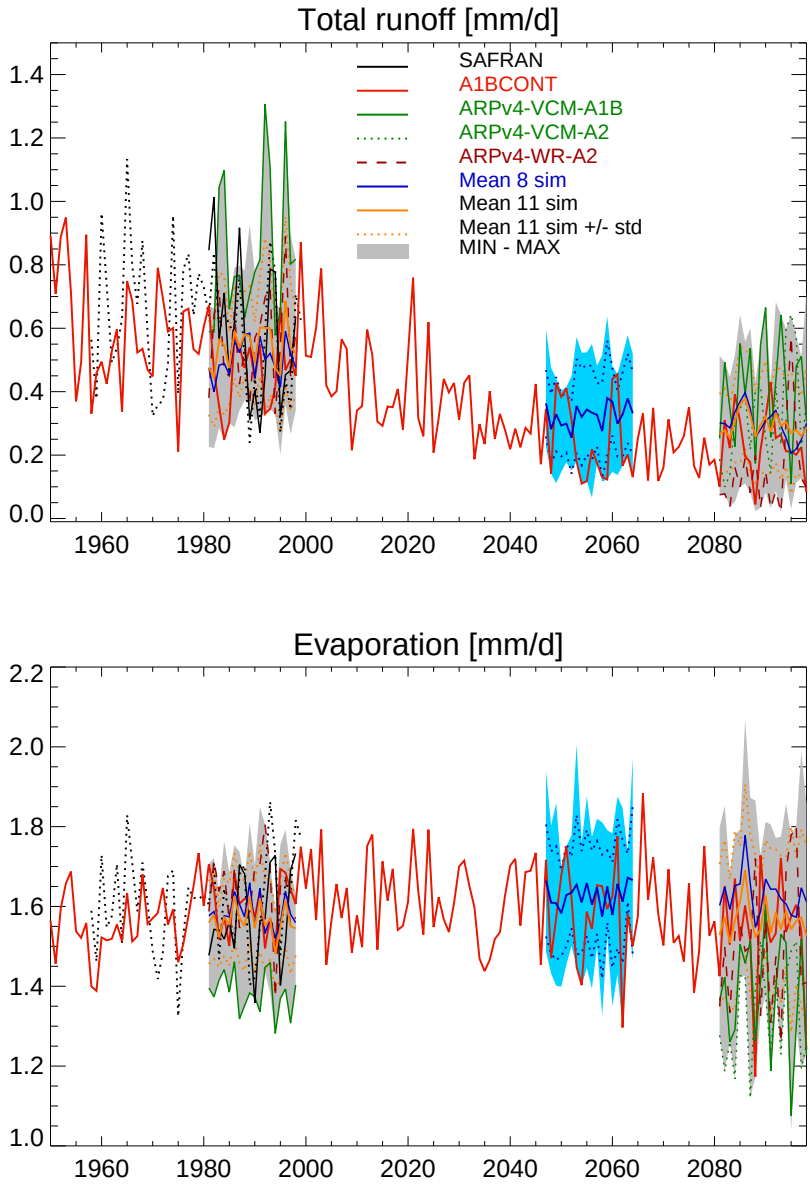

Figure 6.3: Trend on annual mean values for the 11 simulation ensemble over all the catchment at Poses for total runoff and evaporation. Black curve represents SAFRAN present time (1982-2000) observed values. All the other curves are climate change simulations for the 2081-2099 years ("future time" - 21m). Red curve represents A1BCONT simulation (GCM : ARPEGE climat v3+ downscaled with the weather regime approach). Dark green curves come from the ARPEGE climat v4 GCM downscaled with the variable correction method under A2 (dotted line) and A1B GHGs emission scenario (full line). Dashed brick-red curve represent the ARPEGE climat v4 GCM downscaled with the variable correction method under A2 GHGs emission scenario. Blue curve is the mean between 8 simulations (A1BCONT and 7 simulations from IPCC AR4). Orange curve is the mean between the 11 simulations. Dotted orange curves are the standard deviation of this mean curve. The grey shaded area indicates the whole spread of values of the 11 simulations. On 21m time period, only 8 simulations are available (A1BCONT and 7 simulations from IPCC AR4): the mean (full blue line), the associated standard deviation curves (dotted blue lines) and the range of variation (shaded cyan) of these 8 simulations are given.

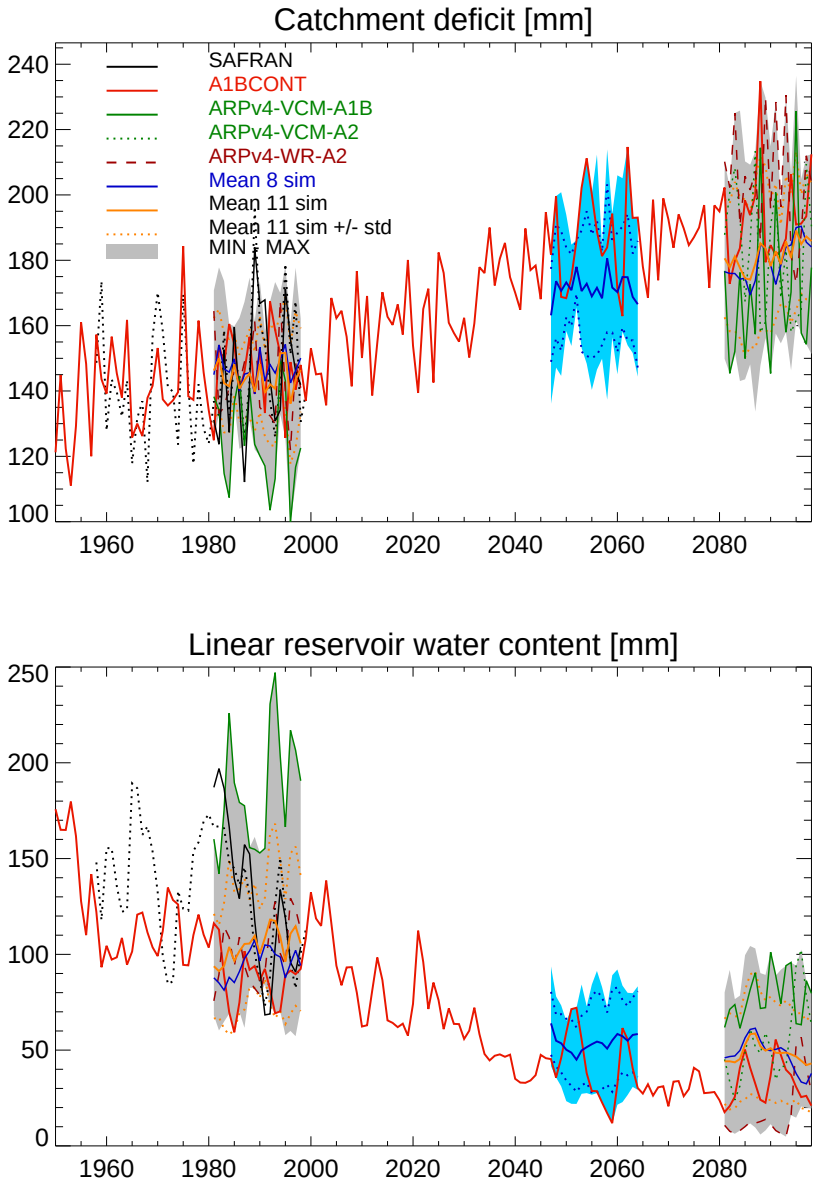

Figure 6.4: Trend on annual mean values for the 11 simulation ensemble over all the catchment at Poses for the catchment deficit and linear reservoir water content. Black curve represents SAFRAN present time (1982-2000) observed values. All the other curves are climate change simulations for the 2081-2099 years ("future time" - 21m). Red curve represents A1BCONT simulation (GCM : ARPEGE climat v3+ downscaled with the weather regime approach). Dark green curves come from the ARPEGE climat v4 GCM downscaled with the variable correction method under A2 (dotted line) and A1B GHGs emission scenario (full line). Dashed brick-red curve represent the ARPEGE climat v4 GCM downscaled with the variable correction method under A2 GHGs emission scenario. Blue curve is the mean between 8 simulations (A1BCONT and 7 simulations from IPCC AR4). Orange curve is the mean between the 11 simulations. Dotted orange curves are the standard deviation of this mean curve. The grey shaded area indicates the whole spread of values of the 11 simulations. On 21m time period, only 8 simulations are available (A1BCONT and 7 simulations from IPCC AR4): the mean (full blue line), the associated standard deviation curves (dotted blue lines) and the range of variation (shaded cyan) of these 8 simulations are given.

	PT : 1982-2000			21m : 2047-2065			21f : 2081-2099			Impact 21f-PT		
	E	Md	LR	E	Md	LR	E	Md	LR	E	Md	LR
	mm/d	mm		mm/d	mm		mm/d	mm		mm/d	mm	
SAFRAN	1,58	145,5	127,9	NO	NO	NO	NO	NO	NO	NO	NO	NO
A1BCONT	1,61	146,7	88,5	1,58	187,6	41,8	1,53	193,0	33,0	-0,08	46,4	-55,4
Mean 8 sim	1,58	146,6	95,2	1,63	171,6	54,0	1,63	179,8	47,7	0,05	33,2	-47,5
Std. dev. 8 sim	0,02	2,6	9,1	0,07	10,0	14,8	0,09	12,5	21,3	NO	NO	NO
Arpv4-WR-A2	1,627	143,4	101,6	NO	NO	NO	1,5	203,8	17,7	-0,13	60,4	-84,0
Arpv4-VCM-A1B	1,382	126,3	184,1	NO	NO	NO	1,38	170,6	77,9	0	44,3	-106,2
Arpv4-VCM-A2	1,382	126,3	184,1	NO	NO	NO	1,33	183,5	54,1	-0,05	57,2	-130,0
Mean 11 sim	1,55	142,9	113,3	NO	NO	NO	1,57	181,5	48,3	0,02	38,6	-65,0
Std. dev. 11 sim	0,09	8,4	36,5	NO	NO	NO	0,14	13,2	22,4	NO	NO	NO
Downscaling	0,25	17,2	-82,4	NO	NO	NO	0,17	20,3	-36,4	NO	NO	NO
Emission scenario	NO	NO	NO	NO	NO	NO	-0,05	12,9	-23,8	NO	NO	NO

Table 6.2: Climate change impacts on evaporation (E), catchment deficit (Md) and linear reservoir water content. For each variable are given the SAFRAN observed reference values on 1982-2000, A1BCONT (ARPEGE version 3+, downscaled with the weather regime approach), ARPEGE v4 downscaled with the variable correction method (ARPv4-VCM) and with the weather regime (ARPv4-WR). ARPv4-VCM is available for future time under the two GHGs emission scenarios A1B and A2. The mean of 8 climate change scenarios (A1BCONT and 7 IPCC) and of the 11 scenarios and their standard deviation is given too. Last column quantify the maximum impact as the difference between 21f and present time value. Last two lines quantify the differences between the two downscaling techniques and between the two emission scenarios.

6.3 Continuation of this work

Results from the present Master's thesis will be used in the framework of the Rexhyss research project. Data will be used to realize an intercomparison between various and different hydrological models (described in § 1.2). Furthermore, discharges will be statistically analysed with a discharge-duration frequency approach for determining climate change impacts on floods and droughts frequencies.

Anthropogenic global warming and climate change is now widely accepted. However too little is done by citizen and decion makers to reduce Green House Gases emission and mitigate climate change. This is also due to the fact that citizens do not link easily global warming (and associated changes in large scale climate) to their daily life. Thus research on climate change impacts has the essential role of making aware citizen and decision-makers of the local scale impacts of climate change.

Climate change impacts, quantified through this thesis and further ascertained within the Rexhyss project, will be very valuable to all the stakeholder of the Seine river basin and particularly to all the decision makers. Hopefully, the dramatic prediction of large and rather robusts impacts on the Seine river basin will encourage the decision-makers to adopt not only local adaptation policies but also to encourage forceful global mitigation policies in terms of Green-House Gases emission reduction.

Bibliography

Alcamo, J., M. Flörke, and M. Märker. 2007. "Future long-term changes in global water resources driven by socio-economic and climatic changes / Changements futurs à long terme dans les ressources en eau globales forcés par les changements climatiques et socio-économiques." *Hydrological Sciences Journal/Journal des Sciences Hydrologiques* 52 (April): 247–275.

Alcamo, J., J.M. Moreno, B. Nováky, M. Bindi, R. Corobov, R.J.N. Devoy, C. Giannakopoulos, E. Martin, J.E. Olesen, and A. Shvidenko. 2007. Chapter Europe of *Climate Change 2007: Impacts, Adaptation and Vulnerability. Contribution of Working Group II to the Fourth Assessment Report of the Intergovernmental Panel on Climate Change*. Cambridge: Cambridge University Press.

Bates, B.C., Z.W. Kundzewicz, S. Wu, and J.P. Palutikof. 2008. *Climate change and water*. Geneve: IPCC Secretariat. IPCC technical paper VI.

Bellier, S. 2008, June. "Calibration d'un modèle de routage hydrologique dans le bassin de la Seine." Master's thesis, Université Pierre et Marie Curie, Paris, France.

Beven, K. 2006. "A manifesto for the equifinality thesis." *Journal of Hydrology* 320 (March): 18–36.

Beven, K. J., and M. J. Kirkby. 1979. "A Physically Based, Variable Contributing Area Model of Basin Hydrology." *Hydrological Sciences Bulletin* 24 (1): 43–69 (March).

Boé, J., F. Terray, F. Habets, and E. Martin. 2006. "A simple statistical-dynamical downscaling scheme based on weather types and conditional resampling." *Journal of Geophysical Research*, vol. 111.

Clapp, Roger B., and George M. Hornberger. 1978. "Empirical Equations for some soil hydraulic properties." *Water Resources Research* 14 (4): 601–604 (August).

Cosby, B. J., G. M. Hornberger, R. B. Clapp, and T. R. Ginn. 1984. "A statistical exploration of the Relationships of Soil Moisture Characteristics to the Physical Properties of Soils." *Water Resources Research* 20 (6): 682–690 (June).

Déque, M. 2007. "Frequency of precipitation and temperature extremes over France in an anthropogenic scenario: Model results and statistical correction according to observed values." *Global and Planetary Change* 57:16–26.

Dickinson, R.E., M. Shaikh, R. Bryant, and L. Graumlich. 1998. "Interactive Canopies for a Climate Model." *J. Climate* 11:2823–2836.

Dingman, S.L. 2002. Chapter "Stream response to water-input events" of *Physical Hydrology*, 408–410. Upper Saddle River, NJ, USA: Prentice Hall.

Ducharne, A. 2008. "Le modèle hydrométéorologique CLSM - travaux récents à l'UMR Sisyphe." Note interne.

Ducharne, A., C. Baubion, N. Beaudoin, M. Benoit, G. Billen, N. Brisson, J. Garnier, H. Kieken, S. Lebonvallet, E. Ledoux, B. Mary, C. Mignolet, X. Poux, E. Sauboua, C. Schott, S. Thery, and . 2007. "Long term prospective of the Seine River system: Confronting climatic and direct anthropogenic changes." *Science of the Total Environment* 375 (1–3): 292–311.

Ducharne, A., R. D. Koster, M. Suarez, M. Stieglitz, and P. Kumar. 2000. "A catchment-based approach to modeling land surface processes in a GCM - Part 2 : Parameter estimation and model demonstration." *Journal of Geophysical Research* 105 (D20): 24823–24838.

Ducharne, A., K. Laval, and J. Polcher. 1998. "Sensitivity of the hydrological cycle to the parametrization of soil hydrology in a GCM." *Climate Dynamics* 14:307–327.

Ducharne, A., Théry, Billen, Benoit, Brisson, Garnier, Kieken, Ledoux, Mary, Mignolet, Mermet, Poux, Saboua, Schott, Viennot, Abu, Alkhair, Baubion, Curie, Ducos, Gomez, Lebonvallet, and O. 2004. "Influence du changement climatique sur le fonctionnement hydrologique et biogèochimique du bassin de la Seine." Technical Report, Rapport final du projet GICC-Seine.

Durand, Y., E. Brun, L. Mérindol, G. Guyomarc'h, B. Lesaffre, and E. Martin. 1993. "A meteorological estimation of relevant parameters for snow models." *Annals of Glaciology* 18:65–71.

Famiglietti, J. S., and E. F. Wood. 1994. "Multiscale modeling of spatially variable water and energy balance processes." *Water Resources Research* 30:3061–3078.

Fowler, H.J., S. Blenkisop, and C. Tebaldi. 2007. "Linking climate change modelling to impacts studies: recent advances in downscaling techniques for hydrological modelling." *Int. J. CLimatol.* 27:1547–1578.

Gascoin, S., A. Ducharne, P. Ribstein, M. Carli, and F. Habets. 2008. "Adaptation of a catchment-based land surface model to the hydrogeological setting of the Somme River basin (France)." Submitted for review to Elsevier.

Gibelin, A.-L., and M. Déque. 2003. "Anthropogenic climate change over the Mediterranean region simulated by a global variable resolution model." *Climate Dynamics* 20:327–339.

Giorgi, F., X. Bi, and J. Pal. June 2004. "Mean, interannual variability and trends in a regional climate change experiment over Europe. I. Present-day climate (1961-1990)." *Climate Dynamics* 22:733–756(24).

Gomez, E., E Ledoux, P Viennot, C Mignolet, M Benoit, C Bornerand, C Schott, B Mary, G Billen, A Ducharne, and D. Brunstein. 2003. "Un outil de modélisation intégrée du transfert des nitrates sur un système hydrologique: application au bassin de la Seine." *La Houille Blanche*, vol. 3.

Habets, F., P. Etchevers, C. Golaz, E. Leblois, E. Ledoux, E. Martin, J. Noilhan, and Ottlé, C. 1999. "Simulation of the water budget and the river flows of the Rhone basin." *Journal of Geophysical Research* 104:31145–31172.

Henderson-Sellers, A., Z.L. Yang, and R. Dickinson. 1993. "The Project for Intercomparison of Land-surface Parameterization Schemes." *Bull. Amer. Meteor. Soc.* 74:1335–1349.

IPCC-AR4. 2007. *Climate Change 2007: Synthesis Report*. Geneve: IPCC Secretariat.

Jamagne, M., R. Hardy, D. King, and M. Bornand. 1995. "La base de donnée géographique des Sols de France." *Etud. Gest. Sols* 2:72–153.

Javelle, P. 2001. "Caractérisation du régime des crues : le modèle débit-durée-fréquence convergent. Approche locale et régionale." Ph.D. diss., Institut National Polytechnique de Grenoble.

Koster, R., and M. J. Suarez. 1996. "Energy and Water Balance Calculations in the Mosaic LSM." Technical Report 9, NASA Technical Memorandum 104606.

Koster, R. D., and P. C. D. Milly. 1997. "The Interplay between Transpiration and Runoff Formulations in Land Surface Schemes Used with Atmospheric Models." *Journal of Climate* 10 (July): 1578–1591.

Koster, R. D., M. J. Suarez, A. Ducharne, M. Stieglitz, and P. Kumar. 2000. "A catchment-based approach to modeling land surface processes in a general circulation model 1. Model structure." *Journal of Geophysical Research* 105:24809–24822.

Koster, R.D., and M.J. Suarez. 1992. "Modeling the Land Surface Boundary in Climate Models as a Composite of Independent Vegetation Stands." *J. Geophys. Res.* 97:2697–2715.

Ledoux, E., G. Girard, and G. de Marsily. 1989. Chapter Spatially distributed modeling : conceptual approach, coupling surface water and groundwater. of

Unsaturated flow in hydrologic modeling, Theory and practice, 435–454. Kluwer Academic Publishers.

Manabe, S. 1969. "Climate and the ocean circulation 1. The atmospheric circulation and the hydrology of the Earth's surface." *Monthly Weather Review* 97 (11): 739–774.

Mancini, M, and N Montaldo. "La formazione del deflusso superficiale." Dispensa per il corso di Idrologia a.a. 2006-2007 - Politecnico di Milano.

Masson, V., J.-L. Champeaux, F. Chauvin, C. Meriguet, and R. Lacaze. 2003. "A Global Database of Land Surface Parameters at 1-km Resolution in Meteorological and Climate Models." *Journal of Climate* 16 (May): 1261–1282.

Meybeck, M, G de Marsily, and E Fustec. 1998, December. *La Seine en son bassin. Fonctionnement écologique d'un système fluvial anthropisé.* Paris: Elsevier.

Monteith, J.L. 1965. "Evaporation and environment." Edited by Cambridge University Press, *Proceedings of the 19th Symposium of the Society for Experimental Biology.* New York, USA, 205–233.

Musy, A., and C. Higy. 1998. *Hydrologie appliquée.* Bucarest: Editions H*G*A*.

Nakinovic, and Swart. 2000. *Emission scenarios - Summary for Policy Makers (IPCC-SRES-2000).* Cambridge: Cambridge University Press.

Nash, J.E., and J.V. Sutcliffe. 1970. "River flow forecasting through conceptual models part I – A discussion of principles." *Journal of Hydrology* 10:282–290.

Perrin, C., C. Michel, and V. Andréassian. 2003. "Improvement of a parsimonious model for streamflow simulation." *Journal of Hydrology* 279:275–289.

Quintana-Seguí, P., P. Le Moigne, Y. Durand, E. Martin, F. Habets, M. Baillon, C. Canellas, L. Franchisteguy, and S. Morel. 2008. "Analysis of Near-Surface Atmospheric Variables: Validation of the SAFRAN Analysis over France." *Journal of Applied Meteorology and Climatology* 47 (1): 92–107 (January).

Randall, D.A., R. Wood, S. Bony, R. Colman, T. Fichefet, J. Fyfe, V. Kattsov, A. Oitman, J. Shukla, J. Srinivasan, R.J. Stouffer, A Sumi, and K.E. Taylor. 2007. Chapter "Climate Models and Their Evaluation" of *Climate change 2007: The Physical Science Basis. Contribution of Working group I to the Fourth Assessment Report of Intergovernmental Panel on Climate Change.* Cambridge: Cambridge University Press.

Richards, A.L. 1931. "Capillary conduction of liquids through porous media." *Physics* 1:316–333.

Sauquet, E, P Javelle, and S Le Clerc. 2003. "Description des régimes hydrologiques des hautes eaux: nouvelle formulation pour l'analyse en débit-durée-fréquence et applications en ingénierie." *Ingénieries EAT*, no. 34:3–16.

Sellers, P.J., Y. Mintz, Y.C. Sud, and A. Dachler. 1986. "A simple biopshere model (SiB) for use within general circulation models." *Journal of Atmospheric Sciences* 46 (6): 505–531.

Stieglitz, M., A. Ducharne, R. Koster, and M. Suarez. 2001. "The Impact of Detailed Snow Physics on the Simulation of Snow Cover and Subsurface Thermodynamics at Continental Scales." *J. Hydrometeor.* 2:228–242.

Terray, L., and M. Braconnot. 2006. "Livre blanc escrime, étude des simulations climatiques réalisées par l'IPSL et Météo france." http://www.ecologie.gouv.fr/Livre-Blanc-Escrime-Etude-des.html.

Thiéry, D. 1990. "Modélisation d'Aquifères par maillage Rectangulaire en régime Transitoire pour le calcul Hydrodynamique des Écoulements. Version 4.3." Technical Report R32210, Rapport BRGM 4S/EAU.

Uppala, S. M., P. W. Kallberg, A. J. Simmons, U. Andrae, V. D. Bechtold, M. Fiorino, J. K. Gibson, J. Haseler, A. Hernandez, G. A. Kelly, X. Li, K. Onogi, S. Saarinen, N. Sokka, R. P. Allan, and . 2005. "The ERA-40 re-analysis." *Quarterly Journal of the Royal Meteorological Society* 131:2961–3012.

Wood, E. F., D. P. Lettenmaier, and V. G. Zartarian. 1992. "A land-surface hydrology parametrization with subgrid variability for general circulation models." *Journal of Geophysical Research* 97:2717–2728.

Zhao, Y. 2006, September. "Modeling fo River-flow routing using a Muskingum and Manning method and application in the Basin of the Seine." Master's thesis, Université Pierre et Marie Curie, Paris, France.